Università degli Studi di Modena e Reggio Emilia

Dipartimento di Ingegneria "Enzo Ferrari"

Dottorato di ricerca in Ingegneria Industriale e del Territorio

"E. Ferrari" – XXXII ciclo

Advances in syngas conditioning for micro-scale gasification power plants

Relatore
Chiar.mo Prof. Ing. Paolo Tartarini

Candidato
Dott. Ing. Nicolò Morselli

Correlatore
Dott. Ing. Giulio Allesina

Coordinatore del Corso di Dottorato
Chiar.mo Prof. Ing. Alberto Muscio

Anno Accademico 2018 – 2019

The typical project starts with new ideas, announcements at meetings, construction of the new gasifier. Then it is found that the gas contains 0.1–10% of 'tars'. The rest of the time and money is spent trying to solve this problem.

Tom Reed, 1998

Al mio bimbo,
Alla sua mamma.

Introduzione

La transizione verso uno sviluppo energetico sostenibile passa attraverso l'efficientamento dei processi, delle tecnologie presenti, e il sempre più largo impiego di fonti energetiche rinnovabili. In questo scenario, le biomasse hanno il potenziale di costituire un serbatoio di energia a basso impatto ambientale che può essere impiegato nella produzione combinata di energia elettrica e termica. Tra i diversi metodi di conversione energetica delle biomasse lignocellulosiche, la gassificazione applicata a gruppi cogenerativi emerge per gli elevati rendimento elettrico e scalabilità, che la rendono applicabile anche al di fuori di contesti prettamente industriali.

La chiave per l'impiego su larga scala di impianti di gassificazione di piccola taglia risiede nella capacità di produrre sistemi di filtrazione semplici, efficaci e dal costo di gestione contenuto.

Per poter perseguire tali obiettivi è fondamentale avere una profonda conoscenza dei fenomeni di fluidodinamica multifase, così come degli scambi termici che avvengono negli impianti di gassificazione.

A tal fine questo lavoro di tesi si articola in due parti: la prima in cui si costruisce il quadro teorico di riferimento, volto a definire le variabili termofluidodinamiche in gioco, e una seconda parte operativa in cui vengono suggerite una serie di soluzioni relative alla filtrazione a caldo.

Nello specifico, i primi due capitoli introdurranno i diversi processi e tecnologie disponibili per la conversione energetica delle biomasse, inserendole nel più ampio scenario europeo delle energie rinnovabili. Sarà descritto il processo di gassificazione delle biomasse legnose per la produzione di energia elettrica, passando in rassegna le principali componenti comuni a questo tipo di impianti. Verrà quindi anticipato il tema cardine di questa tesi descrivendo le tecniche attualmente disponibili per la filtrazione del gas di sintesi, soffermandosi sui metodi di condizionamento delle proprietà fisiche del gas.

Il terzo capitolo tratterà gli effetti degli inquinanti, presenti nel gas di sintesi, sugli organi meccanici dei motori alternativi così alimentati. L'approccio psicrometrico, supportato da metodi computazionali, permetterà di conoscere le condizioni ottimali per un funzionamento in sicurezza di tali generatori.

Nel quarto capitolo si descriverà la caratterizzazione sperimentale di un filtro realizzato con biochar da gassificazione, condotta su un micro cogeneratore a biomassa. Questo studio getterà le basi per quello che sarà trattato nel capitolo

successivo, ovvero la progettazione e lo studio sperimentale di uno scambiatore di calore per gas di sintesi.

Nel sesto capitolo verranno infine descritte le più recenti attività di ricerca che hanno portato sia alla sperimentazione di uno stadio filtrante a sacchi in polimero per un micro cogeneratore a biomassa commerciale.

Nel corso della trattazione saranno esposte le criticità e le potenzialità riscontrate nell'utilizzo dei diversi sistemi di condizionamento del gas di sintesi. La definizione di parametri termo-fluidodinamici chiave risulterà nella semplificazione del sistema multifase iniziale, costruendo una solida base di partenza per il continuo miglioramento di queste tecnologie.

Index

Abstract

The transition towards sustainable energy development involves the efficiency improvement of the processes, the current technologies, and the ever increasing use of renewable energy sources. In this scenario, biomasses have the potential to constitute a low environmental impact energy storage that can be used in the combined production of electrical and thermal energy. Among the different methods of energy conversion of lignocellulosic biomass, gasification applied to CHP gensets emerges due to the high electrical efficiency and scalability, which make it applicable also outside purely industrial contexts.

The key to large-scale using of small-scale gasification plants lies in the ability to produce simple and effective filtration systems with a low maintenance cost.

In order to pursue these objectives, it is essential to have a deep knowledge of multiphase fluid dynamics, as well as of the thermal exchanges that take place in gasification plants.

To this end, this work is divided into two sections: the first in which the theoretical frame of reference is constructed and aimed at defining the thermo-fluid dynamic variables at stake, and a second operative part in which a series of hot syngas cleanup solutions are proposed.

Specifically, the first two chapters will introduce the different processes and technologies available for the energy conversion of biomasses, including them in the broader European renewable energy scenario. The gasification process of woody biomasses electricity production will be described, reviewing the main components common to this type of plant. The key theme of this thesis will therefore be anticipated by describing the currently available techniques for the filtration of the syngas, focusing on the methods of conditioning its physical properties.

The third chapter will deal with the effects of syngas contaminants, on the mechanical parts of internal combustion engines. The psychrometric approach, supported by computational methods, allow to know the optimal conditions for a safe operation of these generators.

The fourth chapter will describe the experimental characterization of a filter made with biochar from gasification, carried out on a micro biomass CHP plant.

This study will lay the foundations for what will be discussed in the next chapter, namely the design and experimental investigation of a heat exchanger for synthesis gas.

The sixth chapter will finally describe the most recent research activities that led to the experimentation of polymer filter bags for a commercial small-scale gasifier.

During the discussion, the critical issues and potentialities encountered in the use of the various syngas conditioning systems will be exposed. The definition of thermo-fluid dynamic key parameters will result in the simplification of the initial multiphase system, building a solid starting point for the continuous improvement of these technologies.

Nomenclature

$\dot{Q}_g$	Thermal power lost by the producer gas	kW
$\dot{V}_{mix}$	volumetric flow of air-syngas mixture	$Nm^3\ h^{-1}$
$P_{el,max}$	maximum electrical power generation	kW
T_{dew}	Dew point temperature [°C]	°C
V_{max}	maximum velocity of the gas	$m\ s^{-1}$
$\dot{m}_g$	Producer gas mass flow rate	$kg\ s^{-1}$
n_{H_2O}	Water vapor mole fraction	
p_{H_2O}	Water vapor partial pressure	Pa
$c_{p,g}$	Specific heat capacity of the producer gas	$J\ kg^{-1}\ K^{-1}$
$D_{g,in}$	Inlet diameter of the HX	m
$D_{g,out}$	Outlet diameter of the HX	m
D_h	Hydraulic diameter	m
D_t	Tubes diameter	m
$D_{w,in}$	Water inlet diameter	m
$D_{w,out}$	Water outlet diameter	m
h_{amb}	Convective heat transfer coefficient	$W\ m^{-2}\ K$
HHV	Higher heating value	$MJ\ kg^{-1}$ or $MJ\ Nm^{-3}$
HTC_g	Overall heat transfer coefficient	$W\ m^{-2}\ K^{-1}$
I	Turbulence intensity	
k	Turbulent kinetic energy	$m^2\ s^{-2}$
l	Turbulent length scale	m
l_b	Distance between the baffles	m
LHV	Lower heating value	$MJ\ kg^{-1}$
		$MJ\ Nm^{-3}$
l_p	Plenum length	m
l_t	Length of the heat exchanging zone	m
MAP	Manifold absolute pressure	Pa
Nm^3	Cubic meter of a gas at 0 °C and 1 atm	
p	Pitch of the twisted tape	m
Re	Reynolds number	

T_{mix}	Temperature of the air-syngas mixture	°C
w	Twisted tape width	m
$wt\%$	Weight total in percentage	%
y	twist ratio pf the twisted tape	
Δp	Pressure difference across the filter stage	Pa
ΔT_{LM}	Logarithmic mean temperature difference	°C

Abbreviations

AFR	Air to fuel ratio
BET	Brunauer–Emmett–Teller
C	Atomic carbon
Ca	Calcium
CCS	Carbon capture storage
CFD	Computational fluid dynamics
CGC	Cold gas clean-up
CH_4	Methane
CHP	Combined heat and power
Cl	Chlorine
CNG	Compressed natural gas
CO	Carbon monoxide
CO_2	Carbon dioxide
DME	Dimethyl ether
ESP	Electrostatic precipitators
FT	Fischer-Tropsch
GHG	Greenhouse gases
H_2	Molecular hydrogen
H_2O	Water molecule
H_2S	Hydrogen sulfide
HCN	Hydrogen cyanide
HGC	Hot gas clean-up
HX	Heat exchanger
ICE	Internal combustion engine
IGCC	Integrated gasification combined cycles
K	Potassium

LHS	Left hand side	
MC	Moisture content	
N	Atomic nitrogen	
N_2	Molecular nitrogen	
N_2O	Nitrous oxide	
Na	Sodium	
NH_3	Ammonia	
NO_x	Nitrogen oxides	
ORC	Organic Rankine Cycle	
PAH	Polycyclic Aromatic Hydrocarbons	
PE	Polyester	
PM	Particulate matter (PM5 indicates particles with diameter $<$ 5µm)	
PP	Polypropylene	
PTFE	Polytetrafluoroethylene	
RANS	Reynolds Averaged Navier-Stokes equations	
RES	Renewable energy sources	
RHS	Right hand side	
RME	Rape oil methyl ester	
TSP	Tar sampling procedure	
TT	Twisted tape	
WGC	Warm gas clean-up	
Greek symbols		
θ	Throttle opening angle	degrees
ε	rate of dissipation of turbulent kinetic energy	$m^2\ s^{-3}$

Chapter 1

Introduction

1.1 The role of biomass in the European energy scenario

On December the 24th of 2018 the revised renewable energy directive EU-2018/2001 (RED II) entered into force, establishing the new future-proof framework by setting a new target of at least 32% renewable energy in gross final energy consumption in 2030 (COM(2019) 225 final, 2019).

The most recent data about the share of renewable energy sources (RES) in Europe is dated to 2017 and it settles to 17.52%. From one hand, the RED I forecast of 16% in 2017 and 20% in 2020 seems to be possible, on the other hand since 2014 the rate of growth of the renewable energy share has slowed down majorly due to policy changing and consequent less investment in RES (Banjaa et al., 2019a; Erbach, 2016).

Within this framework, the wood and other solid biofuels play a key role, producing the 42% of primary renewables production in 2017 (Eurostat, 2019a). The biomass derived from forestry and agriculture has interesting characteristics like renewability, versatility and carbon neutrality (Malico et al., 2019; Shusheng et al., 2019; IPCC, 2012; Krasulina et al., 2012; Mckendry, 2002a).

For this reason, the IEA scenario calculation indicates the crucial role of biomass in order to meet the targets in greenhouse gas (GHG) reduction by 2050 (IEA, 2019) and the literature is by common consent in considering the solid biomass as *the only renewable with significant industrial use* (Malico et al., 2019; Souza et al., 2017; EC-Bioeconomy-KC, 2019). Moreover, the use of bioenergy in combination with carbon capture and storage (CCS) represent a promising negative emission technology (Souza et al., 2017; EC-Bioeconomy-KC, 2019; Rogelj et al., 2016).

However, biomass is not a ready-to-go fuel but must be produced, processed and, only at the very end, can be converted into thermal or electrical energy. Each of this steps has its own criticality, starting from the debates over the convenience to manage or not the forests in terms of CO_2 emissions reduction (Taeroe et al., 2017) to the investigation of the tradeoff between forest as a source for bioenergy production and as a carbon sink (Hoel et al., 2016).

1.2 Bio-energy conversion

As mentioned in the previous paragraph, biomass will be an important player in reaching the GHG reduction target for the near future, but its bulky and inconvenient form hinder the fast shift from fossil to biomass fuel (Basu, 2009). For this reason, a reorganization of the chemical structure of the biomasses is needed with the intent to get gaseous or liquid biofuels with higher versatility and energy density.

The literature is in mutual agreement in dividing the conversion methods of biomass energy into high-value products in two major categories: the bio-chemical/biological and the thermochemical conversions (McKendry, 2002a; Yang et al., 2019; Pang, 2019; Basu, 2019; Malico, 2019; Gonzalez et al., 2019).

The choice of the conversion process is influenced by the type and quantity of biomass feedstock, the desired form of the energy (i.e. end-use requirements), environmental standards, economic conditions, and project specific factors (McKendry, 2002a; Goyal et al., 2008). As a rule of thumb, another way to discriminate the process to be used is to investigate the carbon vs. nitrogen (C/N) ratio of the biomass and its moisture content (MC) For biomass with MC $>$ 50 % and C/N $<$ 30 the biological/bio-chemical route is preferred, spacing from fermentation (production of ethanol) and digestion (production of biogas) (Basu, 2009). In the other cases, the biomass best energy conversion path is the thermochemical one, that it can subdivided in three different subcategories: combustion, pyrolysis and gasification.

Before to introduce those methods of conversion, a short description of biomass properties is reported in the following.

1.2.1 Woody biomass properties

Physical, chemical and thermal properties of the biomass need to be known to understand its behavior in the energy conversion processes. In particular, regarding to the thermochemical conversion methods, the most influencing parameters to be taken into account are: bulk density, heating value, moisture content, elemental composition and ash content (Malico et al., 2019; Quaak et al., 2009).

The ultimate analysis (Tanger et al., 2013) is the most common method to investigate the biomass chemical composition resulting in the relative abundance of individual elements of which the biomass is formed (e.g. C, H, O, N and S).

According to the Energy Research Center of the Netherlands (ECN), an example of biomass properties is reported in Table 1.

Table 1. Solid biomass fuel properties (ECN, 2019; Malico et al., 2019)

	Poplar wood	Willow wood	Wood chips (hybrid poplar)	Bark (pine)	Pellets (wood)
Proximate Analysis (%wt dry)					
Fixed carbon	13.71	15.01	20.3	26.6	17.58
Volatile matter	85.07	83.4	77.9	71.8	82.2
Ash	1.22	1.59	1.8	1.6	0.22
Ultimate Analysis (%wt dry)					
Carbon	49.42	50.19	44	53.9	47.3
Hydrogen	6.0	5.9	5.5	5.8	6.76
Oxygen	43.07	42.22	47.7	38.26	46.02
Nitrogen	0.23	0.1	1	0.4	0.15
Sulphur	0.05	-	0	0.03	0.01
Moisture content (wt%, wet basis, as received)	4.8	43.5	9.2	5	7
Higher Heating Value (MJ kg^{-1}) (dry)	19.5	18.56	16.4	21.37	19.32

Biomass density influences the design of the process control of supply system to the chosen thermochemical conversion plant/device. The density value varies according to its definition defining three type: *true*, *apparent* and *bulk* density.

For the industrial applications, the bulk density plays the most important role. Its definition is based on the ratio between the total mass of biomass particle/stack and the bulk volume occupied by the same biomass particles/stack (Basu, 2009).

Bulk density ranges from even 80 kg m^{-3} for loose materials (Reed et al., 1988) to around 250 kg m^{-3} for wood chips (SERI, 1979).

From these data it's possible to understand how the energy density of the biomass (i.e. the product of higher heating value and the bulk density that ranges from 2.8 GJ m^{-3} for the baled straws to 14 GJ m^{-3} for the wood pellets (Sokhansanj et al., 2006)) is a weak point of this energy source if compared to fossil fuels. From one hand, the high oxygen content lowers its heating value and, on the other hand, the low bulk density results in lower again the product. Biomass densification processes such as pelletization can more than double the energy density (Jenkins, 1995) compared to wood chips, reaching values of bulk density around 500 kg m^{-3}.

Wood chips and pellets were the feedstock used in this study and amongst the options for energy conversion, only those that relates to woody biomass are taken into account and, in the next paragraph, they will be briefly described.

1.2.2 Combustion

Combustion is the oxidation process of the biomass that involves a series of exothermic reactions, and it mainly converts the reactants into H_2O and CO_2 (Basu, 2009) in the form of hot gases around 800-1000 °C (McKendry, 2002b). For woody biomass, this is the most common application to produce heat at domestic and industrial scales (Sansaniwal, 2017; Malico et al., 2019), representing the 12.7 % of the European gross final energy consumption (IEA, 2019). At industrial scales (1-50 MW_e), biomass steam boilers are often used to produce both thermal and electrical power by means of steam turbines with typical electric efficiencies in the range of 15-35 % (Kan et al., 2014 as cited in Malico et al., 2019).

1.2.3 Pyrolysis

Differently from combustion, pyrolysis is the conversion process that takes place in total absence of oxygen by heating the biomass in the range 300-800 °C. The products of pyrolysis are: synthesis gas (syngas) with high calorific value, liquid fuels, chemical products and charcoal (McKendry, 2002b). Biomass, forced to flow inside a container often called a reactor, is supplied with thermal energy

either from the outside (allothermic pyrolysis) or from the combustion of a small part of the biomass itself (autothermal pyrolysis). Based on the heating speed and the temperature, three types of pyrolysis can be distinguished (Brown et al., 2011; Perkins et al., 2018; Basu, 2009; Malico et al., 2019):

- *Light pyrolysis (torrefaction)*: the biomass is heated to 200-300 °C in total absence of oxygen. The method aims at increasing the energy density of the biomass by reducing its hygroscopic properties to guarantee greater stability over time.
- *Slow pyrolysis*: characterized by high residence time of the biomass which is kept at temperatures between 400 ° C and 600 °C. The residence time is enough to convert a large part of the biomass (according to McKendry, 2002b, up to 35 %) into charcoal. This method is also called carbonization and is used, like torrefaction, to increase the energy density of the biomass, completely extracting the humidity and most of the non-combustible components. Transportation costs and fermentation problems in storage are then reduced.
- *Fast pyrolysis*: characterized by strong thermal shocks of the biomass (1000-10000 °C s^{-1}) followed by rapid cooling of the gaseous and vapor products. This method is used when it is desired to maximize the production of liquids and bio-oils.

1.2.4 Gasification

Biomass gasification is the last thermochemical process to be briefly introduced and it will be largely described in the next chapter. Through gasification, the biomass is converted into a gaseous product, termed as *producer gas* or *syngas*[1], which consists mainly of carbon monoxide (CO), hydrogen (H_2), carbon dioxide (CO_2) and methane (CH_4) as well as higher hydrocarbons and nitrogen (N_2) (Pang, 2019; Ahmad et al., 2016).

Gasification offers a high flexibility in using different kind of feedstock materials as well as in the generation of different products. In fact, all kinds of energy or energy carriers (i.e. heat, electrical power, biofuels, hydrogen and biomethane) as well as chemicals can be provided from the syngas. Moreover, synthesis of Fischer-Tropsch (FT) diesel, dimethyl ether (DME), methanol and methane are further established technical processes (Heidenreich et al., 2015) but they will not be part of this study.

[1] Syngas is technically a vapor stream composed of only H_2 and CO derived from a steam and oxygen gasification process (Woodcock et al., 2013) but will be used as a shorthand of producer gas in this work.

The main advantage of the wood gasification process is the generation of a fuel gas instead of only hot flue gases like happens in combustion (Stevens, 2001). The conversion into a gaseous energy carrier enables several possibilities for the syngas to be used as energy source for power generation and every biomass-to-electricity system consists of three main areas: feedstock pretreatment, gasifier and gas conditioning, and electrical generation unit (turbine or engine).

1.3 Gasification process

The process of gasification is, by definition, the thermochemical conversion by partial oxidation of fossil or non-fossil fuels into useful gases and even chemicals (Basu, 2009). The conversion takes place inside a reactor where a *gasifying agent* (also called *medium*) is necessary to make the reactions occur and, for this purpose, pure oxygen, air (air-blown gasifier) or steam can be used (Heidenreich, 2015; Basu, 2009; Ramalingam, 2019).

This work will focus on the air-blown gasification process applied to woody biomass where the air the gasifying agent. In order to better frame this process into the thermochemical conversion methods, a comparison with combustion and pyrolysis can be made by considering the equivalence ratio (ER) i.e. the proportion between the actual air used to oxidize the biomass and its stoichiometric value. According to this parameter, the biomass can be:

- heated in the absence of oxygen following the pyrolysis method and generating bioenergy;
- partially oxidized (ER ~ 0.3) to generate syngas through gasification (Verma et al., 2014);
- fully oxidized through the combustion process, obtaining hot flue gases.

Gasification is then a process where the biomass is partially burned to generate the heat necessary to break down the long molecules of wood into simpler ones. In most of the cases, the process of gasification goes through all the thermochemical methods shown before, passing from the total oxygen depletion via combustion, to a pyrolytic phase where the heat is used to convert the solid biomass mostly into tar vapors and fuel gas and the formation of producer gas through reduction reactions.

According to the reactor technology and the type of biomass used, the volume fractions of the gases can significantly change. Table 2 shows a common producer gas composition range for an air-blown downdraft type gasifier fueled with fir woodchips and using air as gasifying agent. It can be noted how N_2, CO_2 and most of the water vapor that is found in the producer gas is due to the partial

combustion process of air-blown gasifiers. In Table 2 a comparison with oxygen and steam as gasifying agents is also reported.

Table 2. Solid biomass fuel properties (FAO, 1986; Rauch, 2003)

Gas components	Gasifying medium		
	Air	Oxygen	Steam
N_2 [%vol]	50÷54	0÷1	0÷1
CO [%vol]	17÷22	40÷60	20÷25
CO_2 [%vol]	9÷15	10÷15	20÷25
H_2 [%vol]	12÷20	15÷20	30÷45
CH_4 [%vol]	2÷3	0÷1	6÷12
LHV [MJ Nm^{-3}]	4÷5	10÷12	10÷14

The lower heating value (LHV) of producer gas ranges from 4 to more than 5 MJ Nm^{-3} (FAO, 1986; Soares et al., 2019; Susastriawan et al., 2017; Martinez et al., 2012; Wei et al., 2017; Zainal et al., 2002) and 1 kg of dry wood generates approximately 2.5 Nm^3 of gas (FAO, 1986).

Even though the LHV is low, compared to other fossil fuels (e.g. gasoline 44 MJ kg^{-1}, diesel oil 42.5 MJ kg^{-1}, CNG 45 MJ kg^{-1} (Heywood, 1988)), the air to fuel ratio (AFR) for stoichiometric combustion of syngas/air mixture is approximately 1.1:1 (FAO, 1986; Lapuerta et al., 2001) while for other fossil fuels is in the range of 14÷17:1 (Mattarelli et al., 2013).

This results in an energy of the mixture comparable to fossil fuels which makes the syngas, and therefore the gasification, attractive for its application in fuelling internal combustion engine (ICE) for combined heat and power generation (CHP) (Tinaut et al., 2006; Boloy et al., 2011; Martinez et al., 2012; Zabaniotou et al., 2013; Ftwi et al., 2014; Bates et al., 2017; Damartzis et al., 2012; Malik et al., 2013).

Syngas application in ICE started in 1878 with the introduction of the Dowson gas producer, mainly used to fuel big stationary engine for power production. Was Bernier, in 1895, with his "suction gas" generator, that paved the way for small-scale gas producer for power generation (Kaupp et al., 1984). Since then, many studies have followed one another, and different types of gasifiers were patented (including the Georges Imbert model described in the next sections).

Due to the scarcity of fossil fuels, during the Second World War, in Europe, more than one million gasifiers produced syngas from wood, peat or coal to power the engine of vehicles on which they were directly installed (FAO, 1986).

From the definitive advent of natural gas, around 1950, the production of producer gas gradually fell into disuse, remaining confined to the production of chemicals. The ease with which it is possible to produce gas from wood, has brought to the cyclical rediscovery of gasification often in situations of energy emergency, as happened during the oil crises of 1973 and 1979. Only in the last 20 years the progressive spread of an ecological conscience and of dedicated feed-in-tariff subsidies, have allowed the definitive rediscovery of this technology for power generation.

In the following paragraphs the thermochemical reactions that take place in wood gasification will be shown, focusing then to the different designs of the most common air-blown gasifiers and their application in heat and power generation.

1.3.1 Chemical reactions in wood gasification

The gasification process consists of four discrete thermochemical phases, which includes *drying*, *pyrolysis*, *combustion* and *reduction* (Ramalingam et al., 2019).

The various steps of the biomass gasification process will be described below keeping in mind, however, that the phases are not spatially well defined within the gasifier but that there are several promiscuous zones between one process and another.

Drying

Fresh-cut biomass can reach moisture contents around 30÷60 % (Basu, 2009; Ramalingam, 2019) and a drying phase is thus necessary to obtain high quality syngas (Mallick et al., 2017). For this reason, when the moisture content is generally above 20 %, a drying phase outside the gasifier is necessary in order to remove most of the water. The remaining part is eliminated inside the reactor as soon as the wood is heated up. Above 100 °C the drying process becomes irreversible and it proceeds to about 200 °C where the chemical composition of the biomass starts to change with the removal of light volatile compounds (Zhongqing et al., 2012; McKendry, 2002c). Some authors consider this first decomposition stage, above 100 °C, part the pyrolysis phase (Basu, 2009; Ramalingam et al., 2019; Campuzano et al., 2019).

Pyrolysis

Pyrolysis is the endothermic process by which the long polymeric chains that build the biomass are broken down into simpler molecules forming gaseous, liquid and solid compounds.

$$C_nH_mO_p(Biomass) + Heat \rightarrow \sum C_xH_yO_z(liquid) + \sum C_aH_bO_c(gas) + H_2O + C(char) \quad (1.3.1)$$

Heat and the absence of oxygen (ER = 0) are needed to activate the pyrolysis process that evolves according to three crucial parameters: biomass type, pyrolysis temperature, biomass residence time and heating rate (expressed in °C s^{-1}) (Demirbas et al., 2002; Neves et al., 2011 as cited in Campuzano et al., 2019; Pang et al., 2019).

Pyrolysis by itself can be influenced by many other parameters (e.g. biomass particle size, reactor geometries etc.) that play a crucial role in the design of a pyrolyzing reactor. Since the purpose of this study is to stay within the framework of gasification, only the pyrolysis phases that are part of the gasification process of the biomass will be shown in the following.

- *Primary pyrolysis* (200÷300 °C): in this phase the biomass is mostly converted into char (called primary char) and a series of condensable (organic compounds and water) and non-condensable gases. To underline the difficulty of separate these types of processes in discrete phases, consider that primary pyrolysis can proceed even up to 500÷600 °C (Campuzano et al., 2019).
- *Secondary pyrolysis* (300÷600 °C): the volatiles, generated in the first phase, participate to secondary reactions that are strongly influenced by the residence time of the biomass (now decomposed into char, liquids and gases). If this is greater than the time of the pyrolysis reactions, primary char is converted for a large part into secondary char.

Most of the problems inherent to the gasification process of biomass take place during pyrolysis where, together with the products already mentioned, the so-called *tar* is formed. This is present in the state of very viscous liquid at ambient temperature and it is formed by long chains of hydrocarbons which are difficult to split and that cause the premature failure of mechanical components and tubes clogging downstream the gas-making facility. It has been shown how even small amount (ppm) of tar can affect the energy conversion efficiency of end user applications such as fuel cells (Papurello et al., 2016).

This research aims at the investigation and implementation of a series of technical solutions to define the boundaries of a simple and effective filtration system for small-scale biomass gasification power plants.

Combustion

In air-blown gasifiers, the combustion or oxidation zone (even called partial combustion) is the driver of the entire process since, here, the heat necessary to dry and pyrolyze the biomass is generated.

In the combustion zone, the volatiles and char generated during late drying and pyrolysis are partially oxidized through a number of exothermic chemical reactions, generating heat at 1100÷1500 °C (Ramalingam et al., 2019; ECN, 2019). The main reactions involved during this phase are presented below.

$$C + O_2 \rightarrow CO_2 - 394\ kJ\ mol^{-1} \quad (1.3.2)$$

$$C + 0.5O_2 \rightarrow CO - 111\ kJ\ mol^{-1} \quad (1.3.3)$$

$$CO + 0.5O_2 \rightarrow CO_2 - 284\ kJ\ mol^{-1} \quad (1.3.4)$$

$$H_2 + 0.5O_2 \rightarrow H_2O - 242\ kJ\ mol^{-1} \quad (1.3.5)$$

$$C + 2H_2 \leftrightarrow CH_4 - 75\ kJ\ mol^{-1} \quad (1.3.6)$$

$$CH_4 + 2O_2 \leftrightarrow CO + 2H_2O - 803\ kJ\ mol^{-1} \quad (1.3.7)$$

Reaction 1.3.2 and 1.3.3 regard to secondary char partially combustion, while reactions 1.3.4 and 1.3.5 are the oxidation of non-condensable gases (carbon monoxide and hydrogen) generated in the pyrolysis.

Finally, there is a fifth oxidation reaction (1.3.7) concerning the methane generated by the char, which is found to react in a hydrogen-rich environment (1.3.6). This is not our case, as the volume of methane produced is in the order of 2÷4%, but it should be kept in mind (Basu, 2009).

Gasification (Reduction)

Once the oxidation phase is complete, a series of endothermic reactions that delineate the final composition of the producer gas begins in the strongly

reducing environment. As for combustion, the reaction matrix for the gasification phase is the char generated in the previous steps.

Each gasifier aims at converting most of the CO_2 and H_2O formed during the pyrolysis and combustion process into CO, H_2 and CH_4; the gases formed will in fact be the main fuels contained in the final syngas.

Starting from equation 1.3.6, that is on the border between pyrolysis and gasification, other equations are involved in the reduction process and are shown in the following (Basu, 2009; Rauch, 2003; Chawdhury et al., 2013; Kumar et al., 2009; Srivastava, 2013; Pruksakit et al., 2014; Jain, 1999; as cited in Sansaniwal et al., 2017).

Bouduard reaction

$$C + CO_2 \leftrightarrow 2CO + 172\ kJ\ mol^{-1} \tag{1.3.8}$$

Water-gas reaction

$$C + H_2O \leftrightarrow CO + H_2 + 131\ kJ\ mol^{-1} \tag{1.3.9}$$

Water-gas shift reaction

$$CO + H_2O \leftrightarrow CO_2 + H_2 - 41\ \ kJ\ mol^{-1} \tag{1.3.10}$$

1.3.2 Producer gas contaminants

As anticipated in paragraph 1.3.1, during the gasification process a number of undesirable contaminants are generated. A list of all the possible pollutants of the syngas can be found in Abdoulmoumine (2015) and are described in the following.

- Particulate matter: both in updraft and downdraft applications (see section 1.3.3), the producer gas is forced to pass through a packed bed of biomass or char respectively. In this condition, the producer gas is charged with a relevant amount of dust that needs to be removed for downstream applications to avoid corrosion and premature failure of mechanical parts. The particulate matter consists of dust, soot, char, and ashes (Rakesh et al., 2018) with a wide range of particle size scales: between 1 µm to 100 µm (Figure 1) for the soot and in the order of magnitude of few millimeters for char particles (Woolcock et al., 2013).

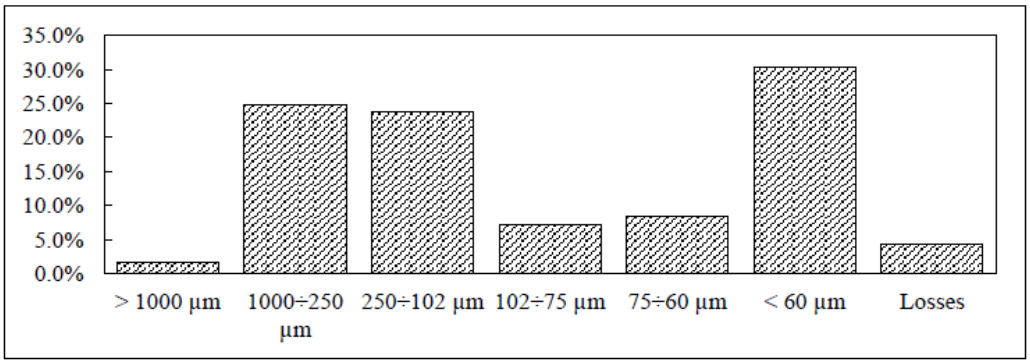

Figure 1. Analysis of wood gas particulate matter (adapted from SERI, 1979).

- Tar: by definition is formed from all the organic compounds, which have the molar mass above the benzene one, hence 78 g mol^{-1} (Devi et al., 2003; Neeft et al., 1999). In the tar are then considered both the aromatic and polyaromatic compounds going from naphthalene to a series of benzenes as reported in Figure 2 (Patuzzi et al., 2016).
  According to the temperature at which are generated, tar can be divided in (Basu, 2009):
  Primary tar: they are generated in the early stages of pyrolysis by the breakdown of cellulose, hemicellulose and lignin. They are mainly formed by acids and sugars of various types, ketones, aldehydes, phenols, etc.
  Secondary tar: they are formed in the gasifier at temperatures above 500 °C, therefore during secondary pyrolysis. They are mainly non-condensable gases and the major constituents are olefins and phenols (Milne et al., 1998).
  Tertiary Tar: these products are formed at higher temperatures than the previous ones (800 - 900 °C) and are organized in the form of polycyclic aromatic hydrocarbons (PAH).

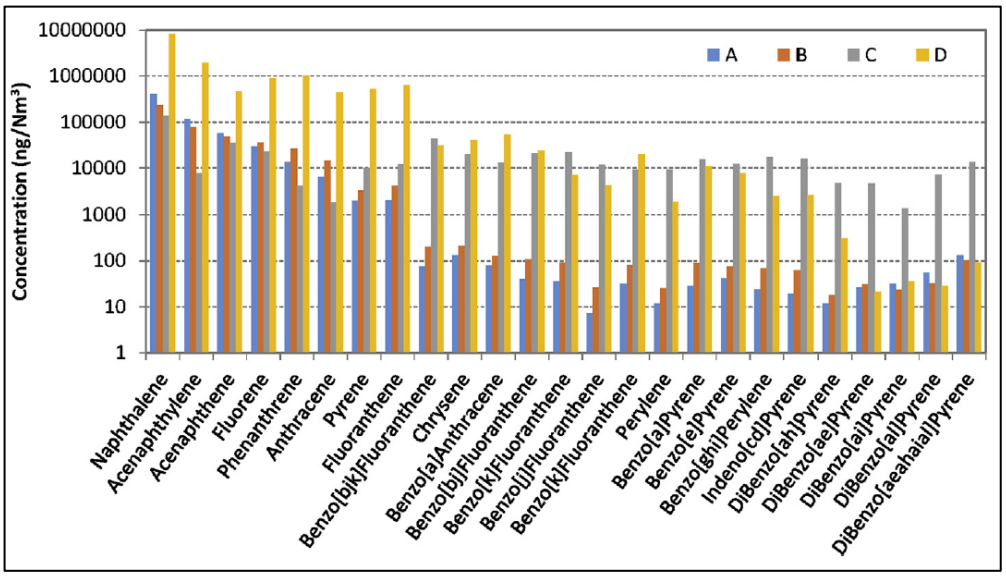

Figure 2. Concentration of tar in the producer gas generated by four (A, B, C, D) different small-scale gasification CHP plants (Patuzzi et al., 2016).

If compared to other contaminants, tar is the most abundant in terms of weight concentration in the final gas composition, contributing to the producer gas HHV for 100-150 kJ Nm^{-3} (Huang et al., 2011). The type of gasifier, the temperature of the gasification process and the feedstock composition and size, can influence its amount (Abdoulmoumine et al., 2015).

Tar is often present in vapor phase downstream the gasifier and the main thermodynamic property that need to be considered for their condensation is the tar dew point. Namely, it is the temperature at which the real total partial pressure of tar equals the saturation pressure of tar. As the actual process temperature exceeds the thermodynamic tar dew point, tar can condense out and cause serious problems, such as clogging and fouling, of the components downstream the gasification facility (Mitsakis et al., 2011 as cited in Rakesh et al., 2018; Richardson et al., 2012). In Table 3, the dew point of major tar components is reported and Figure 3 shows the effect of tar components on the tar dew point calculated according to the ECN complete model. The dashed line represents the amount of condensate tar according to the gas temperature: at 25 °C the 12% of tar are still contained in vapor phase in the gas stream.

Table 3. Tar components dew point (ECN simple model).

Tar class	Compound	Molecular weight [g mol^{-1}]	Number of aromatic rings
Class II	Phenol	92	1
Class III	Toluene	94	1
Class IV	Naphthalene	128	2
Class IV	Phenanthrene	178	3
Class V	Pyrene	202	4
Class V	Benzo(ghi)perylene	276	5

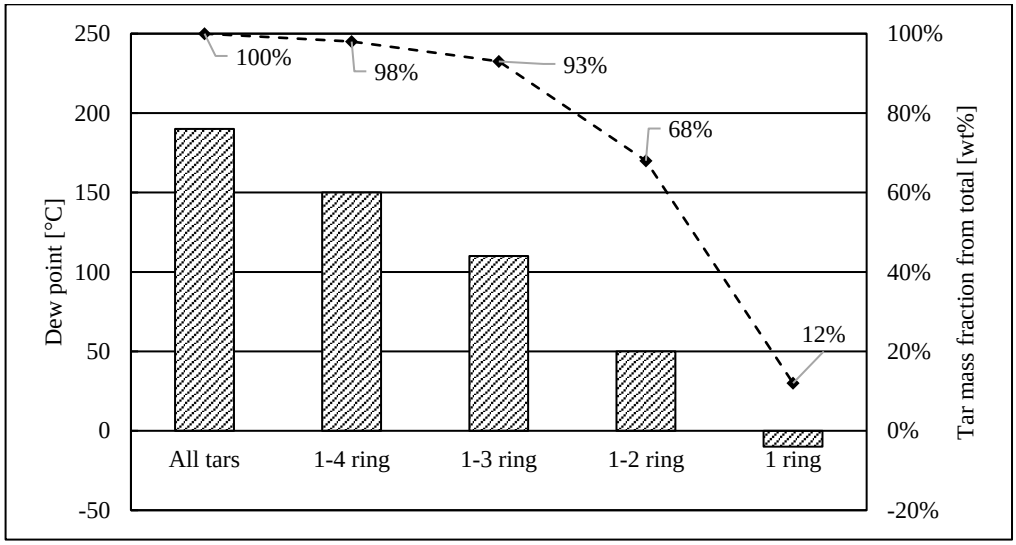

Figure 3. Relation between the tar dew point and the tar composition divided in size of compounds (ECN complete model).

- Nitrogen compounds: as found in (ECN, 2019) the nitrogen content of the biomass ranges from 0.1 to 1 % according to the plant species. During the gasification process, the portion of nitrogen contained in the biomass is sum to the nitrogen of the air necessary for the combustion. Part of it is converted into a series of pollutants such as: hydrogen cyanide (HCN), nitrogen oxides (NO_x and N_2O) and ammonia (NH_3) (Zhou et al., 2000). The remaining part is turned into N_2 (Abdoulmoumime et al., 2015), which has the only drawback to dilute the producer gas, lowering its heating value.

In terms of concentration in the final gas composition, ammonia is the most abundant: its formation is highly competitive, especially at temperatures below 800 °C where the percentage of conversion of the solid nitrogen into ammonia reaches the 60%. The concentration of ammonia in the producer gas usually ranges from 350 and 18000 part per million in volume (ppm_v) according to the biomass composition (Cui et al., 2010; Hurley et al., 2012 as cited in Abdoulmoumime et al., 2015).

- Others: sulfur is the other contaminant present in the feedstock (traces to 0.06 % (Mondal et al., 2011) together with chlorine (Cl) and metals (Na, K). These components can be converted into hydrogen sulfide (H_2S) and hydrogen chloride (HCl) which generate several problems of corrosion to the mechanical parts and pipings downward the gas-making facility (Cui et al., 2010; Hurley et al., 2012; Ohtsuka et al., 2011 as cited in Abdoulmoumime et al., 2015).
  Typical concentration of these pollutants in the syngas are in the order of 100 ppm_v.

1.3.3 Gasifier architectures

Besides biomass characteristics and process parameters, the design of gasifiers is one of the key parameters in gasification process (Susatriawan et al., 2017). Many types of biomass gasifiers are available in various design depending on the shape, size and availability of the fuel as well as the process requirements (Sansaniwal et al., 2017). According to the way of interacting of biomass and gasifying agent, gasifiers can be divided into *fluidized bed* and *fixed bed*.

Fluidized bed

In fluidized bed gasifiers, the biomass is kept in suspension within the reactor by means of a homogeneous flow of gasifying medium (Kunii et al., 1991 as cited in Sansaniwal, 2107). In this configuration, there is not a discrete separation between the different phases of gasification but drying, combustion, pyrolysis and reduction occurs in the whole reactor according to the residence time of the particle. The operating condition is hence nearly isothermal and the working temperatures is between 800 and 900 °C. A powder catalyst can be recirculated in the reactor with the fluid bed to enhance the achievement of the chemical equilibrium of gasification reaction and then to obtain an higher conversion factor of the biomass into gas. (Sansaniwal et al., 2017)

On the one hand, fluidized bed can have a conversion efficiency up to 95%, be suitable for scaling up and work with a wide range of particle size enabling the

use of sawdust and rice husk (Basu, 2009; Siedlecki et al., 2011). On the other hand, they suffer of particles sticking to the reactors wall that tends to modify the internal fluid dynamics and to form agglomerates with the risk of de-fluidization of the bed (Melissari, 2014; Miles et al., 1995; Beenackers et al., 1984, Proll et al., 2007 and Ordys et al., 2004 as cited in Sansaniwal et al., 2017). Fluidized bed reactors are suitable for medium/large-scale power plant applications.

In Figure 4 a schematics of fluidized bed geometry is reported.

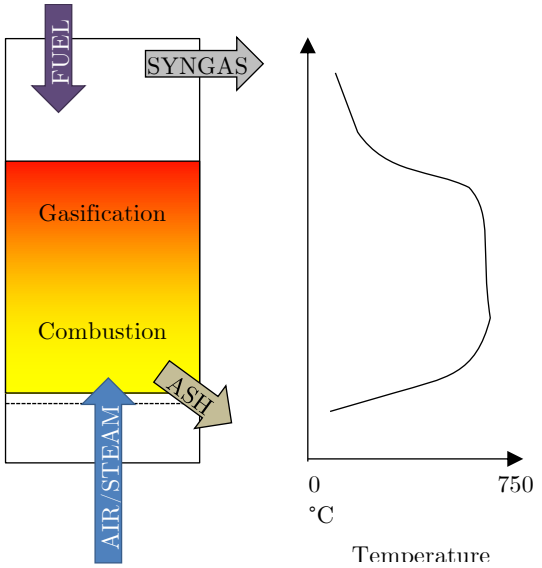

Figure 4. Operating diagram of a fluidized bed reactor. Beside the qualitative trend of the temperature profile vs. the height of the reactor (adapted from Basu, 2009). The nearly uniform temperature trend is shown.

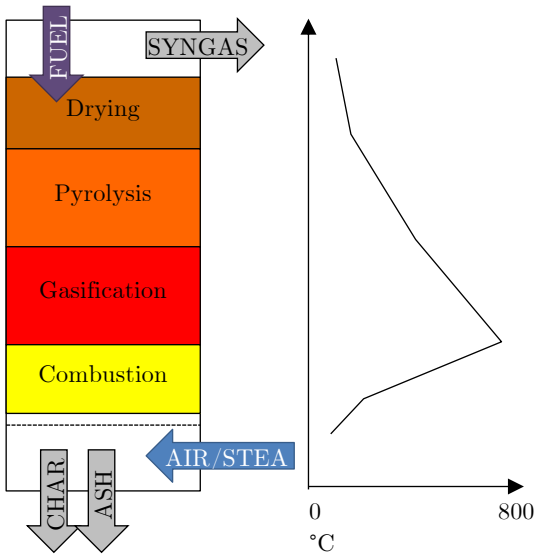

Figure 5. Operating diagram of a fixed bed updraft reactor. The qualitative trend of the temperature profile vs. the height of the reactor is shown (adapted from Basu, 2009).

Fixed bed

Unlike fluidized bed, fixed bed reactors are characterized by a solid packed bed of biomass particles through which gasifying medium and producer gas passes up or downward (Sansaniwal et al., 2017). They are also called moving bed due to the slow motion of the solid with respect to the gas (Ruiz et al., 2013 as cited in Mahipney et al., 2016). Here, the different phases of gasification can be distinguished over the height of the reactor, which is generally formed by a cylindrical stainless-steel vessel. Due to their simplicity and flexibility they are suitable for small-scale heat and power applications (Situmorang et al., 2020; Chopra et al., 2007; Beohar et al., 2012; Gautam et al., 2011; Malik et al., 2013 as cited in Sansaniwal et al., 2017). They also ensure a high specific conversion rate (referred to the volume of the reactor) but they are limited to operate at temperature lower than 1000°C (Warnecke et al., 2000 as cited in Mahipney et al., 2016) to avoid the use of expensive materials. Generally, stainless steel AISI310 (Tomei, 1981) is suitable for this kind of application and guarantees reliability and low costs.

According to the relative movement between the generated syngas and the biomass bed, fixed bed gasifiers can be mainly divided into *updraft* and *downdraft* and are discussed in the following.

1.3.4 Updraft gasifiers

This type of reactor was widely used in the early twentieth century to produce coke using steam as a gasifying agent. In air-blown updraft gasifiers, the air inlet for the combustion reactions is located in the lower area while the outlet of the producer gas is on the top side of the vertical vessel. The air enters the reactor from below and passes through the grate on which a highly reactive layer of char rests. The rapid combustion of pyrolysis products (flaming pyrolysis) in contact with the air sharply raises the temperature (up to about 1000 °C) providing heat by convection and radiation to the biomass contained in the overlying areas. Going up towards the exit, the syngas meets the areas of reduction, pyrolysis and finally drying. The biomass necessary for the supply of the system is loaded from the top and, from the moment that biomass and syngas run in a different direction, are also called *counter-current* reactors. In Figure 5 a schematic representation of the updraft is shown.

PROS: constructive simplicity (Knoef, 2005 as cited in Pedrazzi, 2014), wide range of plant size (Khummongkol et al., 1990; Kurkela et al., 1989; Kirkels et al., 2011; Brammer et al., 2002 as cited in Pedrazzi, 2014), high calorific value of the produced syngas and high gasification efficiency, since when passing

through the biomass layers, the gas goes out at a temperature not too far from the ambient one. It is also useful to point out that these gasifiers are the least sensitive to the size of the inserted biomass (from 5 to 100 mm particle size as reported from Kouhia, 2011), without appreciable changes in the quality of the produced syngas.

CONS: one of the drawbacks of this geometry lies in the distribution of the different phases of the gasification process, in fact, the last reactive zone that the gas crosses when leaving the reactor, is the pyrolysis zone. The pyrolytic tar and vapor produced are torn from the reactor, remaining in suspension in the gas. The tar content in the gas produced by these plants is in fact in the order of 100 g Nm^{-3} (Fjellerup et al., 2005; Sansaniwal et al., 2017), which makes them unsuitable for any application involving the use of internal combustion engines (Rajvanshi, 1986).

The only feasible application is the direct combustion of the syngas in torch to produce thermal and/or electrical energy using Stirling cycle (Marini, 2012 as cited in Allesina, 2013a) engines or ORC turbines.

1.3.5 Downdraft gasifiers

One of the drawbacks of updraft gasifiers is the high amount of tar in the producer gas. Tar formation is reduced using downdraft reactors because the combustion stage follows the pyrolysis stage (Ruiz et al., 2013 as cited in Mahinpey et al., 2016). As can be seen in Figure 6, the reactor is fed with biomass from the top while the gas is drawn from the bottom of the reactor. For this reason, they are also called *co-current* gasifiers given the same path followed by biomass and syngas (Basu, 2009 as cited in Morselli, 2012).

PROS: this technology theoretically allows the almost total abatement of tar, reducing the costs of post-treatment of syngas. The average tar concentration in the syngas from downdraft ranges from 0.15 to 1.00 g Nm^{-3} (Bhattachary et al., 2001 as cited in Martinez et al., 2012) and, for this reason, downdraft gasifier systems are more appropriated to provide producer gas with allowable quality for ICEs. The application range between 10 and 100 kW makes them particularly interesting for the construction of small biomass plants.

CONS: the main weaknesses of these reactors lie in the limited flexibility regarding the size of the biomass to be processed (which is calibrated according to the size of the reactor), the possibility of sintering the ashes due to the high operating temperatures and the production of an average syngas with lower heating value than an updraft gasifier (Kihedu et al., 2014).

According to Martinez, downdraft gasifiers can be divided in open top and close top designs.

Open top

Open top reactors are also called *stratified* because the air is forced to move downwards through the biomass bed, generating a homogeneous temperature distribution all over the reactor diameter. These gasifiers are versatile and reduces the sensitivity of the process to the biomass size, enabling the operation with a large range of particle dimension. Open top gasifiers are widely diffused in the literature (Prando et al., 2016; Prasad et al., 2015; Jayamurthy et al., 1997) but will not be part of this study.

Closed top

Closed top downdraft gasifiers are characterized by a single or multiple injection of air placed in the height of the reactor. According to the presence of a restriction (*throat*) in the reactor core, they can be distinguished in *no-throat* and *throated* gasifiers.

The most diffused (Pathak et al., 2008; Sheth et al., 2010; Ouadi et al., 2013 as cited in Pedrazzi, 2014) type of throated downdraft reactor is the Imbert gasifier (Reed, 1988 as cited in Martinez et al., 2012) which takes its name from the homonymous inventor Georges Imbert (Figure 7).

This type of reactor has the particularity to have a series of nozzles upstream the throat, that provides the combustion air and generates a zone at temperature up to 1200-1400 °C (Valderrama et al., 2018) but often limited to 1000 °C due to materials resistance. The high temperatures increase the chance for the pyrolytic tar vapors to be cracked (Anca-Couce et al., 2016) and hence to obtain a cleaner gas, suitable for power generation through ICEs (Chaves et al., 2016).

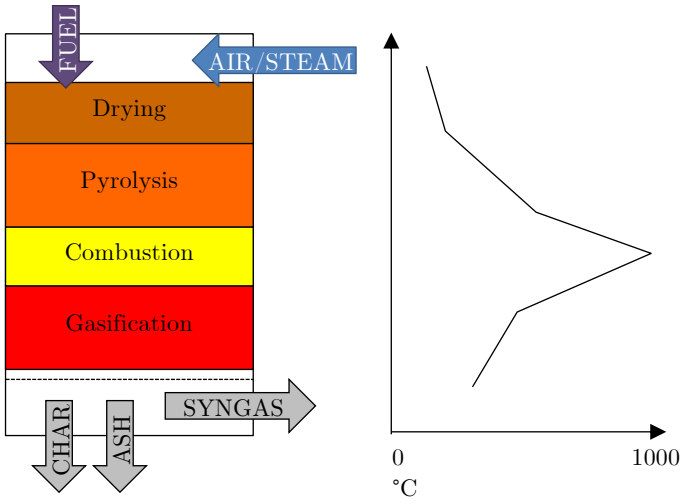

Figure 6. Operating diagram of a fixed bed downdraft reactor. The qualitative trend of the temperature profile vs. the height of the reactor is shown (adapted from Basu, 2009).

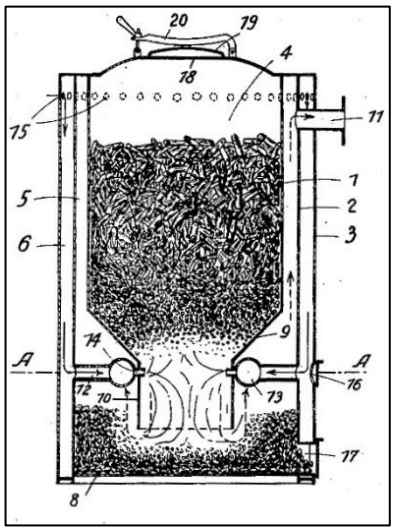

Figure 7. Imbert gasifier design (SERI, 1979; US Patent 1821263)

1.4 Power production technologies

The flexibility of the producer gas enables several possibility of its application in heat and power generation, ranging from the district heating to the decentralized power generation (Borjesson et al., 2010; Buragohain et al. 2010 as cited in Kirsanovs et al., 2017; Bridgwater, 1998; Bocci et al., 2014).

Figure 8. Biomass thermal gasification power plant distribution in Europe (IEA Task 33 database). Green and red flags represent respectively the operational and non-operational power plants.

Different power plant scales can be thus defined depending on the thermal or electrical power generated: many authors suggest that small-scale power plants can have a maximum power output between 100 and 150 kW_e while medium and large-scale systems go up to 1-2 MW_e and to over 10 MW_e respectively (Omar et al., 2019; Bshit et al., 2019).

As anticipated in the previous paragraph, each reactor technology is characterized by an operational range in terms of maximum gas flow rate and, thus, in terms of maximum power output. The choice of an optimal type of gasifier mainly depends on the dimensions of the power plant and on the quality of the available biomass.

Instead of listing all the ways in which the producer gas can be exploited to produce electricity and heat, some virtuous examples of biomass power plants of different scales are reported below, explaining the technology used for each one.

1.4.1 Steam turbine in Kalundborg power plant

In co-firing configuration, the biomass is converted into producer gas, which is usually fired together with the pulverized coal for steam production and steam turbine feeding for electricity and heat generation. The advantages of this solution are the reduction of carbon dioxide, sulfur and nitrogen oxides emissions of the coal power plant. As reported in NREL, 2019, up to 15% of the total energy input can be substituted by biomass without modification to the coal burner, making this technology attractive to upgrade already existing power plants. In the Kalundborg power plant, the gasifier consists of three main components: a pyrolysis chamber, a char reactor and a recirculating cyclone. Since the gas is directly fired afterward its production, the filtration stage is simply composed by a second single stage cyclone for ash and fines recovery. The thermal power given by the biomass co-combustion is 6 MW_{th} (Hrbek, 2019).

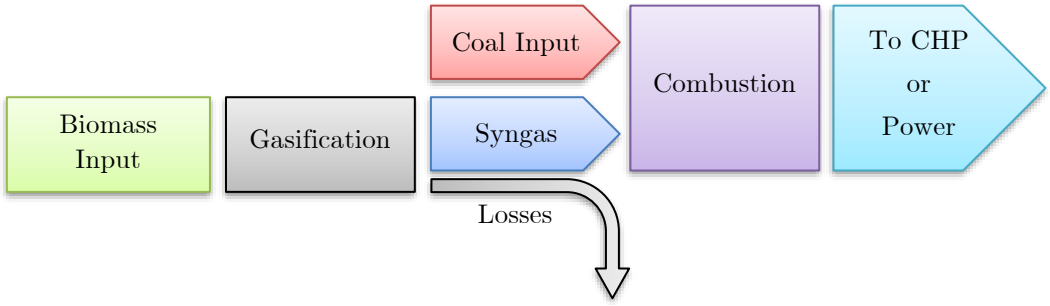

Figure 9. Biomass thermal gasification for coal boiler power production (adapted from Rüegsegger et al., 2018)

1.4.2 IGCC power plant of Värnamo

Thermal gasification process can be applied both to non-fossil and fossil fuels such as fossil carbon, for which Integrated Gasification Combined Cycles (IGCC) have been first developed. In IGCC systems the solid feedstock is thermally converted into syngas by means of a gasification reactor, the gas is then filtrated, compressed using centrifugal compressor and fired inside a gas turbine. Here, the first tranche of electrical energy is generated. The hot exhausts from the gas turbine serves as heat source for the generation of steam which feeds a steam turbine for the second tranche of electrical power generation. A heat recovery system closes the circle by cooling down the steam that exits from the second turbine which is often used for district heating. The Värnamo (Sweden) power plant is the first virtuous example of IGCC technology applied to biomass

conversion. The plant started in 1996 and was capable of 6 MW_e and 9 MW_{th} for district heating with an overall efficiency of 83 % and net electrical efficiency of 32 % (Stahl et al., 1998).

The chipped biomass is dried using flue gases to a moisture content of 5-20 % and is then fed into the gasifier, which uses the fluidized bed technology (air as gasifying medium). A classical tubes-and-shell heat exchanger cools down the gas to 350 °C and a ceramic filter is used to remove the particulate matter before entering into the gas turbine (Stahl et al., 1998).

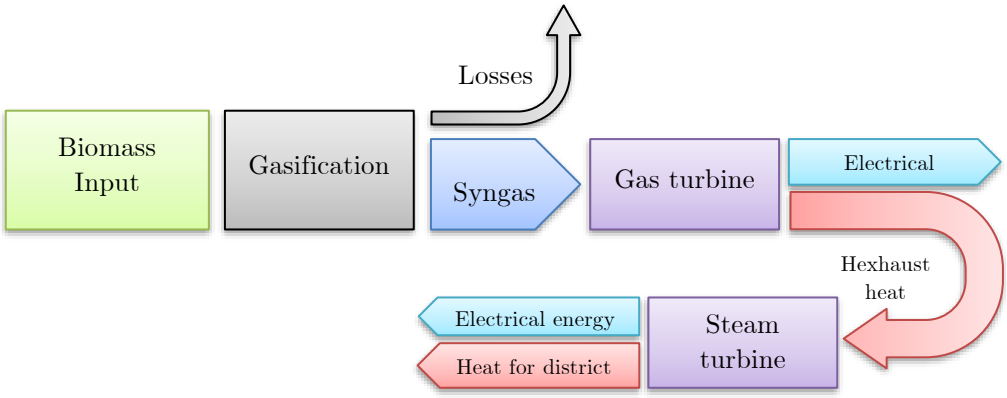

Figure 10. Scheme of the Värnamo gasification plant.

1.4.3 Power plant of Güssing

This power plant is composed of a fluidized bed reactor and steam is used as gasifying medium. This solution allows the generation of nitrogen-free, high-grade syngas that feeds a turbo-charged V 20 – cylinder Otto engine from GE – Jenbacher able to generate up to 2 MW_e and 4.5 MW_{th} in CHP configuration for district heating. The gas exits from the reactor at 850 – 900 °C and it is cooled down to 160 – 180 °C using a water-cooled heat exchanger. Unlike in the previous case, the particulate matter of the gas is removed by means of fabric filters while tar is separated using a scrubber, in which rape oil methyl ester (RME) is used as solvent. The power plant is supplied with woodchips by means of screw conveyors and the total fuel consumed is around 2300 kg h^{-1}. Electrical efficiency is 25 % while the overall power plant efficiency is 80 %.

After almost 100.000 hours of operation, the biomass CHP of Güssing was shut down by end of October 2016 due to economic reasons. The project was in fact supported by feed-in tariffs that ends in October 2016 and, without this tariff, no economic operation was possible (Hrbek, 2019).

The project of Güssing was replicated even in Senden (Germany) building a CHP plant capable of 4.55 MW_e and 15.1 MW_{th}. The electrical efficiency was increased from 25 % to 35 % by integrating a biomass drying unit and an Organic Rankine Cycle (ORC) module. In ORC systems, an organic fluid is used to follow the Rankine cycle at lower temperatures instead of steam. This enables the possibility to recover low-grade waste heat from engines or production cycles for electrical energy production by means of a turbine.

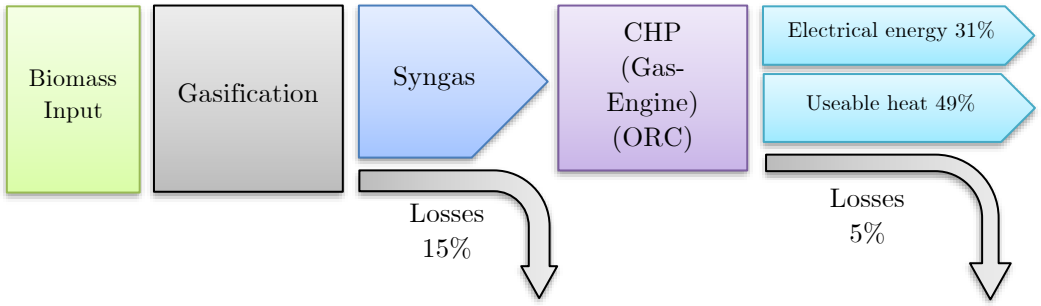

Figure 11. Biomass thermal gasification for CHP engine or ORC powering (adapted from Rüegsegger et al., 2018)

1.4.4 Burkhardt

Despite to previous systems that work with woodchips, Burkhardt is a company that produces inverted downdraft gasifiers fueled with wood pellets for CHP applications. The gasifier technology is comparable to co-current gasifiers but the difference with standard downdraft is that, here, air and biomass are fed from the bottom of the reactor and the gas is drawn from the top.

The power plant is proposed in three different sizes: 50 kW_e, 165 kW_e and 185 kW_e, and all of them are characterized by a syngas/water heat exchanger and baghouse filters for tar and particulate removal. An internal combustion engine is used to generate both heat and power: a common spark ignited gas engine is used for the 50 and 165 kW_e versions, while a Diesel ignited one is used in the 185 kW_e CHP plant. In the latter, a pilot ignition of Diesel oil is used as liquid spark in substitution of the spark plugs (Burkhardt, 2019). In Figure 12 the 50 kW_e model is shown.

1.4.5 SPANNER RE[2]

Spanner is a German producer of downdraft fixed bed biomass gasifiers for combined heat and power applications. The company produces several model of power plants, named according to the electrical power output: HKA 10/35/45/49/70 ranging from 9 to 67 kW_e and 22 to 123 kW_{th} respectively. The plant consists of a series of feeding auger that feed the gasification reactor, which converts the woodchips into producer gas. The gas is cooled down by means of tube-in-tube gas/water heat exchangers (red arrow in Figure 14a – solution adopted also by ESPE Chip50 gasifier in Figure 14b) and the engine coolant is used as cooling fluid. The gas is then filtered using a baghouse filter and then fired into a turbocharged Otto-cycle engine. The HKA70 machine can be organized in clusters reaching up to 2 MW_e power output (Spanner, 2019).

1.4.6 Portable cogenerating unit: the Power Pallet series

One of the most interesting companies regarding small-scale gasification is the Californian All Power Labs (APL). The project of their first semi-automatic[2] gasifier, called GEK TOTTI, started in 2008, resulting in a wider work of construction of a micro gasification power plant capable of 15 kWe and 30 kW_{th}: the Power Pallet 20 (PP20). Its name comes from the dimensions of the installation base 1000x1200 mm, standard of the US pallet 40x48" and this feature gave the chance to carry it over a truck where there is biomass and energy is needed.

During the years, many upgrades have followed, and the ultimate APL small-scale plant is the Power Pallet 30 (PP30). The machine is shown in Figure 13 and it still consists of an Imbert type gasifier, a gas filtration and cooling stage and an internal combustion engine that is capable of 25 kW_e and almost 40 kW_{th}.

The PP20 and PP30 are the basis of the researches reported in this thesis and will be described in more detail in the following chapters.

1.4.7 Summary

In the previous paragraphs the most diffused biomass-to-syngas conversion technologies are shown. It is clear, even from these few but representative examples, how fluidized bed reactors are confined to medium/large scale

[2] Despite the other gasifiers here shown, in the Power Pallet series the feeding of the biomass and the discharge of the ashes/char is done manually.

applications and are often coupled to ORC or steam generation systems for both thermal and electrical power production via turbine expansion. Fixed bed gasifiers find place in small-scale power plants instead and are often coupled with internal combustion engines.

Although syngas production can be used for energy generation in systems that are technologically very distant from each other, every biomass gasification power plant can be divided into four main areas: feed pretreatment (chipping/pelletizing and drying the biomass), gasifier, gas conditioning (cooling and clean-up), and a turbine or engine to generate heat and power.

The main difference between large and small-scale power plants lays in the chance, for the former, to afford advanced pre-processing, gasification and gas conditioning technologies. The power plant of Güssing is an example of how large-scale biomass gasification is technically feasible but strongly related to feed-in tariffs. In small-scale gasification systems, the technical feasibility is still a challenge, but the smaller size has several advantages that will be described in the next paragraph (Hrbek, 2019).

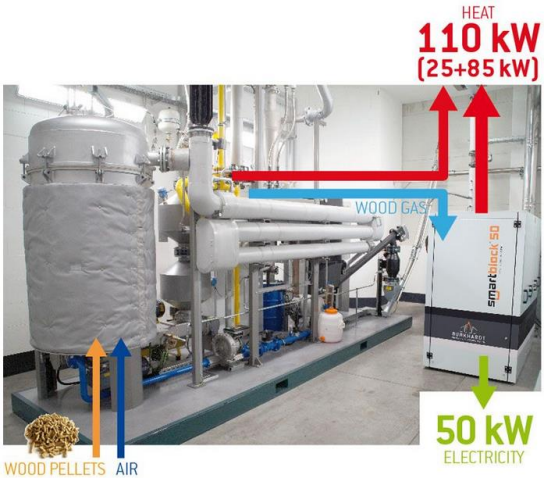

Figure 12. Burkhardt 50 kW_e gasification system (Burkhardt website)

Figure 13. Power Pallet 30 (All Power Labs website)

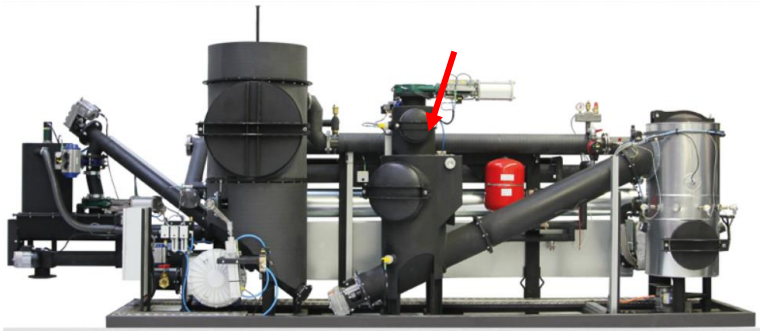

(a)

(b)

Figure 14. Spanner HKA 35[3] (a) and ESPE Chip 50[4] (b) biomass gasification power plant. Red arrow indicates the tube-in-tube HX.

[3] Image from the link https://www.holz-kraft.com/images/produkte/holzvergaser.png
[4] Image from the link http://www.espegroup.com/biomassa/cogeneratore-a-biomassa/

1.5 Why small-scale gasification power plants?

Biomass for thermal gasification is mostly used in medium/large-scale power plants (> 150 kW_e) for heat and power generation via IGCC or steam generation processes. As seen, these processes lead to high electrical conversion efficiencies up to 40% in IGCC cycles. Drawbacks of large-scale power plants lay in the feedstock supply: these plants often use biomass from farmed sources which leads to a competition of bioenergy with the food sector (Nuss et al., 2013 as cited in Ahmed et al., 2019) and, secondly, large power plants require tons of biomass per hour which is only available in large geographic areas around the plant (100-150 km radius). The logistics and transport have then a significant influence on the feedstock costs for large-scale power plants and on the total carbon dioxide emission of the power plant (Rüegsegger et al., 2018).

In the context of a circular economy, the waste-to-energy approach is the most promising alternative to biomass farmed source. Biomass waste residues can derive from tree trimming, forest fire risk reduction, wood-borne pest remediation and from the pruning process of fruit tree or vineyards. It is estimated that the potential of wood waste can cover up to the 70 % of the current use of biomass for energetic purposes (Langholtz et al., 2016 as cited in Ahmed et al., 2019) but since most of the waste biomass is geographically dispersed is not economically convenient its harvesting and transportation to large-scale power plants. For this reason, most of the times, the biomass is left to decompose, or it is burned in open piles. This is the case of vineyards in Italy that produce around 2500 tons/year of pruning whose are often disposed via direct in-situ combustion or shredded and left on the field for natural decomposition (Ruiz et al., 2013; Ntalos et al., 2002).

Both open burning and decomposition are unable to recover the huge amount of energy obtainable using residual biomass as fuels and moreover lead to the production of a series of pollutants and greenhouse gases (GHG) that include CO_2, CH_4, CO, NO_x, SO_x, particulates, volatile organic compounds and CO_2, N_2O and CH_4 respectively (Akagi et al., 2011; Petrov et al., 2017; Permadi et al., 2013 as cited in Ahmed et al., 2019). In Table 4 a comparison in terms of pollutants emission between the different pathways of biomass usage is shown. It can be noted how decomposition and open burning lead to the highest values of equivalent emitted CO_2 into the atmosphere.

In this inconvenient scenario, small-scale gasification power plants can provide economically and environmentally competitive alternative and generate heat and power from wood-waste biomass, reducing the GHG emissions by as much as 58 % compared to other pathways for biomass disposal (Campbell et al., 2010 as cited in Ahmed et al., 2019).

Table 4. Mass emission comparison for various path of biomass usage on a dry mass basis compared to small-scale gasification power generation (Well-to-Wheels Analysis, 2011; Akagi et al., 2011; Wihersaari, 2005; Sinha et al., 2004; Bhattacharya et al., 2002; Christian et al., 2003; Aurell et al., 2015; Liu et al., 2014; Yokelson et al., 2011; Ozgen et al., 2014 as cited in Ahmed et al., 2019).

Pathway	CO_2 (kg/kg)	NO_x (g/kg)	CO (g/kg)	CH_4 (g/kg)	Soot (g/kg)	N_2O (g/kg)	CO_2e (g/kg)
Open burning	1.62	2.9	97.2	4.6	15.5	–	1888
Residential	1.56 – 1.62	0.05–2.7	19–154	6–10	1.2–10	–	1740–2112
Decomposition	1.74	–	–	33.3	–	0.04	2584
IGCC turbine	1.84	0.17	0.16	0.07	0.05	–	1841
Steam turbine	1.83	1.13	5.82	0.6	2.57	–	1854
Small-scale gasifier	1.34 – 1.60	1.6–3.6	9.6–21.6	8.6–13.3	0–0.26	–	1570–1966

The advantages of gasification technology applied to residual biomass are multiples:

- The feedstock necessary to operate small gasifiers can be harvested from local areas and the energy generated can be entirely used by the local community reducing the economic issue of power dispatching over the grid and promoting the emergence of new job opportunities. In Figure 15 and Table 5 it is shown the comparison, in terms of CO_2 emitted, of the different conversion path considering the impact of the transportation over the total amount of CO_2. Giving a different point of view respect of Ahmed et al., 2019, these data shown not that gasification is convenient respect of open burning if the biomass is harvested within 25 km of radius from the plant. But that biomass gasification is always convenient respect of open burning (that does not generate useable heat or power) and, if the transportation stays within 25 km of radius, small-scale power plants generates the possibility to store CO_2 through the biochar and gain lower emissions as briefly explained below.
- Small scale gasification systems often use fixed-bed downdraft reactor which lead to the formation of low PAH[5]-content biochar[6] as byproduct

[5] Polycyclic Aromatic Hydrocarbons

[6] During the reduction phase of the gasification process, the pyrolytic gases are forced to pass through the bed of char at the bottom of the reactor where the temperatures are around 600-

of the gasification process. This highly porous material consists of 80-90 %wt of recalcitrant organic carbon that can be used as soil amendment to mitigate GHG emissions acting as a very stable carbon storage. Moreover, it has recently received increased attention due to its capability of improving soil fertility and water holding capacity (Wang et al., 2017; Coninck et al., 2018). To sum up, the win-win-win scenario offered by the biochar is the opportunity to pump atmospheric CO_2 into the soil, increasing the soil properties and the productivity of the rural areas around the power plant.

- The implementation of CHP systems on small-scale gasification units allows to design the plant to fulfill the seasonal thermal load request of the local community.

Table 5. Modified biomass emission factors including feedstock preparation (adapted from Ahmed et al., 2019).

Pathway	CO_2 (kg/kg)	NO_x (g/kg)	CO (g/kg)	CH_4 (g/kg)	Soot/PM (g/kg)	Total CO_2e (g/kg)
IGCC turbine (160 km)	1.9	0.37	0.2	0.07	0.054	1902
Steam turbine (160 km)	1.89	1.33	5.9	0.6	2.58	1914
Small-scale gasifier (16 km)	1.36–1.62	1.7–3.7	9.7–21.7	8.6–13.3	0.01–0.27	1590–1987

700 °C. If the char is extracted from the reactor at temperatures lower than 400 °C, part of the heaviest tars contained into the gas stream may be absorbed within the char porosities leading to formation of char with high level of PAH. If this situation is avoided by extracting the char at higher temperatures, and the levels of PAH are lower than 6-20 mg kg^{-1} (IBI, 2013 as cited in Wang et al., 2017) the char can be defined biochar, be safe for human health and be used as soil amendment.

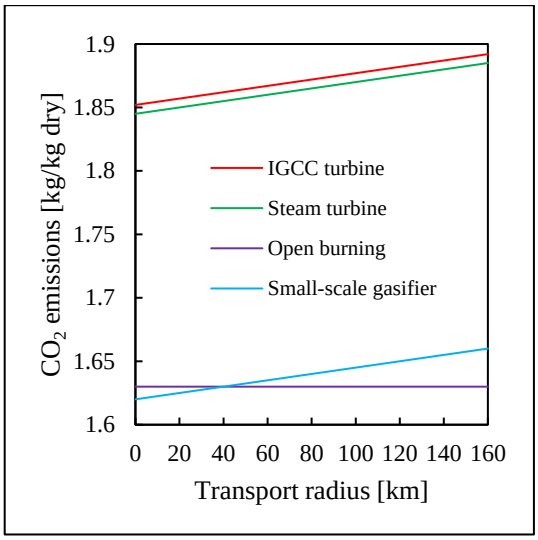

Figure 15. CO_2 emissions factor of four biomass pathways as a function of biomass transport distance (adapted from Bridgwater, 1995 and Ahmed et al., 2019).

On the other hand, small-scale gasification power plants are penalized by several factors:

- Lower electrical efficiencies if compared to large plants that ranges from 10 to 20 % for plants < 50 kW_e (Bsiht et al., 2019; Bridgwater et al., 2019).
- Higher cost per kW_e of installed power: IGCC power plants ranges from 1500 to 1800 €/kW_e while small gasification systems are around 2800 €/kW_e (Wei et al., 2009).
- As shown in Figure 16, for gasification facilities the operating cost is the major part of the total cost and small plants are associated to an increased labor cost. This is often generated by the incapability of small plants to afford sophisticated automation systems and by the necessary and daily-based maintenance of the syngas filtration system (Wei et al., 2009).

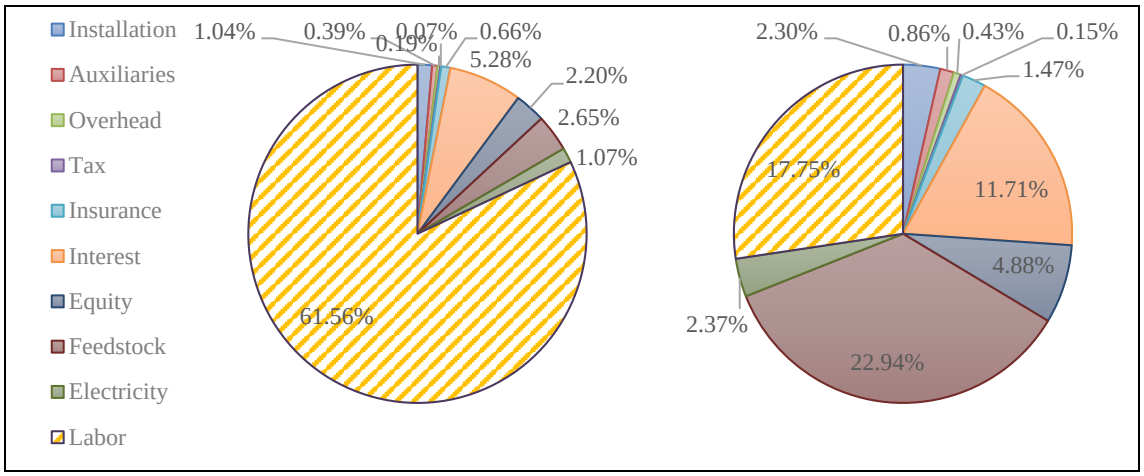

Figure 16. Annual production cost composition for a 20 kW_e (a) and a 800 kW_e (b) power plants (adapted from Wei et al., 2019)

Small-scale gasification systems can thus be the key to exploit the residual biomass energy potential, offering a carbon-negative technology that can play a fundamental role in GHG emission reduction. These plants cannot however be applied in every context and their installation must be preceded by a careful analysis of the quantity of biomass available in a narrow radius, together with the certainty of being able to use thermal and electrical energy on site. The labor cost is the most significant contribution to annual costs in small-scale applications, meaning that they can even be a reason for the formation of new job opportunities but also that their maintenance operations should be made as simple and quick as possible. Concluding, in small gasification power plants most of the development work should be concentrated in balancing cost, effectiveness and maintainability of the filtration stages and in this work will be studied different technical solutions aiming for this goal.

Chapter 2

Syngas conditioning

2.1 Introduction

Syngas conditioning can refer to different strategies depending on the context in which it is used:

- Devi and Park use the term conditioning referring to the gas reforming processes that lead to the decomposition of tar into non condensable gases (Devi et al., 2002; Park et al., 2010 as cited in Savuto et al., 2019).
- Other authors extend the concept of syngas conditioning to hydrogen separation and carbon dioxide elimination in order to obtain high quality syngas to be used in fuel-cell or Fischer-Tropsch synthesis (Dagle et al., 2011; Richardson et al., 2012; Stevens, 2001).

These processes are generally confined to medium-large scale gasification power plant and often included into the larger group of syngas *upgrading* techniques. For this reason, in this work the term conditioning is used according to Rakesh (2011), Risnes (2018) and Kirkels (2002) interpretation, that is, describing all the processes and treatment necessary to use the producer gas inside ICEs. Conditioning strategies can be subdivided into syngas cooling and cleanup systems that will be reviewed in the following and are taken up in the body of this thesis work investigating new approaches.

2.2 Syngas cleanup

In the decades, many efforts were destined to the design and study new gasifier concepts to directly reduce the contaminants contained in the raw gas. An example of this is the Viking gasifier (Henriksen et al., 2006) for which a partial combustion enables the tar reduction down to 15 mg Nm^{-3}, or the Fraunhofer ISE gasification process that generates producer gas with a tar content less than 50 mg Nm^{-3} (Burhenne et al., 2013 as cited in Heidenreich et al., 2015). The drawbacks of these benchmark systems are their complexity and high cost.

For this reason, many gasifier producers focused on the design of simpler and cheaper reactors, obtaining tar and particulate content in the raw gas between

0.15-1.00 g Nm^{-3} (Sandeep et al., 2014; Salzmann et al., 1996 as cited in Rakesh et al., 2018). As reported in Table 6, these contaminants concentrations are not suitable for end-user applications and, hence, gas cleanup and conditioning systems are required to meet those targets.

Table 6. Final tar and particulate concentration in syngas applications for power generation

Application	Concentration (mg Nm^{-3})		Reference
	Tars	Particulate	
Steam turbine	No limit specified[7]	No limit specified	Stevens, 2001 and Milne et al., 1998
Internal combustion engine	< 30	$< 50 \div 100$	Milne et al., 1998
	< 50	< 100	Richardson et al., 2012
		< 50	Abatzoglou, et al., 2000
Gas turbine		< 30 (PM5)	Richardson et al., 2012
			Abatzoglou, et al., 2000
	< 5	< 15 (PM5)	Milne et al., 1998
Fuel cell	< 0.1		Richardson et al., 2012
	< 1		Milne et al., 1998
		< 0.02	Stevens, 2001

Gas cleanup technologies can be divided either by the position respect to the gasifier, or to the temperature range of the filtration process.

In the first case, cleanup approaches can be defined as *primary* if the raw gas pollutants are minimized within the gasifier, or, *secondary* if the cleanup is made downstream the gas making facility.

In the second and most diffused case, filtration technologies are classified in hot gas cleanup (HGC), warm gas cleanup (WGC) and cold gas cleanup (CGC). Since, the definitions hot, warm and cold are ambiguous, a more rigorous separation between the different filtration strategies can be based on the condensation temperatures of the different compounds (Woolcock et al., 2013). This allows to determine which categories of pollutants will be collected in the filtering stage and to understand the state of the contaminants upstream the end-user application (e.g. solid, liquid or vapor phase).

[7] Steam generation is achieved by directly burning the producer gas, the tars and the particulate matter contained in it, in a separated furnace.

According to these criteria, in the following paragraphs a review of the different gas cleanup and conditioning technologies are reported. The attention will be focused only on the two major (in terms of concentration) contaminants of the producer gas: tar and particulate matter.

2.2.1 Hot gas cleanup (HGC)

Hot gas cleanup devices usually operate at temperature higher than 400 °C avoiding the condensation of all the tar vapors contained in the gas stream. The maximum temperature reached by hot cleanup systems can be up to 1300 °C (Korens et al., 2002 as cited in Woolcock et al., 2013) even if most of the application tend to keep the filtration device temperature under 600 °C in order to limit the use of expensive materials (Woolcock et al., 2013).

HGC systems are mainly focused on the reduction of tar and particulate matter from the producer gas and first devices were applied to fluidized bed combustors (Lyczkowski et al., 2002) in the early '70 due to the more stringent environmental standards. The increasing knowledge on these systems has led to the development of solutions not only related to syngas combustors but also to biomass power plants for power generation.

Following the approach of Woolcock, the discussion is divided into particulate matter removal and tar removal underlining the different approach and devices currently available.

2.2.1.1 HGC - particulate matter removal

HGC technologies for particulate removal are based on three different physical principles:

- Inertial separation
- Barrier filtration
- Electrostatic interaction

and has been continuously improved in the last three decades obtaining important improvement in commercial syngas applications.

Cyclones (Inertial separation)

Cyclones are devices that exploit the mass and acceleration of solid particles to separate them from a gas flow. These are the most common, cheap and oldest devices for solid separation which utilize centripetal acceleration to decrease the time needed by the particle to settle down (Woolcock et al., 2013).

The balance between particle drag force and centrifugal force defines the *cut point* of the cyclone at which, a particle of that size, has the 50% of chances to be captured by the swirl flow and then collected (Hoffman et al., 2008).

Despite their robustness, conventional cyclones have a collection efficiency (referred to particles diameter greater than 5 µm) slightly higher than 90%, restraining these devices usually as a first stage of a more complex filtration system.

Relatively new cyclone designs, studied with the aid of CFD software, reached collection efficiencies greater than 99.6% (Salcedo et al., 2002) making them competitive with other filtrating devices, such as bag filters, that are though limited in temperature.

Multi-cyclone configuration is possible, enabling the capability to collect almost the 90% of PM as small as 0.5 µm with the drawback to be economically not feasible for large volume gas streams (Hoffman er al., 2008 as cited in Woolcock et al., 2013).

Other options such as dust agglomerates and impact separators are based on the same principle of cyclones and are widely discussed in Atimtay (2001) and Cummer (2002) works.

Ceramic and metallic filters (Barrier filtration)

These devices are usually formed by a rigid metal mesh or a porous ceramic media and guarantee collection efficiency over 99.99% at operating temperatures higher than 400 °C (Sharma et al., 2008; Channiwala et al., 2002). Ceramic filters are usually built as candles, where the dirty gas enters radially from the outer part of the porous media and reaches the hollow inner tube. PM build up on the external surface of the ceramic candle generating a layer called “filter cake” which acts as further filtration barrier increasing both the filtration performances and the pressure drop. For the latter, the filter cake needs to be removed time by time in order to maintain the fluid-dynamic efficiency of the gasification facility. One of the filter cake removal methods is to use a pulse jet of inert gas (e.g. nitrogen, carbon monoxide or the same compressed producer gas) to a cleaning shock wave. The drawback of this solution is the thermal

shock, to which the candles are subjected, that shorten their life cycle (Sharma et al., 2008).

To overcome this issue, metal foam and metal mesh filters can be adopted. The structure of a metal filter is less sensitive to thermal shock, especially if metal fibers are used instead of foams (Gardner et al., 2005 as cited in Woolcock et al., 2013).

Granular bed filters (Barrier filtration)

In this filtration devices, the raw gas, rich in particulate, flows through a granular material placed in a vessel. Bed particles generally are spherical and have dimensions of 1 mm (Stanghelle et al., 2007) but other applications of bigger particles can be found in literature (Macìas-Machìn et al., 2006). Typical material for granular bed spheres is limestone, sand, sintered bauxite, alumina and mullite.

These filters can operate up to 870 °C with collection efficiencies above 99.9 % (Smid et al., 2005 as cited in Woolcock et al., 2013) that, combined with the possibility to incorporate adsorbents and catalyst in the bed material, make them promising for high temperature and low maintenance applications.

Electrostatic precipitators (ESP)

The electrostatic interaction between the particles and the gas can be used to lower the particulate concentration in the syngas. The operating principle of ESP lies in the generation of a strong electric field in which the particle-laden gas is forced to pass through. The solid particles become charged when they enter in the electric field and are removed due to their difference in dielectric properties compared to the gas molecules (Lloyd, 1988, as cited in Woolcock et al., 2013).

The collection efficiency of ESP can be up to 98% (McDonald, 1982 as cited in Woolcock et al., 2013) and it is strongly influenced by the resistivity of the particle material and the operating temperature.

Decreasing the resistivity, the collection efficiency increases and increasing the temperature the ESP efficiency tends to decrease. For this reason, ESP can find application up to 400÷450 °C (McDonald, 1982; Lloyd, 1988).

2.2.1.2 HGC - tar removal

At high temperatures, four different paths can be followed to remove or reduce the amount of tar in the producer gas: thermal cracking, catalytic cracking, non-thermal plasmas and physical separation.

Thermochemical equilibrium

The first three approaches of tar reduction trying to restore the thermochemical equilibrium of gasification reactions. Since tar conversion efficiency is directly correlated to the process temperature, thermal cracking is based on the generation of a high temperature zone (1000÷1300 °C) to decompose large organic compounds (Han et al., 2008; Tregrossi et al., 1999 as cited in Woolcock et al., 2013). Catalytic cracking aims at reducing the activation energy of decomposition of tar compounds, allowing lower process temperatures (Woolcock et al., 2013). Non-thermal plasma process generates atmospheres of free radicals, ions, and other excited molecules that can initiate decomposition of tar molecules (Pemen at al., 2003 as cited in Woolcock et al., 2013).

Physical separation

All the tar vapors are in vapor phase at temperatures above 450 °C. In order to remove tar using physical methods such as ESP and inertial separation devices, the temperature need to be lowered below 450 °C to allow the partial condensation of the heavier ones that form an aerosol. Since the dew point of tar compounds ranges between 80 and 450 °C it is not possible an efficient separation of those at high temperature and, thus, HGC processes have limited collection efficiency (Stevens, 2001; Zanzi et al., 1996 as cited in Woolcock et al., 2013).

2.2.2 Cold gas cleanup (CGC)

Cold gas cleanup systems operate at temperature lower than the ambient air dew point and, for this reason, are also called wet processes. Liquid adsorbents are used in wet systems, to remove syngas contaminants, maintaining the operating temperatures between 10 °C (when the adsorbent liquid is water) and -62 °C when methanol is used (Korens et al., 2002 as cited in Woolcock et al., 2013). The low process temperature hides the shortcoming to decrease the thermal efficiency of the overall gasification process but, when the syngas is used

in volumetric applications (e.g. ICE), the increase of volumetric efficiency of the application can mitigate this penalty.

2.2.2.1 CGC – particulate matter removal

Water scrubbing is the main method for particulate removal at ambient temperature. The simplicity and effectiveness of this process led to the design of different devices based on this principle.

Spray scrubbers

In spray scrubbers, the gas is passed in a chamber where spray nozzles or atomizer disperse the adsorbent liquid in co-current or counter-current way. The large surface area increases the chances of impaction of the particulate contained in the gas stream. The PM collection efficiency of spray scrubbers is above 90 % for PM5 and around 40 % for submicron particles (Schifftener et al., 1996 as cited in Woolcock et al., 2013).

Wet dynamic scrubbers

In dynamic scrubber, the mixing between water droplets and particle-laden gas is enhanced by means of spinning fans. The inertial impaction is then increased reaching collection efficiency of 95 % for PM5 and between 60 to 70 % for submicron particles (Woolcock et al., 2013).

Cyclonic scrubbers and impactors

Cyclonic scrubbers' acts following the cyclonic principle with the addition of water spray at the inlet, while, in impactors, the gas is forced to pass through a series of perforated trays continuously washed by the adsorbent liquid. Such devices are almost not effective on submicron particles but can reach 98% of collection efficiency for particle greater than PM5 (Schifftener et al., 1996 as cited in Woolcock et al., 2013).

2.2.2.2 CGC - tar removal

The solubility of tar in the adsorbent material plays a crucial role in tar removal for CGC processes. When water is used in wet scrubbing devices, non-soluble tar condenses by coming into contact with water and can be physically separated

from the water using settling tanks or filter meshes. Other lighter tars, such as phenol, condenses as well but, being soluble in water, cannot be easily separated and, accumulating time by time, reduces the effectiveness of the adsorbing liquid. Moreover, the generated wastewater cannot be discharged to the environment and need to be chemically/biologically treated before the disposal, increasing the maintenance costs of the power plant (Woolcock et al., 2013).

2.2.3 Warm gas cleanup (WGC)

Cold gas cleanup systems offer a high collection efficiency of both particulate matter and tar, adding fixed costs of plant management. This strong shortcoming can be avoided using cleanup processes that work above the water vapor dew point allowing to some tar and other contaminants (chlorides and alkalis) to be anyway condensed and removed from the raw gas (Woolcock et al., 2013).

2.2.3.1 WGC – particulate matter removal

Some of the solutions available for the HGC systems, such as gas cyclones and ESP, can be applied to particulate removal even at temperature slightly higher than ambient (80÷250 °C). Fabric filters is the third option that can be applied only in this temperature range and will be discussed in the following.

Fabric filters

Fabric filters (also called bag-house filters) are often used in gas-solid separation, since they are easy to use, relatively cheap and highly efficient in collecting particles (Song et al., 2006 as cited in Tambe et al., 2011). Those filters are usually formed by fibers, that can be woven or non-woven (e.g. felt), and operate according to the principle of barrier filtration that is subdivided into three different mechanisms of particles removal:

- Inertial impaction: particle-laden gas is forced to pass through the porous of the fabric and, when a particle is enough large, its inertia prevents it from turning around the fiber and escape. The particle will proceed straight impacting the fiber's surface.
- Direct interception: for medium-sized particles, the inertia is too low to generate the impaction but can be sufficient to divert their trajectory making them sticking to the side wall of the fibers and being thus intercepted.

- Diffusion: for submicron particles, Brownian motion becomes strong in defining the random trajectory of each particle that can collide with a fiber and be collected.

Bethea, 1978, proved that almost the 99% of particle greater than 1µm are collect through inertial impaction and direct interception. Often, in bag-house filter devices, an inlet plenum is required to distribute the flow across several bags; in this case, very large particles (hundreds of microns), can be collected on the bottom of the plenum by effect of gravitational force (Beachler et al., 1995).

At the macroscopic level, the filtration process can proceed following three different phases.

The first one, called *depth filtration*, is characterized by the retaining of the particulate matter between the fibers and takes place at the beginning of the process, when the bags are clean. During filter operation, the collected particles increase the surface of the fibers, by adding a sort of dendrites that act as new collecting elements. In this phase the pressure drop generated by the fabric filter start to increase. Eventually, when the space between the fibers is almost saturated, a particle layer starts to buildup on the bag's surface, creating the so-called *filter cake*. This is the *surface filtration* mechanism and it is the most effective but has the drawback of generating high pressure drop over the filtration stage (Song et al., 2006).

For this reason, the filter cake needs to be reduced (Callè et al., 2002) or removed over time and the most common technique are mechanical vibration, reverse air flow and pulse jet (Mao et al., 2008).

Successful and reliable gasifier-engine systems can be operated using these filtration systems (Breag, 1982; Kjellstrom, 1981 as cited in Reed et al., 1988).

According to the fabric material, the collection efficiency of filter bags ranges from 99 to 99.9 % (Fritz et al., 1990 as cited in Hasler et al., 1999) for even submicron particle scales. Several studies report the difficulties generated by tar condensation while using barrier filtration device at temperatures below 500 °C (Risnes, 2002). This study proves that barrier filtration can be adopted even at temperature slightly above 50 °C.

2.2.3.2 WGC - tar removal

The advantages of warm-gas-cleanup techniques lay in the good collection efficiency of tar, if compared to HGC systems with the advantage of not generating tarry water. At WGC operation temperatures, most of the heavier tar can condensate or be adsorbed by the particulate matter suspended in the

gas stream. For this reason, it is difficult to separate the filtration of tar and PM properly because often happen at the same time.

In the literature, the most important WGC tar filtration approach is the OLGA technique (Raveendran et al., 1995) which is an oil-based gas scrubber that remove and reuse valuable tar compounds without generating wastewater. The process works between 60 °C and 450 °C, with 100% of collection efficiency for heavy tar and 99% for the lighter compounds such as phenols and 1-2 ring aromatics.

OLGA based filtration stage is currently operational in several gasification facilities, up to 800 kW of thermal power (Rabou et al., 2009; Han et al., 2008 as cited in Raveendran et al., 1995).

2.3 Syngas temperature control

Syngas is generated by the gasification reactor at temperatures that can exceed 800-1000 °C (SERI, 1979; Lozza, 2017) and it has been shown how it needs to be properly cooled down according to the chosen cleanup technology. The most effective cleanup strategy, for small-scale application, lays in the combination of hot and warm gas cleanup devices (Reed, 1988; SERI, 1979). In this way, it is possible to benefit from the advantages of separating each contaminant at the right temperature. In fact, the HGC processes are effective in particulate matter removal, leaving tar in vapor phase, while, WGC systems are more effective in heavy tar collection leaving the water in vapor phase, thus not generating tarry water.

Moreover, when the end-user application of a gasification power plant is the heat and power generation through an ICE, the final syngas temperature need to be low enough to not affect the volumetric efficiency of the engine and, thus, the overall performances of the power plant (SERI, 1979).

Many technologies have been developed during the World War II to cool down the wood gas in portable gas generators. All these systems used the ambient air as cooling fluid and, thus, were often placed in front of the vehicle in order to exploit its movement for the cooling. Some of these technologies include:

- *Baffle plates coolers*: often used in early portable gasifier prototypes, they consist of a metal pipe with a series of orthogonal perforated plates welded inside. The particle-laden gas is forced to pass through the misaligned holes and changing its direction several times, the dust particles are then removed according to the inertia principle. The external surface area of baffle plates systems is exposed to the flux of ambient air and they also acts as gas coolers (Figure 17).

- *Finned coolers*: also called radiators, they have higher performances compared to the previous ones, but they need cleaner gas. Filtration devices need to be installed upward this kind of systems. They consist of a series of finned tubes, where the gas passes through and it is cooled down by the air that flows across the heat exchanger panel. Often, a catch can for water condense were placed on the bottom of these devices and the condensed tarry water served as a producer gas scrubber to clean it even more (Figure 18). Water was often sprayed on the external surface of the HX to increase the heat transfer coefficient under high engine load conditions.

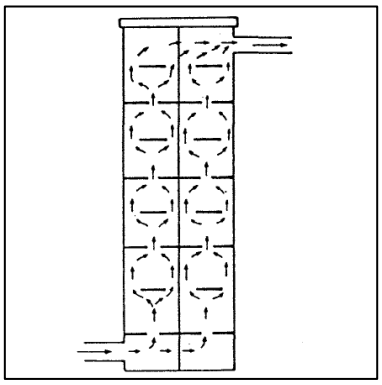

Figure 17. Baffle plates heat exchanger (SERI, 1979).

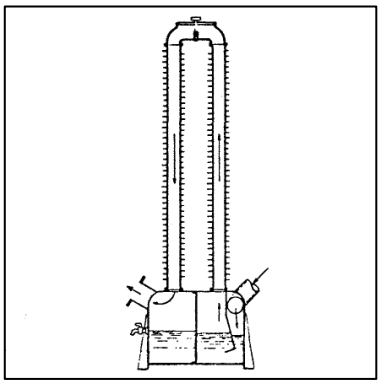

Figure 18. Finned tubes heat exchanger (SERI, 1979).

If during WW II more than one million of cars were fueled with wood and charcoal portable gasifiers (FAO, 1986), nowadays the interest in biomass gasification has shifted towards combined electrical and thermal energy production by means of stationary engines. In such power plants the quantity of recoverable heat from gas cooling is not negligible (Lozza, 2017) and, to make it more available for end-user application, water is often use as cooling fluid instead of ambient air.

Water cooled systems for biomass gasification power plants are based on different technologies:

- *Tube-in-tube heat exchanger*: it is the simplest version of heat exchanger and it consists of two concentric tubes where the two different fluid passes through. Two configurations are possible according to the relative velocity of the fluids: co-current and counter-current. They are often used in small-scale biomass gasification power plant (e.g. Spanner HKA 35 (Holz-Kraft website) and ESPE CHiP50 (Espegroup website)) due to their simplicity and low maintenance costs. The small heat exchange surface area make them not suitable for compact applications even if heat

transfer enhancement can be improved by means of differend kind of inserts such as twisted tapes (Vashistha et al., 2016; Eiamsa-ard et al., 2010; Bhuiya et al., 2013; Chokphoemphun et al., 2015 as cited in Zheng et al., 2020). Usually, in biomass power plant, the hot producer gas flows in the inner tube while the cooling fluid (i.e. water) flows in the annular section.

- *Tubes-in-shell heat exchanger*: it consists of a baffled cylindrical shell which contains a series of tubes. Usually the cold fluid flows in the shell and the hot fluid in the tubes. Several configurations are available according to the number of baffles placed in the shell and according to the number of passages of the tubes in the shell. Even if the 90% of industrial heat exchange applications use tubes and shell technology (Zheng et al., 2020), for small-scale biomass power plant this solution is less common than the simpler tube-in-tube due to the higher complexity and cost. However, this technology allows high flexibility, more compact design (Wang et al., 2016 as cited in Zheng et al., 2020) and it can be found in the Power Pallet 30, a small-scale biomass generator from All Power Labs (All Power Labs website). In this version, the hot fluid (i.e. the raw producer gas) flows in the shell, across the baffles, and the cooling water flows in the rack of tubes. This configuration was implemented in order to increase the heat exchange surface area between the two fluids, by both reducing the diameter of the cooling tubes and increasing their number.
  When it is the raw gas that flows into the tubes, the minimum diameter of those is limited to a lower value to reduce the clogging phenomenon due to syngas contaminants. This configuration is thus less compact than the previous one, but it has several advantages that are discussed in Chapter 5.

2.4 Gasifier-engine coupling

Producer gas technology is useful to convert biomass into mechanical, thermal and electrical power by means of an internal combustion engine. Given the stringent limits on the concentration of contaminants in the producer gas (see Table 6), updraft and fluidized bed are unsuitable for engine application in small-scale plants and, thus, many commercial applications use downdraft technology (Susatriawan et al., 2017).

Due to the mass diffusion of engines for vehicle application, they are often adopted in small-scale gasification power plant, going toward a necessary conversion and modification of some components according to the engine architecture.

The mechanical power output of an internal combustion engine is described in Eq. 2.4.1 (Allesina et al., 2015b)

$$P = \rho_{air} V_d \lambda'_v \eta_i \eta_o \eta_{th} \frac{K_v}{\alpha_s} \phi \frac{n}{2} \tag{2.4.1}$$

where P is the mechanical power [kW] at the engine shaft, ϱ_{air} is the air density in the intake manifold [kg m^{-3}], V_d is the engine displacement [m^3], λ'_v is the engine volumetric efficiency [ad], η_i [ad] is the indicated engine efficiency [ad], η_o is the mechanical efficiency, η_{th} [ad] is the thermodynamic efficiency, a_s is the stoichiometric ratio [ad], K_v is the fuel calorific value [MJ kg^{-1}], Φ is the equivalence ratio [ad] and n is the engine revolution speed [rad s^{-1}].

As shown in Eq. 2.4.1 the engine power output is directly proportional to the air density and, hence, in spark-ignition engines the load is controlled varying the *quantity* (i.e. the density) of the fuel mixture by means of a single or multiple throttle valves upstream the intake manifold.

When an ICE is connected to a gasifier, its pumping work is exploited to draw the syngas from the gasifier and, at the same time, the engine needs to draw also the air necessary for the stoichiometric combustion of the mixture. The gasifier is a complex system that generates a considerable pressure drop and affects the parameter λ'_v by reducing it from 0.96 of naturally aspired gasoline engine (Heywood, 1988) to less than 0.80 (FAO, 1986) on producer gas operation.

The parameter a_s indicates the mass ratio between the fuel and the air for combustion at stoichiometric regime. For gasoline fueled engines this value is 14.7 while for producer gas ranges from 1.1 to 1.4 (FAO, 1986; Allesina et al.,

2015b) which means that for each kg of drawn producer gas, the engine needs to aspire 1.1 kg of ambient air to provide stoichiometric combustion.

Power derating of automotive spark-ignited engine converted to syngas fuel is calculated to be in the order of 40 % (Allesina et al., 2015b).

Due to the low value of a_s, the fuel flow rate cannot be governed by a Venturi device as can be for CNG or LPG engines (Reed, 1988) but it needs a secondary throttle valve as shown in Figure 19.

The secondary air throttle is feedback controlled by an oxygen sensor installed in the engine exhaust manifold and it governs the quantity of mixing air maintaining the set equivalence ratio (which is respectively equal to *1*, *<1* or *>1* at stoichiometric, lean and rich mixture conditions).

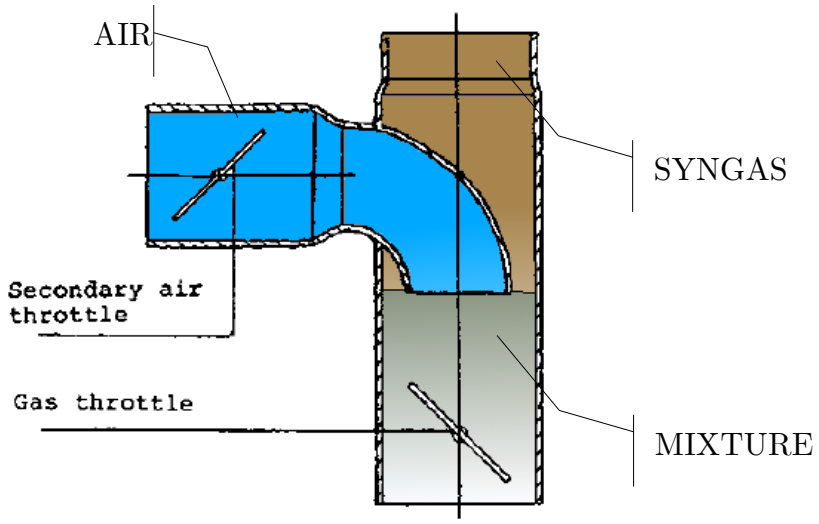

Figure 19. Air-fuel mixer for syngas engine operation (adapted from FAO, 1986 as cited in Morselli, 2012).

As will be shown in the next chapter, the mixer represent a crucial point for tar and water condensation due to the temperature of the air, often lower than the dew point of the producer gas (50÷60 °C as mentioned in SERI, 1979). A safety filter is often installed after the mixer and right upstream the engine to collect condensates, if present (examples are SPANNER and AllPowerLabs power plants).

Chapter 3

Multi-phase fluid dynamic of syngas flow across a throttle body in a gasifier-engine system

3.1 Introduction

In a gasifier-engine system for stationary application, the engine throttle is a fundamental part of the power plant because it controls the speed of the engine, maintaining it at the value required for electrical energy production, usually set to 1500 or 3000 rpm for small-scale generators (Glover et al., 2012).

The way the throttle works is well known in literature and consists in a variable pressure drop (Ferrari, 1996; Heywood, 1988; Cashco, 2017; Sinaiski et al., 2007). When the gasifier-engine system is used in stand-alone mode, and not grid connected, the throttle became even more important in the power production control due to variable power demand.

While the design developed and perfected during the years in gasoline engines has few or no side issues, its application to syngas-engine systems arises a complete new series of phenomena rarely described in other applications. The major difference between standard liquid fuel and syngas engines lays in the psychrometry of the fuel mixture that is often near saturation, as well as in the presence of particulate and liquid phase pollutants (char, ashes and tars) (Allesina et al., 2015a).

The differences described above result in boundary conditions across the throttle blade that generates unique phenomena of condensation which can slightly modify the engine performance (Sinaiski et al., 2007). In fact, when droplets are generated during the throttling, they cease to move following the perfect laws hypothesis and start to behave accordingly to the high inertia originated by their mass. In such a way a series of unwanted effects may happen i.e. post throttle line fouling, unequal conditions in between the engine cylinders etc.

The first part of this work investigates the previously described phenomena starting from a psychrometric analysis of the fluid conditions upstream the

throttle. The goal of the first part is to find the dew point temperature of water vapor inside the air-syngas mixture flow. The further step taken in this paper consists in a CFD analysis of the temperature drop effects related to high pressure drops across the throttle blade. This model, coupled to the psychrometric one, allows to determine the areas where the temperature drop overcome the pressure drop and condensation occurs.

Finally, a qualitative experimental analysis is set up for a qualitative comparison with model prevision. The tar and water deposition afterwards a throttle body of a gasifier-engine system was assessed to confirm the simulated phenomenon.

Results showed that the coupling of the psychrometric and the CFD models allows a good level of understanding of the phenomenon that occur across the throttle blade in a gasifier-engine system. The awareness about this phenomenon allows a better design of these systems in order to prevent condensation and related issues. This work reports the boundary limits for preventing condensation.

3.2 Materials and methods

3.2.1 Gasification facility description: the PP20

The framework facility of the chapters 3 and 4 is the Power Pallet 20 gasifier by All Power Labs (All Power Labs website). The gasification system is composed of a gasifier, a filtration stage and a spark-ignited internal combustion engine. As shown in Figure 21, the gas making facility consists of an hopper that contains the drying stage, a pyrolyzing stage, named “Pyrocoil” where engine exhaust gases provide the sufficient heat to pyrolyze the biomass, and a gasification stage where biomass, tar gases and pyrolyzed biomass are converted into producer gas passing through combustion and reduction zones. Typical biomasses used in these systems range from wood chips (Malaguti et al., 2017; Allesina et al., 2013) up to agro-industrial waste such as chipped vine prunings (Allesina et al., 2018a), corn cobs (Allesina et al., 2015c), corn stover (Allesina et al., 2014; Allesina et al., 2015d) wood residues from river maintenance (Pedrazzi et al., 2017; Allesina et al., 2018b), solid residues from vegetable oil production (Allesina et al., 2014b), solid residues from cotton crops (Allesina et al., 2018c), municipal green waste (Pedrazzi et al., 2019a) etc.

The gas generated encounters a first cyclonic filtering stage where most of the dust is separated and collected. The gas exiting temperature from the cyclone varies according to the load and it can reach 450 °C. For this reason, the gas is

cooled down using an air/gas heat exchanger with the classic tubes and shell scheme (syngas in the tubes and air in the shell with multiple passages). The gas is cooled down to approximately 100 °C and it flows into the last filtering stage made by a packed bed filter that uses woodchips and char as filtering medium. Once filtered, the gas is mixed with air and the stoichiometric mixture is drawn by the internal combustion engine (GM Vortec 3.0 L) that it is connected to a Meccalte synchronous generator that produces 15÷20 kW_e of electrical power output.

Figure 20. Power Pallet 20 (All Power Labs website).

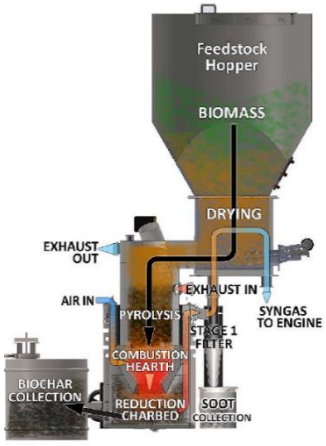

Figure 21. All Power Labs PP20 gas generation unit (All Power Labs website).

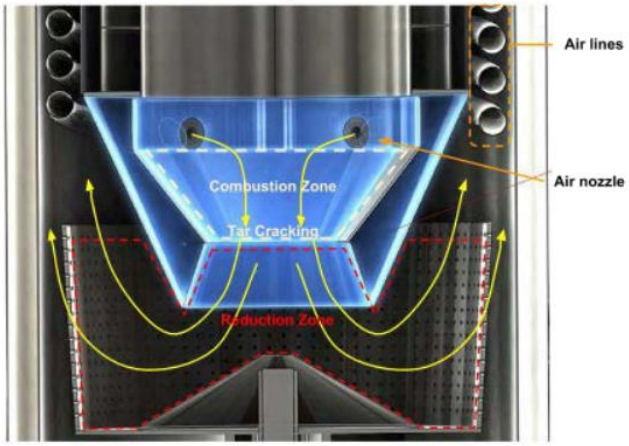

Figure 22. All Power Labs v5 reactor detail (All Power Labs website).

3.2.2 Psychrometric model

The model here implemented has the goal to calculate the dew point temperature of the syngas where condensation of the water vapor occurs. The syngas is

considered as a perfect gas with the composition reported in Table 7. In this model, no tar and particulate matter are considered. Wet syngas composition is derived from the datasheet of the gasifier producer (All Power Labs) considering a molar fraction of water vapor of 0.08 given by a modeling evaluation (Allesina et al., 2015a).

The syngas is mixed with dry air in stoichiometric proportion following the mathematics reported in the work of Allesina et al. 2015b. Table 7 resumes the air-syngas mixture composition.

Table 7. Species mole fraction in syngas, air and stoichiometric syngas-air mixture.

	N_2	H_2	CO	CO_2	H_2O	CH_4	O_2
Syngas	0.42	0.18	0.20	0.09	0.08	0.03	-
Air	0.79	-	-	-	-	-	0.21
Mixture	0.62	0.08	0.09	0.04	0.04	0.01	0.12

In order to calculate the dew point temperature T_{dew} [K] of the mixture, the water vapor partial pressure p_{H_2O} [kPa] is necessary. This can be evaluated using the following equation:

$$p_{H_2O} = n_{H_2O} p_{tot} \tag{3.2.2}$$

where n_{H_2O} [ad] is the water vapor mole fraction in the syngas-air mixture, p_{tot} [kPa] is the total pressure in front of the governor. This pressure was measured in the experiment and the average value at full load is 94 kPa. Eq. 3.2.3 is used to calculate T_{dew} as function of p_{H_2O}. This correlation was achieved interpolating the water vapor data reported in (Cengel, 1997).

$$T_{dew} = 16.8 * \ln(p_{H_2O}) + 6.871 + 273.15 \tag{3.2.3}$$

3.2.3 Geometrical model

A simplified geometrical model was created considering a throttle plate inserted in a straight pipe with internal diameter D of 36 mm. The thickness of the plate s is 0.1 mm. According to the chosen Woodward 36 mm throttle body (Woodward, 2014) a clearance of 0.1 mm is considered between the plate OD and the pipe, resulting in a plate diameter d of 35.8 mm. In accordance with the correct assembly, the plate is fixed to a downstream central pin of 4 mm radius r.

The opening angle ϑ is reported in Figure 23.

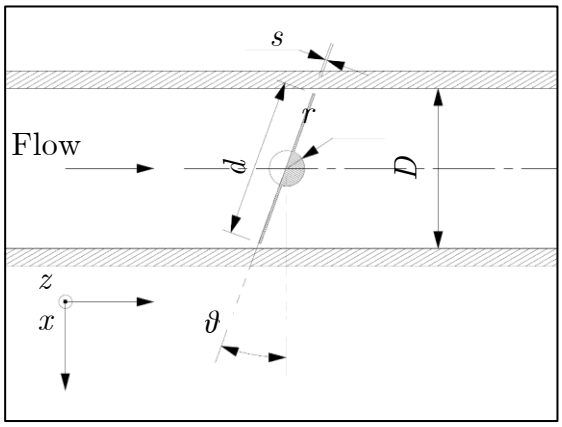

Figure 23. Geometrical model of the throttle body.

3.2.4 Numerical model

Starting from the CAD geometry, a numerical model was created. In this preliminary study, the thickness of the pipe is not relevant since only the internal volume is investigated and all the walls are considered adiabatic, impermeable and satisfies no-slip condition. Considering the x-y symmetry of the problem, it was modeled just a half of the fluid volume as reported, together with the BC's, in Figure 24.

The mixture composition reported in Table 7 is assumed and, for simplicity, a gas with the mean properties of the mixture was considered. Fully developed flow conditions are assumed at inlet and outlet boundary conditions. To ensure this, the pipe was chosen 4.5D long upstream the plate and 14D long downstream it.

Considering the internal combustion engine as volumetric pump, varying the throttle opening angle, the gas velocity at the fluid domain outlet should be

approximately always the same. Therefore, the maximum velocity of the gas V_{max} [m s^{-1}] was calculated through Eq. 3.2.4.

$$V_{max} = \dot{V}_{mix}/A \tag{3.2.4}$$

$$\dot{V}_{mix} = 3.6 * P_{el,max}/(HHV_{mix} * \eta_{IC} * \eta_{GEN}) \tag{3.2.5}$$

$$HHV_{mix} = HHV_{H_2} n_{H_2} + HHV_{CO} n_{CO} + HHV_{CH_4} n_{CH_4} \tag{3.2.6}$$

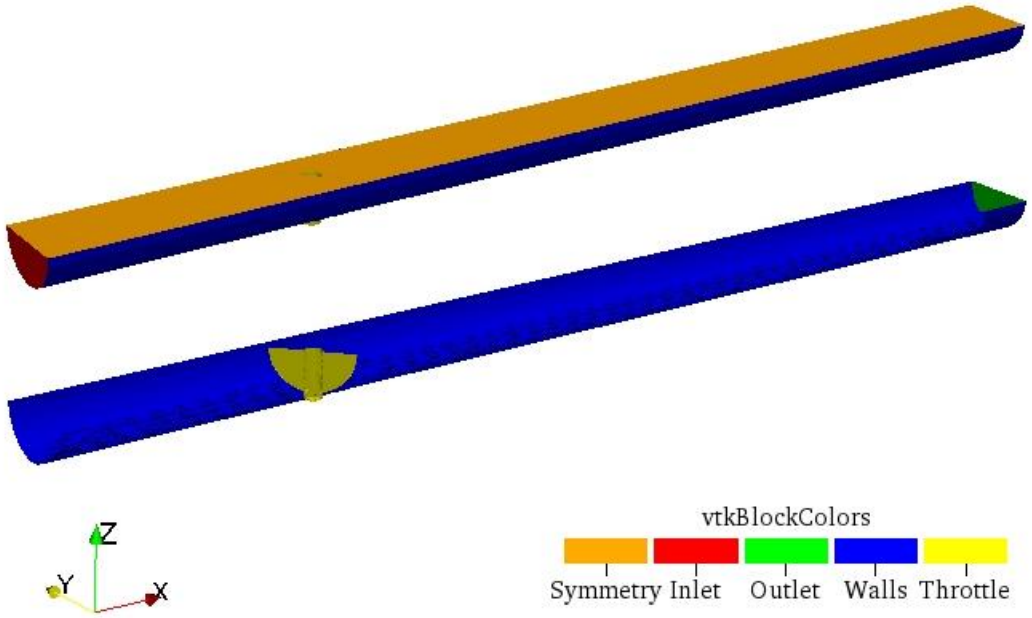

Figure 24. Fluid symmetrical model with BC's.

where $\dot{V}_{mix}$ [Nm^3 h^{-1}] is the volumetric flow of air-syngas mixture, A [m^2] is the throttle area, $P_{el,max}$ [kW] is the maximum electrical power generation (13 kW$_e$ is achieved during the experimental campaign), HHV_{mix} [MJ Nm^{-3}] is the mixture higher heating value, HHV_{H_2} [MJ Nm^{-3}] is the hydrogen higher heating value (Cengel, 1997), HHV_{CO} [MJ Nm^{-3}] is the carbon monoxide higher heating value (Cengel, 1997), HHV_{CH_4} [MJ Nm^{-3}] is the methane higher heating value (Cengel, 1997), n_{H_2} is the hydrogen molar fraction in the mixture, n_{CO} is the carbon monoxide molar fraction in the mixture and n_{CH_4} is the methane molar fraction in the mixture. From the calculation, a maximum velocity of 29.38 m s^{-1} was found.

A velocity outlet boundary type was chosen and a velocity $u = V_{max} = 29.38$ m s^{-1} was set in positive x direction. Temperature and pressure are calculated. At the inlet, a pressure inlet condition is used. According to a real operating condition, the pressure is set to 94 kPa and the temperature to 323.15 K. On the symmetry plane, symmetric boundary condition is used. Since the Reynolds number Re is always above $2 \cdot 10^4$, according to (Launder et al., 1974) and (Shih et al., 1994) the realizable k-ε turbulence model was chosen and the model coefficient are shown in Table 8.

Table 8. Turbulence model coefficients.

σ_k	σ_ε	C_1	C_2	C_μ
1.0	1.2	1.44	1.9	0.09

Turbulence intensity I (Russo et al., 2016) and turbulent length scale l (Versteeg et al., 2007) are calculated according to the following equations and properly set to inlet and outlet boundaries.

$$I = 0.16 Re^{-\frac{1}{8}} \tag{3.2.7}$$

$$l = 0.07 D_h \tag{3.2.8}$$

where D_h is the hydraulic diameter of the pipe at the specific boundary and k is the turbulence kinetic energy calculated according to (Versteeg et al., 2007).

$$k = \frac{3}{2}(Iu)^2 \tag{3.2.9}$$

According to Del Toro, 2012, a $y^+ > 30$ formulation was adopted to better balance the necessity of a fine mesh near the plate profile and the selected k-ε turbulence model.

A fluid model was created for several throttle opening angle ϑ (15°, 30°, 45° and 60°) following the same procedure.

Continuity equation, energy equation and momentum equations for the gas phase were numerically solved by using the open source code OpenFoam.

The solver selected for the scope was *sonicFoam*, which enables the solving of compressible fluid flows up to transonic velocities, often reached in the chocking section of the throttle valve at idle.

The results with three meshes, from 133 thousand to 287 thousand cells, have been analyzed in order to establish the suitable computational mesh size. For these tests, the half-way position of the throttle (i.e. 45°) was chosen, adding the boundary conditions listed before.

From Figure 25 to Figure 27 the results of the sensitivity analysis are reported, showing the effect of the mesh size on the numerical result. In particular, the solution seems not to be sensible to the mesh far away from the throttle plate nevertheless more differences are reported in proximity to the obstacle. The most important parameter of this calculation is the temperature and the conclusion of this sensitivity analysis is that the mesh size has a relevant influence in its the calculation.

The results of the computational meshes of 175k and 287k cells are similar, and this indicates that further refinements of the computational mesh will not bring relevant changes in the numerical results. Therefore, the mesh resolution of 287'000 cells was selected as a reference in all of the simulations.

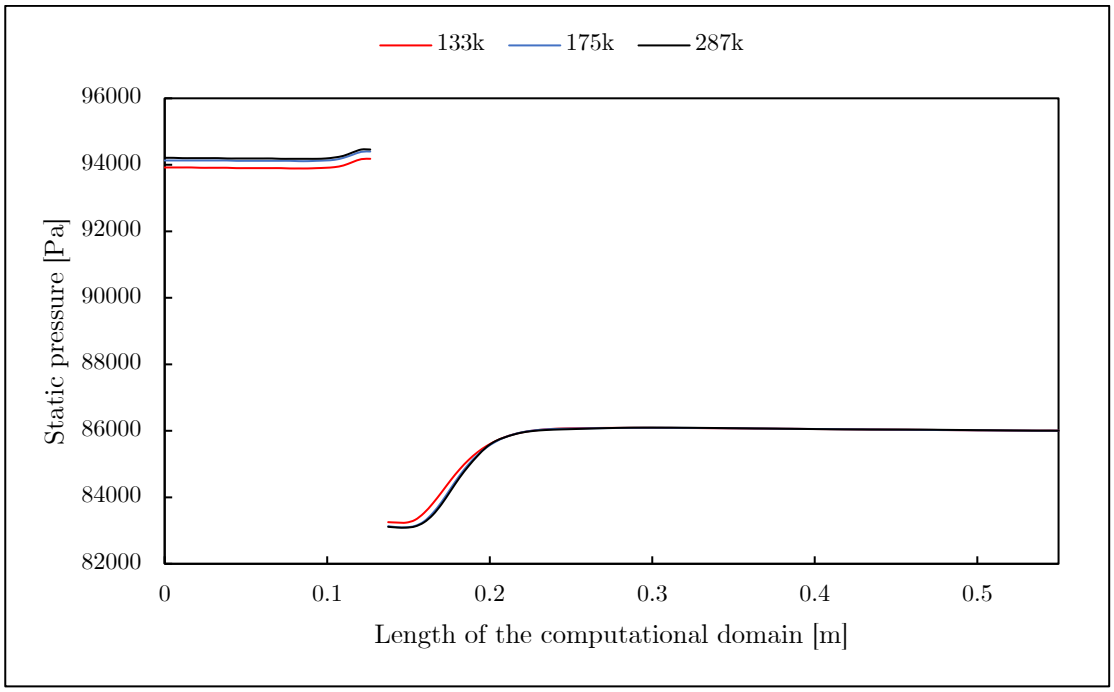

Figure 25. Mesh sensitivity analysis: average static pressure.

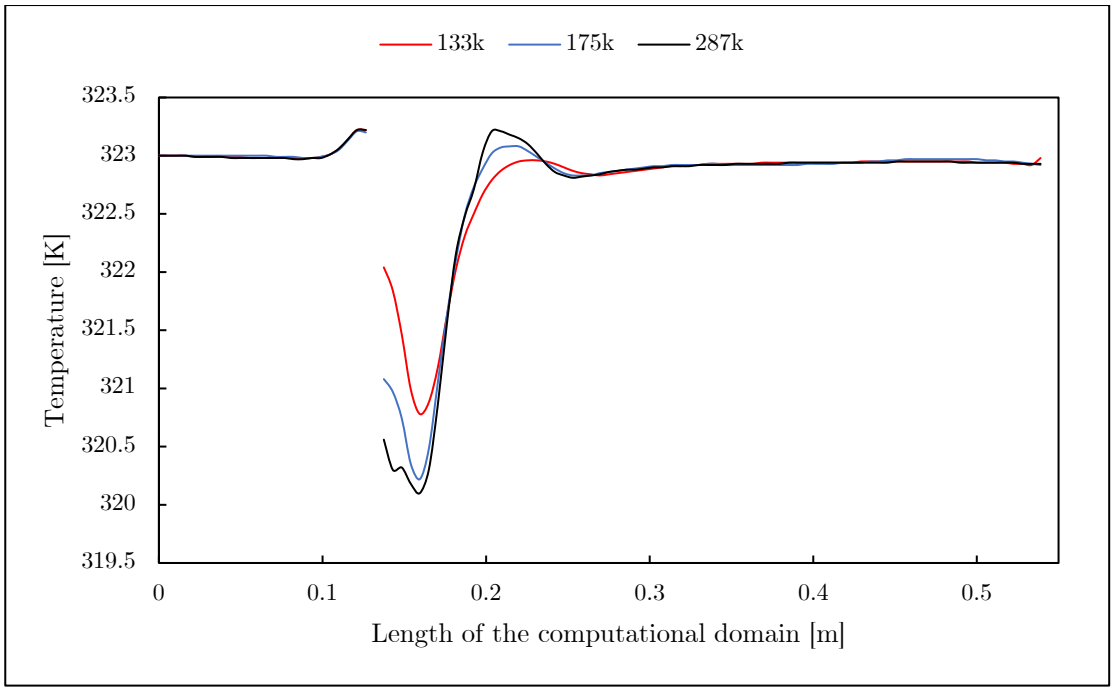

Figure 26. Mesh sensitivity analysis: average temperature.

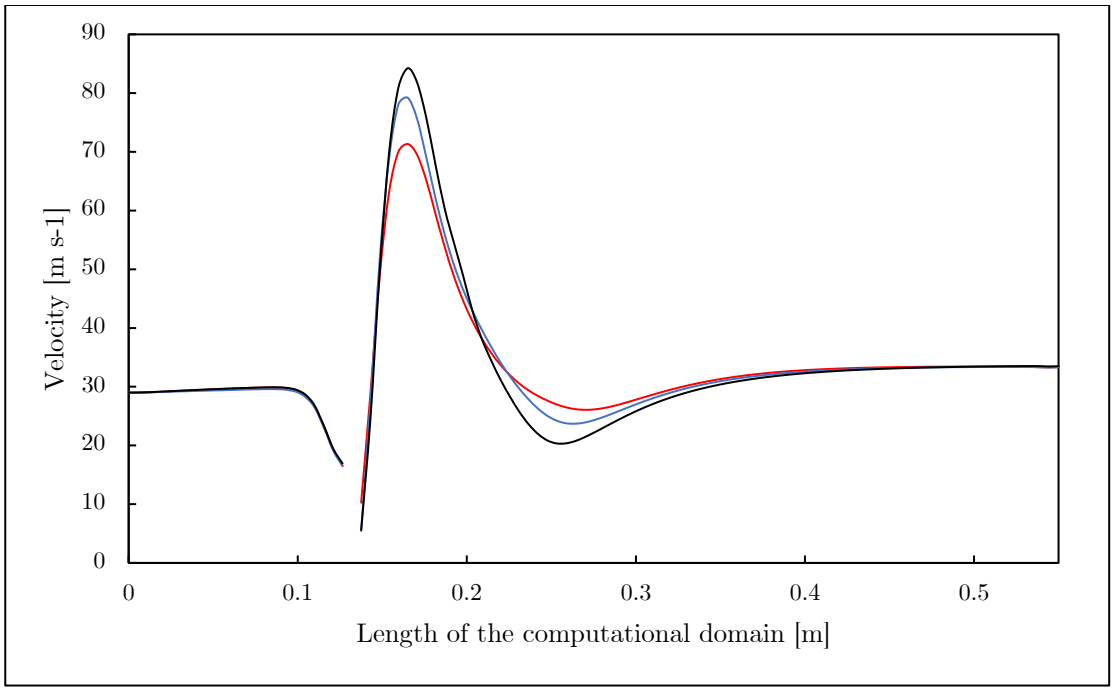

Figure 27. Mesh sensitivity analysis: average velocity in x-direction.

3.3 Results and discussion

3.3.1 CFD model output

To investigate the gas pressure and temperature scalars behavior through the throttle plate, a set of RANS (Reynolds Averaged Navier-Stokes Equations) simulations was performed. In Figure 29, Figure 30 and Figure 31, for each throttle opening angle, pressure, temperature and velocity contours are shown.

For small throttle opening angles, due to the high pressure drop across the plate, chocked flow condition is achieved in the annulus. This local phenomenon produces a strong temperature drop that stretches for few diameters towards the outlet.

With the assumed BC's, the two major outputs of the analytical model are the water vapor partial pressure $p_{H_2O} = 3.38\,kPa$ and the dew point temperature of the mixture $T_{dew} = 300.49\,K$. The calculated T_{dew} was introduced as upper limit in the CFD model and, for each simulation, a volume threshold was created. For each of them, the average temperature $T_{threshold,avg}$ [K] and the threshold volume $V_{threshold}$ [m³] were calculated. In Figure 28 those results are plotted and the dashed trend line shows that no water condensation ($V_{threshold} = T_{threshold,avg} = 0$) should occur for $\theta > 37°$.

Figure 32 shows the set of corresponding 3D representations of the volume threshold for each ϑ. These results reveal the different shapes of the fluid region where the gas temperature drops below the dew point.

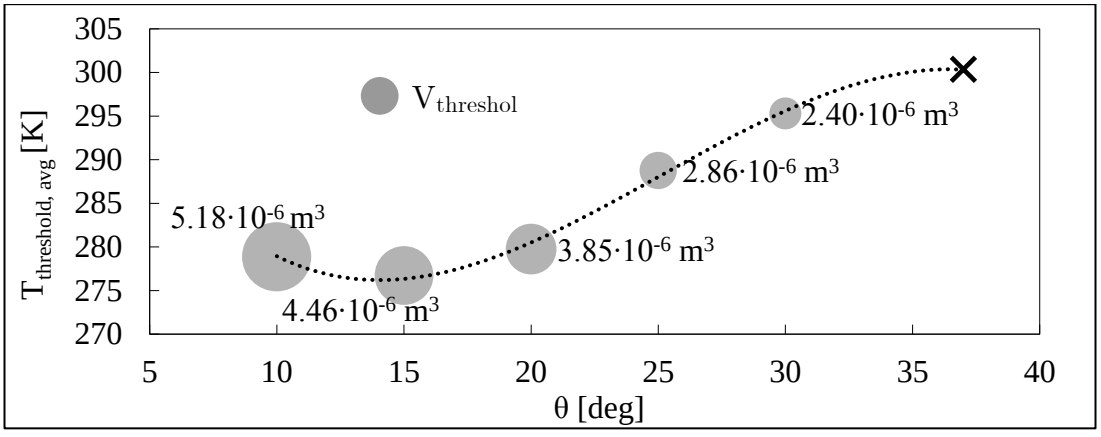

Figure 28. Temperature average of the threshold volume represented for each angle ϑ.

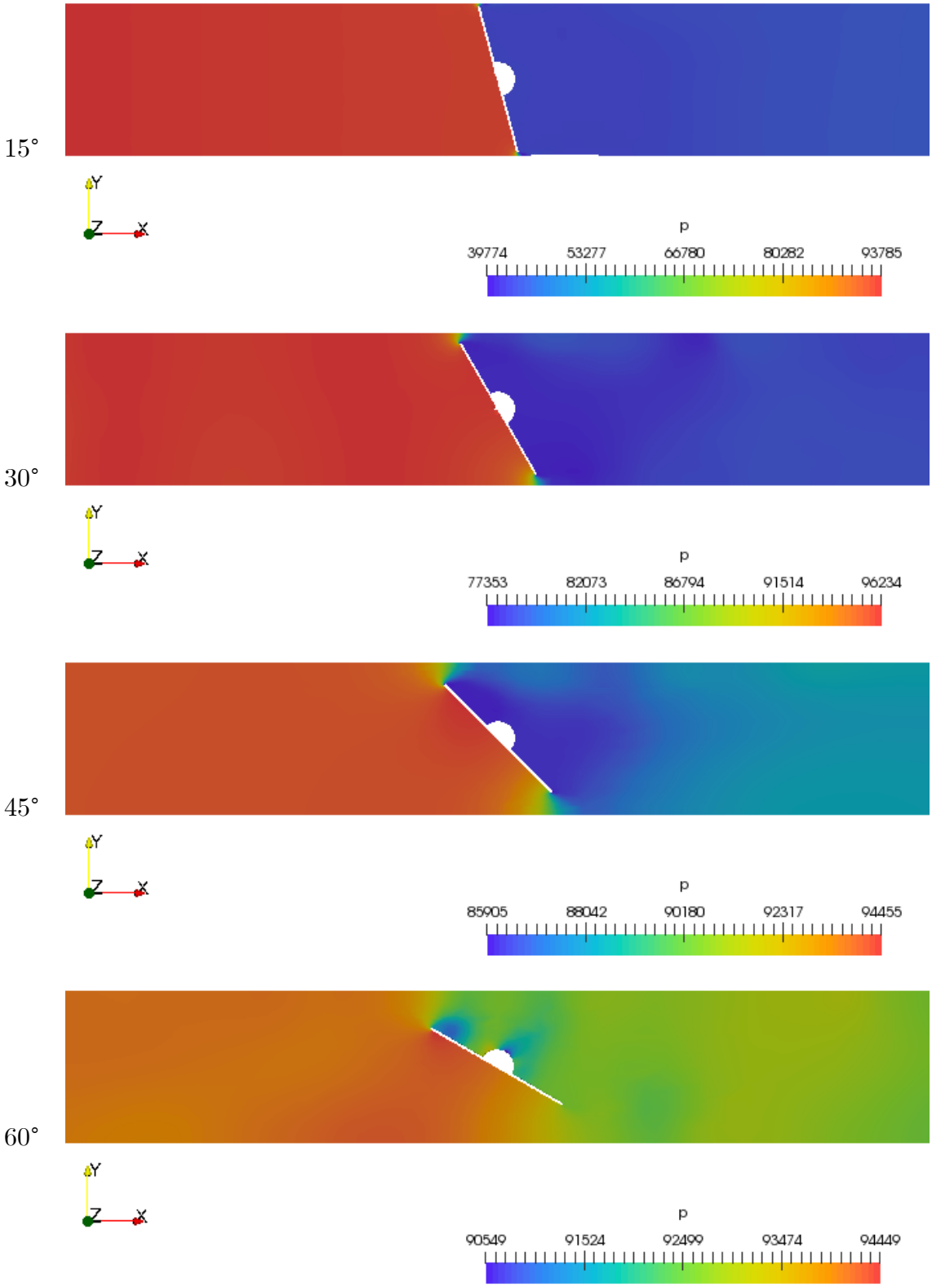

Figure 29. Pressure contours [Pa] at different ϑ.

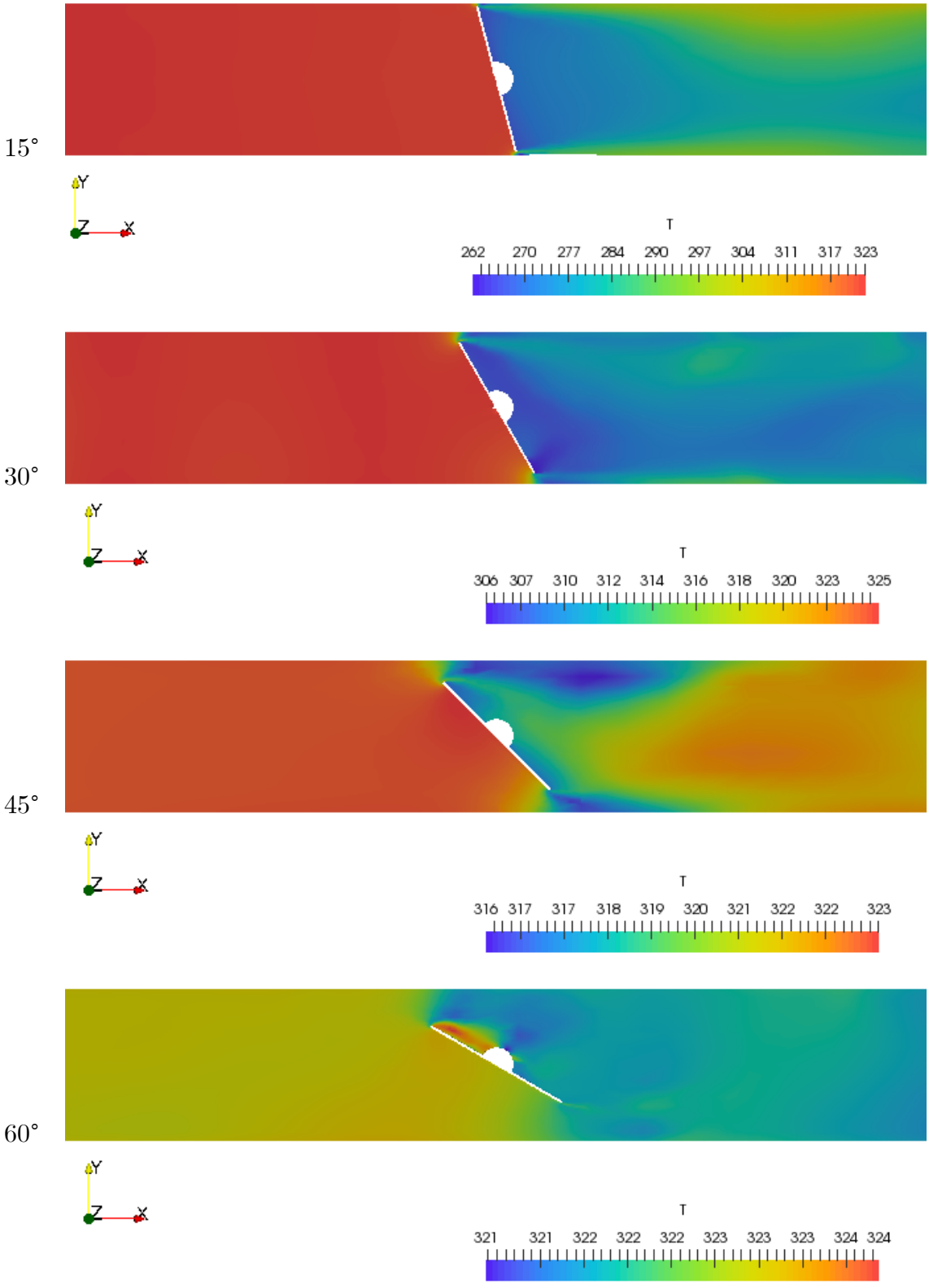

Figure 30. Temperature contours [K] at different ϑ.

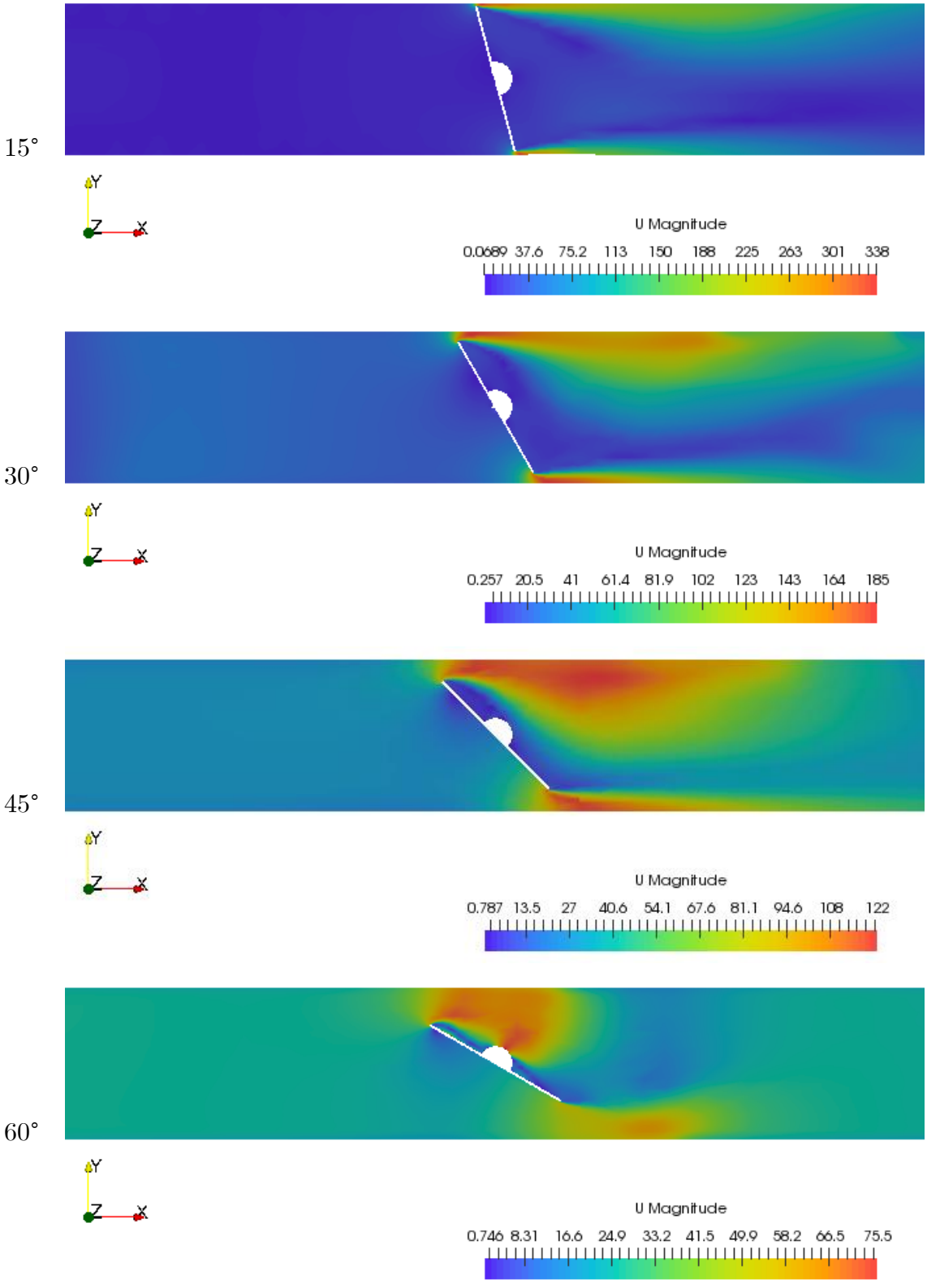

Figure 31. Velocity contours [m s^{-1}] at different ϑ.

3.3.2 Qualitative comparison between combined psychrometric-CFD model output and experimental analysis

In order to validate the results given by the volume threshold method, an experimental campaign was carried out maintaining the throttle opening angle at $\theta = 25°$ while running the engine on producer gas. At this value, the engine produces the electrical power of 10 kW. In Figure 32 a comparison between the CFD output at $\theta = 25°$ and the throttle system after the test is shown. Temperature regions under the calculated water vapor dew point are reported in grayscale on the LHS, showing that the chance of tar and water condensation increase right across the throttle plate, as shown in the experimental result on the RHS.

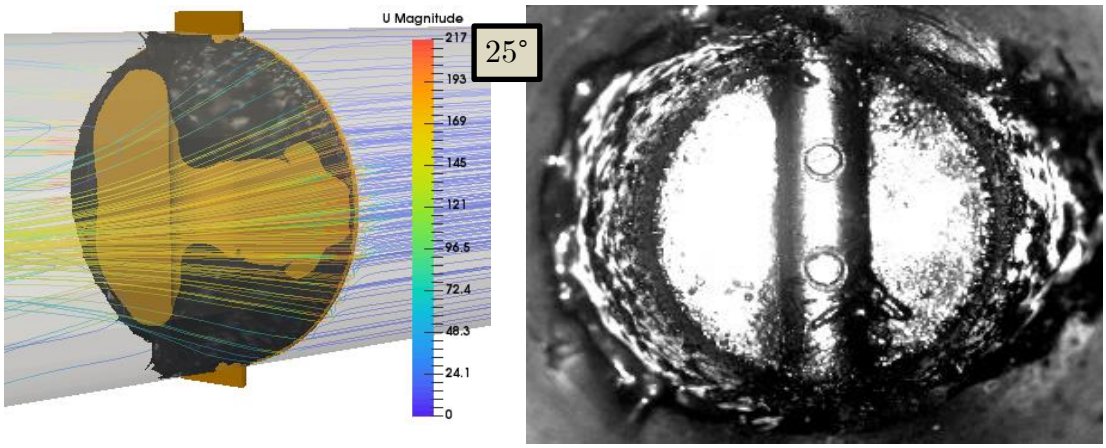

Figure 32. comparison between CFD model prevision (LHS in grayscale temperature contour under the water dew point derived from Figure 28) and real throttle body fouling (RHS) after testing it at 10 kW_e.

3.4 Chapter summary

An analytical model was created in order to investigate the psychrometric conditions of the fluid upstream a commercial throttle body installed on a small-scale woodchips gasifier. It was found that, with the assumed gas mixture composition, the air-syngas flow passing through the governor is close to its dew point.

A series of CFD simulations were done to study the behavior of air-syngas mixture throttling, using as BC's both experimental values, and psychrometric model outputs.

Combined CFD-psychrometric model showed that the pressure drop across the throttle plate is followed by a strong temperature drop that is the main cause of the condensation phenomenon.

The comparison of experimental results, on the throttle fouling, and the model output, revealed a qualitative but strong correlation between flow path, temperature distribution and condensates shape downstream the throttle plate.

Extensions to this study include the upgrade of the developed psychrometric model in order to also investigate the flow through and downstream the governor. A more detailed and validated CFD model can also be studied, both for calibrate the parallel analytical model, and to investigate new throttle geometries that can prevent or reduce the condensation phenomenon.

Chapter 4

Use of gasification char for hot gas filtration in a micro-scale plant

4.1 Introduction

As mentioned in Chapter 1, producer gas is generated together with a series of contaminants and it must be filtered before its utilization as fuel into ICEs for energy production. Among other pollutants, such as nitrogen, sulfur and chlorine compounds, the most common are particulate matter and tar (Ntalos et al., 2002; Puglia et al., 2017a).

Tar is a wide family of aromatic compounds with different boiling temperatures. Except for very light compounds that are usually not classified under the general tar family, condensation starts at 180-220°C (Puglia et al., 2017a). Above this temperature no condensation occurs, while, between this temperature and -15 °C almost all the aromatic compounds condense. Water content in producer gas is far from being negligible and originates from three sources, from the higher to lesser affecting: moisture content in the biomass, water originated during the thermochemical conversion, moisture content in the gasification agent. The final output is the 1-8 % of the whole gas (Ntalos et al., 2002). Even in a simplified approach, where producer gas is composed of gaseous compounds and water only, the dew point will range from 30 to 55 °C (Reed, 1988) depending on the above-mentioned water sources. Several strategies are commonly used in filtration systems to remove tar and particulate and most of them are resumed in Chapter 2.

In small-scale biomass gasification system, the most attractive filtration strategies are HGC and WGC. WGC systems work above water dew point filtration avoiding the water vapor to not condense as well as some light tar species. However, heavy tar still condenses below 100 °C, therefore it is fundamental to have an adsorbent media in the filtration stage.

This chapter focuses on a possible solution that derives from the use of the very porous char produced in the gasification process. This char is characterized by high porosity and well-known filtering capacity (All Power Labs, Channiwala et al., 2002). To efficiently use the char, two char candle filters depicted were

designed and built. Experimental tests were done on an All Power Labs PP20 gasification system by All Power Labs. Two candles were fabricated and filled with the char produced by the gasifier during conventional operations. For 12 days the system ran at various electrical loads. In all the tests, characteristic temperatures and pressures of the system were monitored, while, after every test, the engine throttle valve was used as standard point for the quick evaluation of the effectiveness of the filtration stage. Six tar content gravimetric tests were performed using the Tar Sampling Procedure (TSP) (Basu, 2009). Results showed the capability to build dry filtration systems with encouraging filtering performances. On the other hand, the pressure drop across the candles quickly increased during all the tests to values too high for an efficient IC engine running. This phenomenon outlines the necessity to provide the system with a regeneration strategy that can renew the outer layers of char, more affected by the fouling phenomenon due to the producer gas pathway.

4.2 Materials and methods

4.2.1 Char properties

As result of the gasification process, char is formed and collected downstream the combustion zone inside a stainless steel perforated bucket that sets the boundaries of the reduction zone (Figure 22). Since the gas is forced to pass through the reduction zone, the bucket is connected to a shaking system that provides char removal when pressure drop across it is too high. Then, the char, is finally pulled out from the gasifier through an auger and disposed in stainless steel vessel. The extraction temperature of the char is between 600 and 700 °C, high enough to minimize the tar content.

Char composition analyses were conducted using the FLASH 2000 Organic Elemental CHNS Analyzer and the result is shown in Table 9. Ash content, BET superficial area and real density are also reported.

Surface properties of the gasification char are often similar to the activated carbon which enables the aromatic compounds (i.e. tars) adsorption as reported in Ravenni et al., 2019.

Table 9. Char characterization in dry conditions.

Parameter	Value
N [%w/w]	0.22
C [%w/w]	81.12
H [%w/w]	0.82
S [%w/w]	0.00
ASH [%w/w]	19.98
BET superficial area [m^2 g^{-1}]	394.443
Real density [g cm^{-3}]	2.1454

4.2.2 Char candles

Since the maintenance operations on the filter stage should be weekly performed by a single operator, a char filter was designed in order to ensure quick maintenance and easy handling and retrofitting on the current filter design and to maximize the filtering surface. Result of the conceptual phase was the design of two filtering candles shown in Figure 33a,b. Each candle is 130 mm diameter wide (D), 560 mm high (H) and the external part supports the 1 mm stainless steel mesh. An annular space was created within each candle by inserting the 38 mm diameter (d) slotted pipe from where the syngas is drawn by the internal combustion engine. An annular volume of 6.80 liters was hence generated allowing the storage of 0.9 kg of char for each candle (Figure 33c).

4.2.3 Testing procedure and recorded data

Thirty tests were performed on the char candles filter for a total of 40 hours of engine operation at 10 kW_e and 10 hours of gas flaring needed for the startup and shutdown of the gasifier (from Figure 68 to Figure 74 in the Appendix for the details). Eight tests lasted more than 2 hours each while the remaining tests lasted less than 30 minutes. The test bench is shown in Figure 34 and it consists of an air-producer gas heat exchanger (HX) connected upstream the char candles filter. The 'air side' of the HX was connected to a dimmable 12 volts air blower by which the outlet temperature of the producer gas could be set.

The electronic controlled throttle valve (AirServo) has the purpose of maintaining the stoichiometric value of the engine air/fuel mixture. A hot air

gun was used to preheat the air entering from the AirServo in order to qualitatively evaluate the effect of cold mixing air in tar condensation.

(a) (b) (c)

Figure 33. Char candles components (a, b) and installation of the tested filter inside its housing (c).

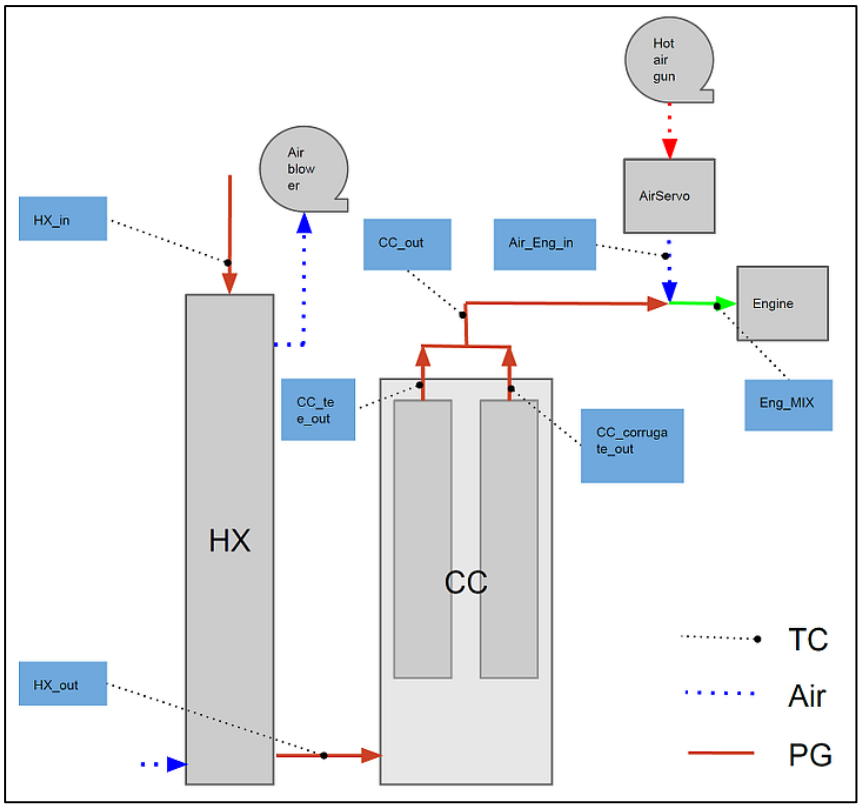

Figure 34. P&I of the char candles testing facility.

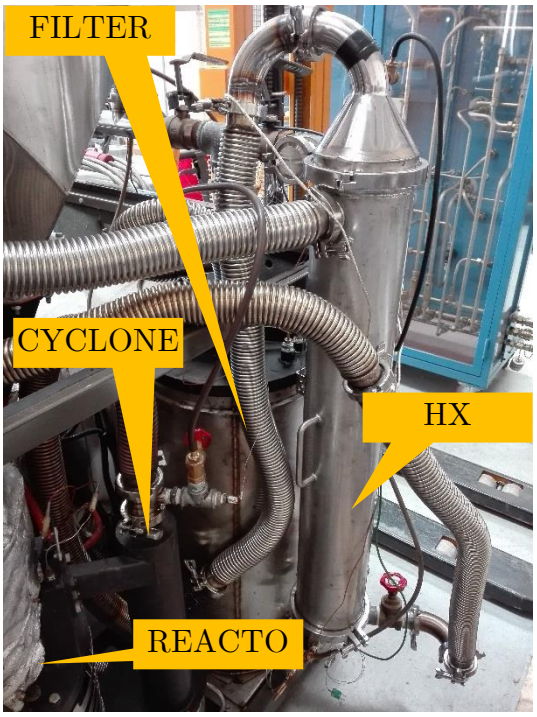

Figure 35. Installation of the testing facility.

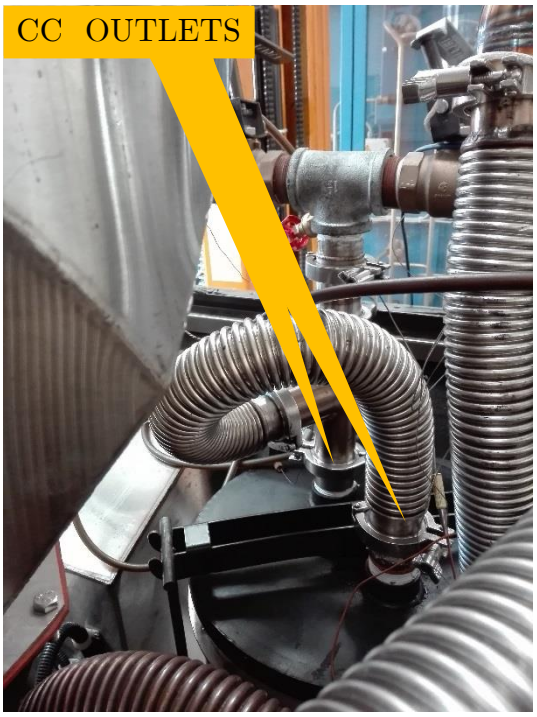

Figure 36. Detail of the two filter outlets: one for each char candle.

As described in the following paragraph, several gas samplings were done investigating the quantity of tar and particulate matter in the gas stream before and after the filtration stage. Since it was not possible to apply the tar sampling procedure for the very short tests, qualitative analyses were carried out by observing the fouling of the engine throttle governor after each test. In conventional operation, tar and water find a way of condensing right downstream the governor plate because of the high pressure drop that is present when the engine runs choked (Reed, 1988). A visual assessment of the condensates was carried out and a picture of the throttle plate was taken. After each test, the throttle body was cleaned to reset the fouling conditions.

During each test the pressure drop across the filter was recorded. Since pressure drop lowers the engine performances, a series of tests from 0 to 10 kW_e were performed in order to calculate the characteristic curve of the gasifier circuit plotted in kPa vs. kW_e. These tests were carried out both on new and on exhaust char candles filter. Coupling this result with the characteristic curve of the engine was possible to set different operation points predicting the engine performance in function of the filter fouling.

4.2.4 Simplified tar testing procedure

This paragraph treats the tar sampling procedure, adopted in this case. It is a simplified procedure, following some of the expedients shown in CEN BT/TF 143. The principle is based on a gravimetric analysis of the tar collected during the discontinuous sampling of a gas stream containing particles and organic compounds. The gas sampling system consists of a series of impinger bottles containing isopropyl alcohol as solvent for tar absorption. The impinger bottles are placed in a cooled glycol bath. The gas is sampled for a specified period through the sampling line and filter. The flow rate is maintained constant with the aid of an air pump.

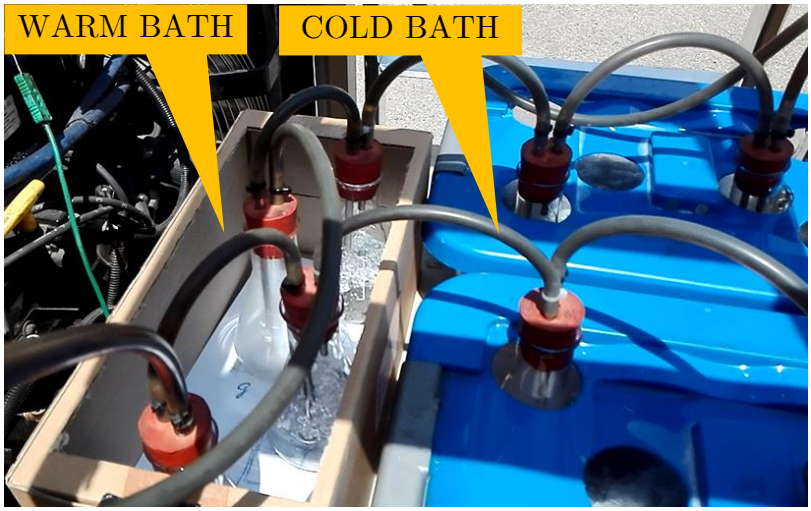

Figure 37. Gas sampling on the tested candle filter.

The tar collection occurs both by condensation and absorption in isopropanol, which was found to be the most suitable solvent. The volume, temperature, pressure, and gas flow rate through the equipment are measured. The gases from by-pass lines and sample gas are vented safely to atmosphere. The tarry isopropanol is then filtered using a paper filter. This procedure is needed in order to assess the particle content of the syngas before and after the filtration and it consists in a gravimetric analysis of the paper filter. Afterwards, the isopropanol is distilled in order to measure the tar content of the syngas, by mean of a gravimetric analysis. The solution starts to boil at around 78 °C at atmospheric pressure and process is interrupted as soon as the temperature start to rise again. The next step is to put the remaining material into an oven set at 90 °C for about 24h in order to evaporate all the water and the final step is the measurement of the mass of the remaining liquid and waxy tars. Eventually,

given the mass of tar for each sampling and given the volume, temperature and pressure, it has been possible to figure out the concentration of tar and particulate matter before and after the filtering stage.

4.3 Results and discussion

4.3.1 Producer gas filtration performances

Filter performance was evaluated at different filter and engine operating conditions. During each test the electrical power output was set to 10 kW_e and kept constant.

To separate the effect of char candles working temperature and condensation due to cold mixing air entering the engine, the latter was preheated and tests were performed at engine mixture temperatures (T_{mix}) ranging from 50 to 70 °C and shown in Figure 41. No liquid condensates were collected downstream the governor. The higher the mixture temperature, the lower the fouling of the throttle plate.

The working temperature of the two char candles (T_{cc}) was set from 60 to 80°C by using the air to producer gas heat exchanger. Results are shown in Figure 42. Increasing the working temperature of the candles, filtering performances get worse, showing the optimum in the range from 50 to 60°C.

During all the tests the filter was never regenerated, and a fouling phenomenon was observed by measuring the pressure drop (Δp_{filter}) across the char candles. Figure 43 shows the recorded filtering performances at same filter temperatures and engine conditions but at different filter pressure drops. Filtering performances clearly increase according to the increase of the filter pressure drop. In particular, the amount of particulate matter is negligible over 11 kPa of pressure drop.

In Figure 38 the isopropyl alcohol collected during the TSP is shown. It can be noted the absence of particulate matter in the sample on the left, collected downstream the filtration stage. The presence of tar is qualitatively shown by the resulting yellowish color of the IPA.

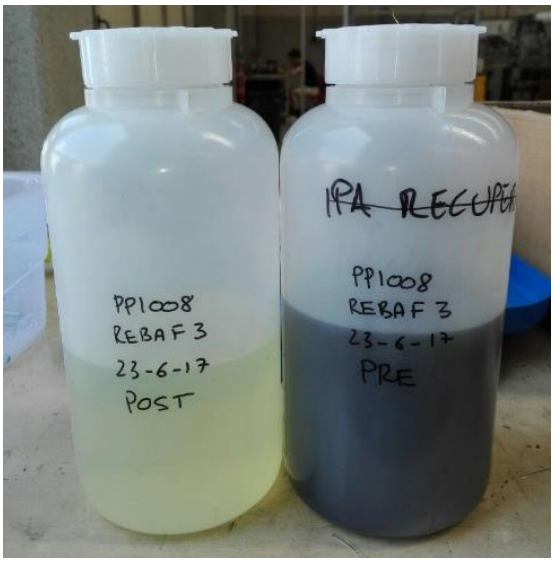

Figure 38. IPA collected downstream (left) and upstream (right) the filtration stage.

Figure 39. Char candles after 50 hours of tests.

During the filter life span (measured in kWh_e produced by the Power Pallet), six gravimetric tar and particulate analyses were performed and results of the gas sampling campaign are shown in Figure 40. In Table 10 test conditions of each gas sampling are reported. Test no. 1 was carried out also upstream the filtering stage in order to have a point of comparison for filtering performances. In Figure 39 the filter conditions after 50 hours of tests are shown.

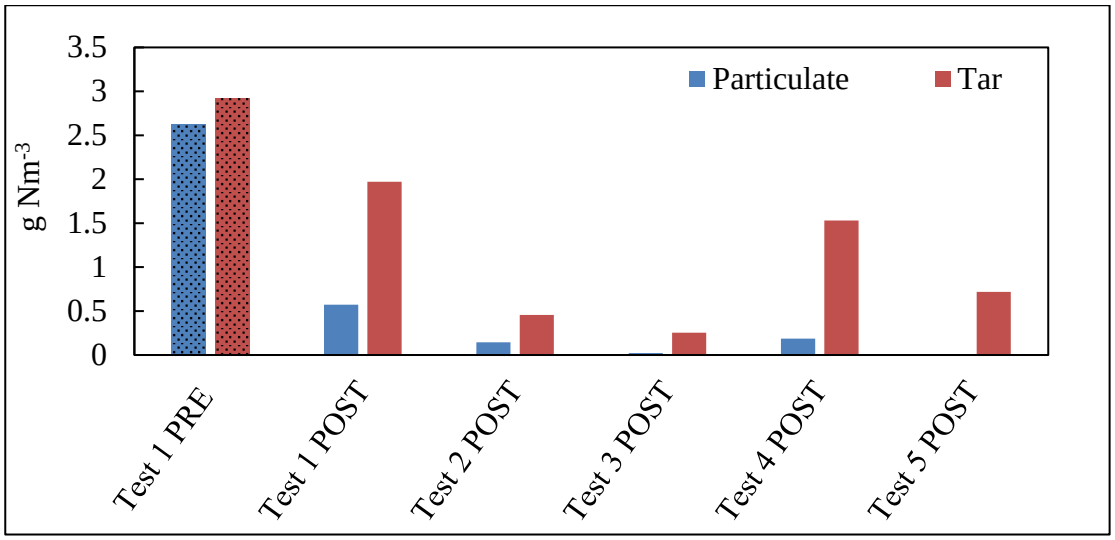

Figure 40. Gravimetric tar and particulate analyses results.

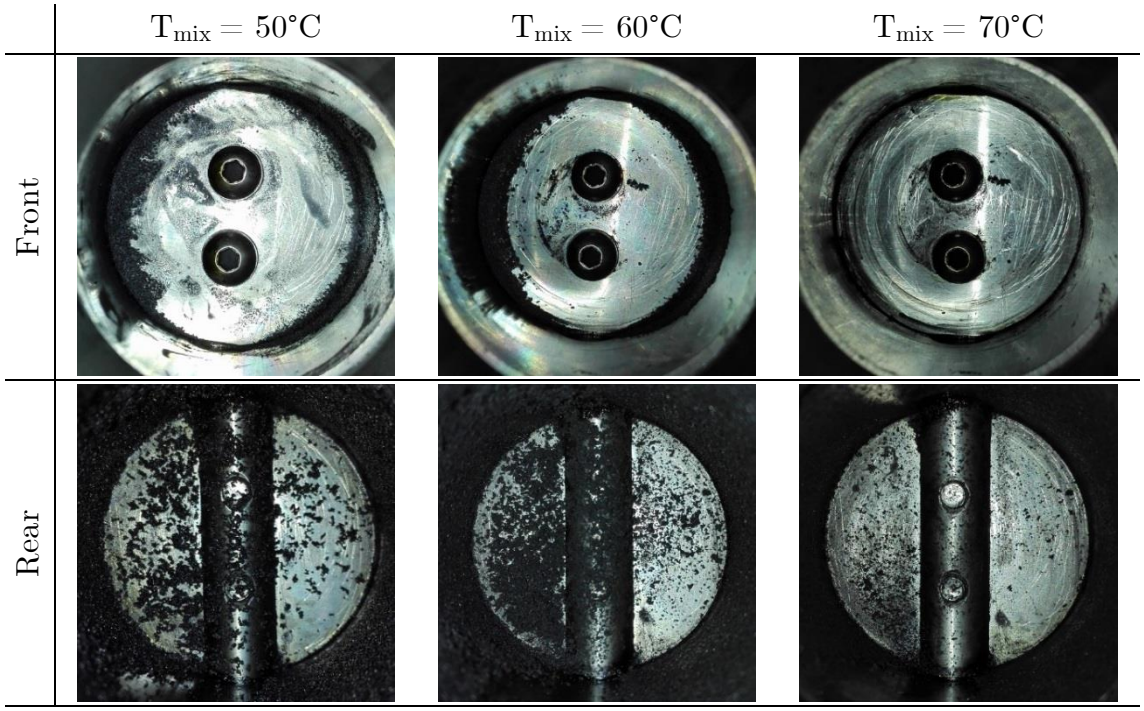

Figure 41. Qualitative assessment of tar condensation across the governor during tests at 50, 60 and 70°C of engine mixture temperature. Char candles working temperature set to 50°C.

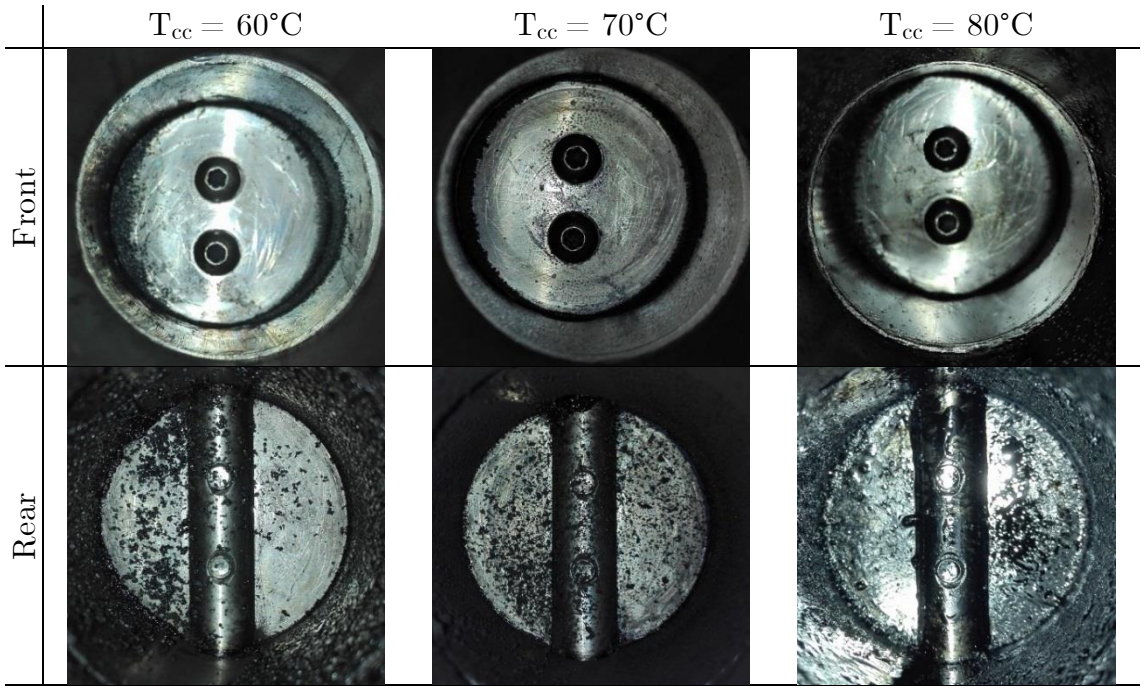

Figure 42. Qualitative assessment of tar condensation across the governor during tests at variable working temperatures of the char candles.

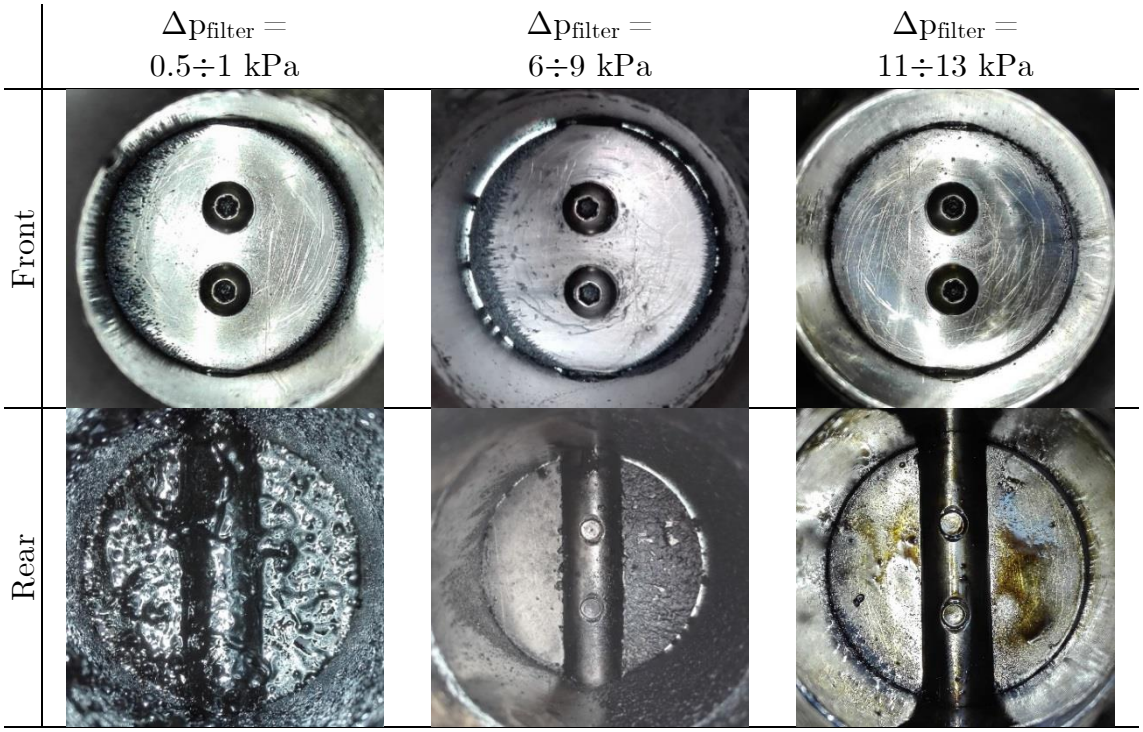

Figure 43. Qualitative assessment of tar condensation across the governor during filter lifetime at different filter pressure drop.

Table 10. Temperatures and filter conditions during TSP tests

Test no.	Test conditions	Filter lifetime [kWh_e]
1	CC not cooled	0
2	CC not cooled	70
3	T_{cc}=60°C	287
4	T_{cc}=70°C	334
5	T_{cc}=80°C	350

4.3.2 Filter pressure drop analysis

To understand and predict how filter pressure drop affects the maximum engine power output, a series of tests were carried out at different electrical power output recording the absolute pressure downstream the filtering stage (p_{filter}). Blue line in Figure 44 represents the test performed with a clean char candles filter by running the engine from 0 to 10 kW_e where p_{filter} was recorded for each power output step. This curve represents the characteristic of the gas making and filtering system in its power pressure drop conditions.

The same test was performed at the end of the filter life (clogged filter) running the engine between 2 and 8 kW_e since at 0 kW_e the engine ran unstable due to high filter pressure drop the green line in Figure 44 shows the result.

A range of pressure variability is generated during gasifier operation due to biomass and char flow inside the reactor. The biomass flow it is in fact regular but not continuous because it is mainly governed by the intervention of the grate shaker, which generates such variability in the reactor pressure drop that was measured and it is shown in Figure 44 (blue and green areas) for each of the filter conditions. Those ranges need to be considered to not overestimate engine performances during filter lifetime.

The absolute pressure of the engine intake manifold (MAP) was also measured at different engine loads. The intersection between the MAP line and the two p_{filter} curves shows the expected engine electrical power output at different filter conditions. The calculated maximum power output ranges from 16.2 kW_e in clean filter conditions to 11.3 kW_e at the end of the filter life. Those values were calculated for a T_{mix} of 40°C and need to be re-evaluated for different intake mixture temperatures.

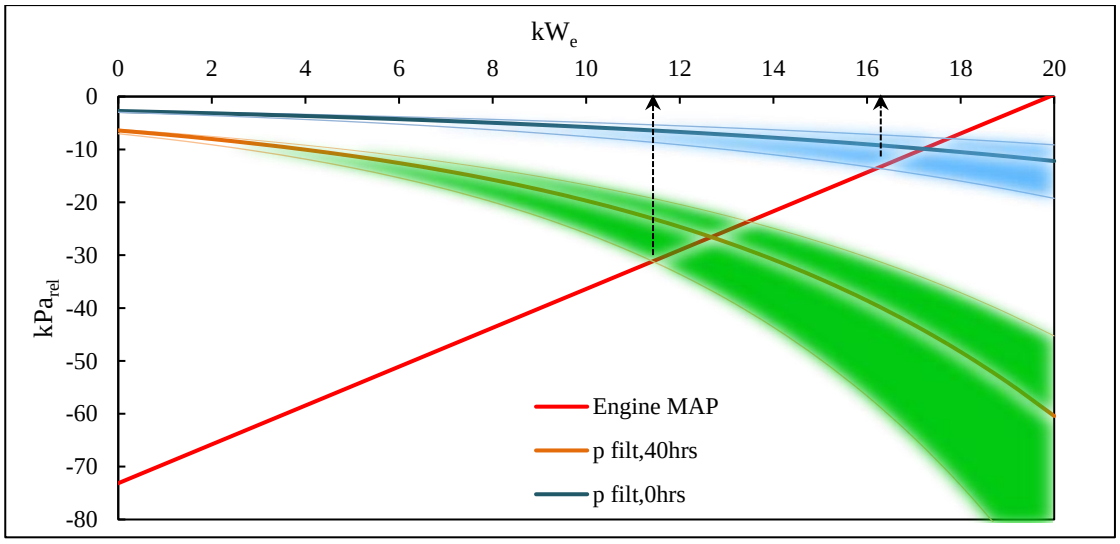

Figure 44. Comparison between gas making and filtering system pressure drops in clean conditions (p filt,0hrs) and after 40 hours of engine operation (p filt,40hrs)

4.4 Chapter summary

Experimental tests supported the literature estimation of water vapor dew point around 50-60 °C in the producer gas, above this temperature the filter is kept "dry". The condensation of the heavies' tar compounds likely still occurs on the char medium. In fact, partially dry filtration can be performed in the window of opportunity above water condensation. Char was proven to be an effective medium for filtration of the particulate matter. Since this filtration system generates high pressure drops, future work will focus on 'in situ' regeneration of the filtering systems in order to achieve constant filtering performances avoiding the excessive engine power loss during filter lifetime. At this stage the proposed technology is in fact suitable for discontinued engine operation. From a qualitative point of view, preliminary tests demonstrated that controlled temperature char filtration can achieve high filtration performances, alike wet filtration, without the well-known disadvantage of generating tarry water.

Chapter 5

Experimental evaluation of possible solutions for compact design of producer-gas heat exchangers

5.1 Introduction

Taking up what was already anticipated in the two introductory chapters, gasification reactions take place at high temperatures up to 1100 °C, the overall energy balance is endothermic and the different reaction kinetics drop in speed when temperature falls below 600 °C (Basu, 2009).

For this reason, the large majority of downdraft reactor designs produce syngas in a temperature range between 500 and 700 °C depending on the reactor capability to self-recover some of the gas heat for internal use (Wu et al., 2015; Pan et al., 2018; Arthur et al., 2018). Hot gas must be cooled down before reaching the power generation unit otherwise it will reduce the engine volumetric efficiency and will increase the risk of knocking (Heywood, 1988).

Gas temperature conditioning is also a strategic part of the filtration stage. At different temperatures the pollutants traveling within the gas can be filtered through a variety of systems. The control over the gas temperature allows to selectively work on specific pollutants. Dust and particulate matter are usually filtered at high temperature (300 to 600 °C), while tarry compounds and other condensable compounds are separated at lower temperature (Reed, 1988).

This chapter focuses on the design of a water-cooled gas heat exchanger able to cool down the producer gas while keeping it above water vapor condensation. The challenge is to take advantage of the literature about flue gas turbolated heat exchanger (Saha et al., 1990) in biomass boilers and to import it into gasification systems. Several techniques are available to improve the heat transfer between two different continua in tubes and shell heat exchanger, such

as: coil wire inserts, conical tube inserts, helical screw inserts and twisted tape inserts (Bipin et al., 2018). The common ground of these devices is to use the energy already available in the system to work, they can thus be named as passive systems. They aim at reducing the convective resistance between the solid and the fluid domains by promoting the recirculation of the flow reducing the thickness of the boundary layer (Bipin et al., 2018; Eiamsa-ard et al., 2012).

It is known from literature (Saha et al., 1990) that the regularly spaced twisted tapes perform better than the full-length twisted tapes in terms of pressure drop at constant heat duty. Since, here the aim of this device is not only to promote the heat exchange but also to keep the tubes clean from the tar and particulate matter, in this work a set of 7 full length (1.5 m long and 2 mm thick) TT were inserted in the 7 tubes of the HX. In this way it was avoided the use of inserts with centred rod that needs welding techniques instead of simple tape twisting. The cleaning mechanism consists in moving up and downward the twisted tapes in order to remove the soot from the tube walls and restore the heat transfer effectiveness. The final system was tested in a 25 kW_e small-scale commercial gasifier.

5.2 Materials and methods

5.2.1 Gasification facility description: the PP30

To evaluate the performance of the gas cooling device a PP30 gasifier by All Power Labs (All Power Labs website) was used. This power plant is the evolution of the PP20 model, and it consists of a gas generating unit, a gas temperature control system, a filtration stage and a spark-ignited internal combustion engine. Despite the previous model which had an air-cooled producer gas HX, now the HX is placed between the cyclone and the filtering stage and the water of the engine cooling system (~ 85 °C) is used to cool down the syngas. The standard heat exchanger uses the tubes and shell technology: the raw gas flows into the shell across several baffles while the coolant flows in the tubes making two passages. To reduce the risk of clogging of the shell, where the raw gas passes in, a cleaning mechanism that moves a series of baffles up and down is installed. The packed bed filter was replaced by four bag-house filters that guarantees higher reliability and performances in syngas cleanup. The engine now installed is an Ashok-Leyland 4 liters naturally aspired capable of up to 27 kW_e running on wood gas.

Table 11. Producer gas composition and resulting higher heating value from vine pruning pellets.

Producer gas composition					HHV [MJ Nm^{-3}]
CO_2	CO	N_2	CH_4	H_2	
11.84 %	23.99 %	41.23 %	1.77 %	21.18 %	6.20

Figure 45. Power Pallet 30 (All Power Labs website).

The standard HX was replaced with the tubes and shell HX subject of this work.

As known, many kind of biomass can be used to fuel All Power Labs machines and for the tests detailed in this chapter, vine prunings pellets were used. Table 11 shows a typical producer-gas composition from vine prunings biomass (Allesina et al., 2018a) and the resulting higher heating value (HHV) calculated according to Eq. 5.1.1 (Basu, 2009).

$$HHV = \frac{12.75H_2 + 12.63CO + 39.72CH_4}{100}\left[\frac{MJ}{Nm^3}\right] \quad (5.1.1)$$

5.2.2 Syngas-water heat exchanger

5.2.2.1 Tubes and shell HX

The heat exchanger (*HX*) prototype was purposely designed to fit in the existing filtration stage and, as shown in Figure 46, the *HX* needed to be placed between the cyclone and the filtration stage. The other key parameter was to bound the minimum and maximum temperature of the gas to cool down. From one hand is not advisable to exceed 150°C at the gas outlet to avoid the filter failure, but from the other hand, it is necessary to maintain the producer-gas at the minimum temperature of 50-60 °C to avoid the condensation of light tar and water (Allesina et al., 2017a) that cause the premature failure of mechanical components (Quinlan et al., 2017a,b). For this reason, the coolant water of the internal combustion engine was used. A mechanical thermostatic valve automatically regulates the minimum temperature of the coolant at 78°C, preventing the overcooling of the ICE, while its maximum temperature (95°C) is kept under control by the cooling system of the engine.

The HX layout was chosen to be multiple tubes in shell: the gas passes through the tubes and the water runs between the outer layer of the tubes and the shell. Five equispaced (l_b) baffles were added to the water path in order to reduce stagnation points and thus increase the heat transfer. The inlet of the HX ($D_{g,in}$) is connected to the cyclone with a 2" flanged joint and its outlet ($D_{g,out}$) is connected to the filtering stage with a 6" sanitary type joint. The net length of the heat exchanging zone (l_t) is 1500 mm and a 250 mm long plenum (l_p) was added on the top in order to provide better distribution of the gas and to contain the mechanism for the tubes cleaning. In the 6" diameter shell 7 tubes (D_t) 1" ¼, regularly spaced, were placed. The water inlet ($D_{w,in}$) and outlet ($D_{w,out}$) are chosen to be 1" of diameter. In Figure 49 the HX dimensions are detailed.

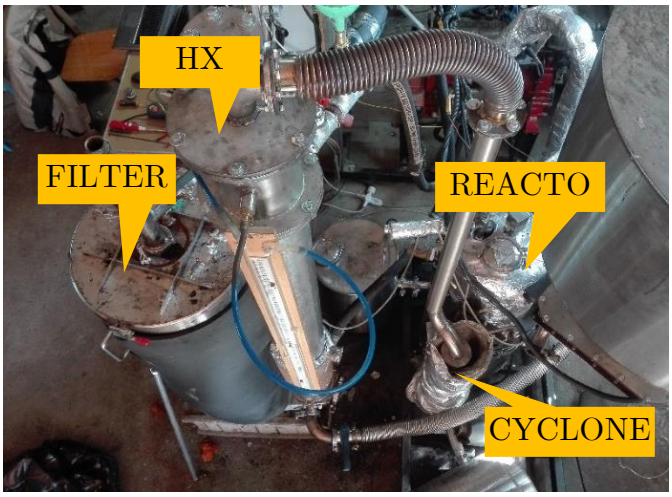

Figure 46. Layout of the All Power Labs PP30 prototype at the testing site.

Figure 47. Top of the HX.

Figure 48. HX installed on the PP30.

5.2.2.2 Twisted tape inserts

The two characterizing parameters of the twisted tapes are the pitch (p) and the twist ratio (y) that is the ratio between the pitch and the width of the tape. Figure 4 illustrates the mentioned parameters that, for this prototype were chosen to w=35 mm, p=200 mm and thus y=5.88. The clearance between the tube and the tape was designed to be 1 mm per part in order to reduce the tendency of the tape to stick to the tube surface, acting on a thicker layer of tar and particulate matter in the cleaning movement. Figure 47 shows the tubes distribution in the *HX* and the installation of one the mentioned twisted tape.

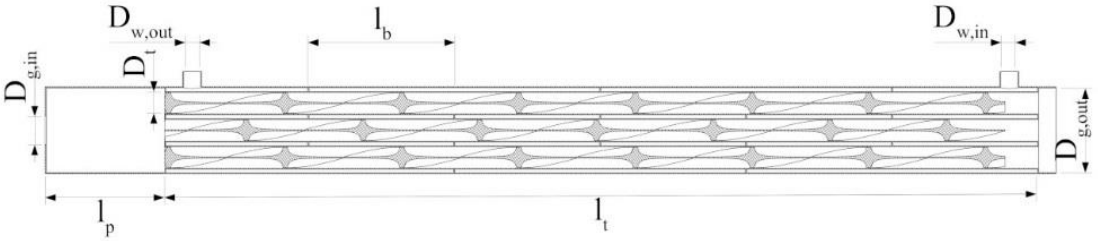

Figure 49. Longitudinal section of the HX.

Figure 50. Dimensions of the twisted tape inserts used.

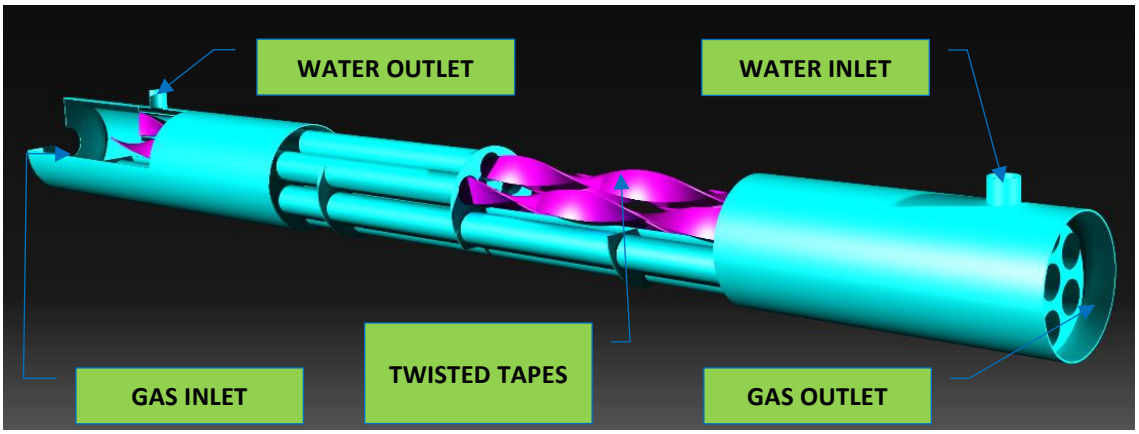

Figure 51. Exploded view of the HX.

5.2.3 Experimental setup and procedures

Four different tests were performed to assess the response of the heat exchanger at three different gas mass flow rates. Since, the gas volumetric flow rate is almost directly proportional to the internal combustion engine power output, tests were carried out at three different electrical power output of the cogenerator: 7.7, 11.6 and 16 kW_e, both with and without twisted tape inserts. During each test the inlet and outlet temperatures of the gas were measured using K-type thermocouples, while the water inlet and outlet temperatures were measured using T-type thermocouples. The datalogging system used was a Picotech TC-08 thermocouple datalogger.

Both gas and water flow rate were measured using respectively a calibrated orifice meter and an impeller meter for hot water. The orifice meter was placed downstream the filtering stage of the Power Pallet and, for this reason, the temperature of the gas from the filter outlet was used to calculate the volumetric flow rate from the pressure difference measured across the orifice. The pressure loss generated in the gas stream by the heat exchanger was measured through a water U-tube manometer. In Figure 52 the experimental setup is shown.

During each test, the steady state condition was reached before to start to sample the temperatures and flow rates. The sampling lasted for 300 s for every case and the mean value of each parameter was used to setup the relative boundary conditions in the CFD model. For each test, the thermal power lost by the producer gas ($\dot{Q}_g$) and the overall heat transfer coefficient (HTC_g) of the tested *HX* version were calculated according to Eqs. 5.1.2 and 5.1.3. The thermal power is referred to the gas mass flow rate ($\dot{m}_g$) and the specific heat capacity of the gas ($c_{p,g}$). The overall HTC calculation is referred to the tubes internal surface area (S) and the logarithmic mean temperature difference (ΔT_{LM}) calculated using gas and water inlet/outlet temperature.

$$\dot{Q}_g = \dot{m}_g c_{p,g}\left(T_{g,in} - T_{g,out}\right) \tag{5.1.2}$$

$$HTC_g = \frac{\dot{Q}_g}{S\,\Delta T_{LM}} \tag{5.1.3}$$

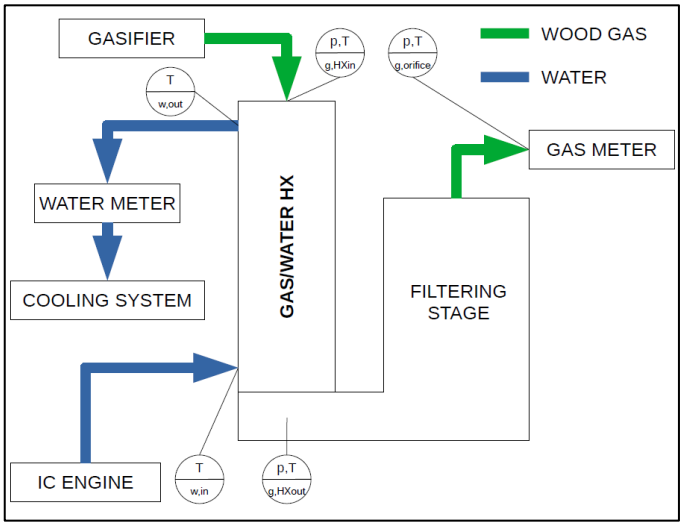

Figure 52. Setup scheme of the instrumentation.

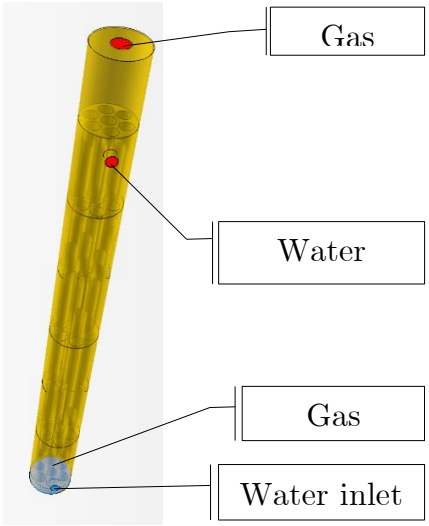

Figure 53. Boundary conditions of the HX.

5.3 Results and discussion

The engine power outputs, selected to characterize the performances of the tubes and shell heat exchanger led to three different gas mass flow rates: 0.0071, 0.0086 and 0.0103 kg s^{-1}. Each mass flow rate was averaged on a period of 300 s after steady state condition was reached.

The gas inlet and outlet temperatures are reported in Table 12 while the temperature of the coolant ranged between 77.5 and 82.4 °C according to the engine power output selected. In Figure 54 and Figure 55 the results on the overall *HTC* and thermal power output of the *HX* are shown. The uncertainty on the overall *HTC* calculation was estimated to be 5% maximum. The thermal power output was calculated based on the gas stream temperature difference, the temperature-corrected specific heat capacity of the gas and the mass flow rate. It was noticed that the pressure drop across the heat exchanger was under the instrument sensitivity in the case of plain tubes and it was assessed to be 20 Pa during the test with *TT* at the maximum tested mass flow rate of producer-gas.

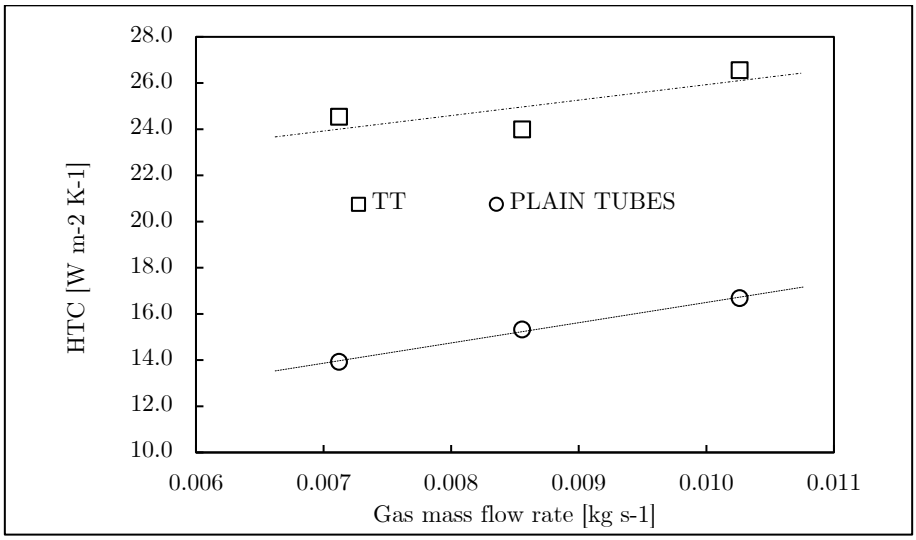

Figure 54. Experimental results on heat transfer coefficient.

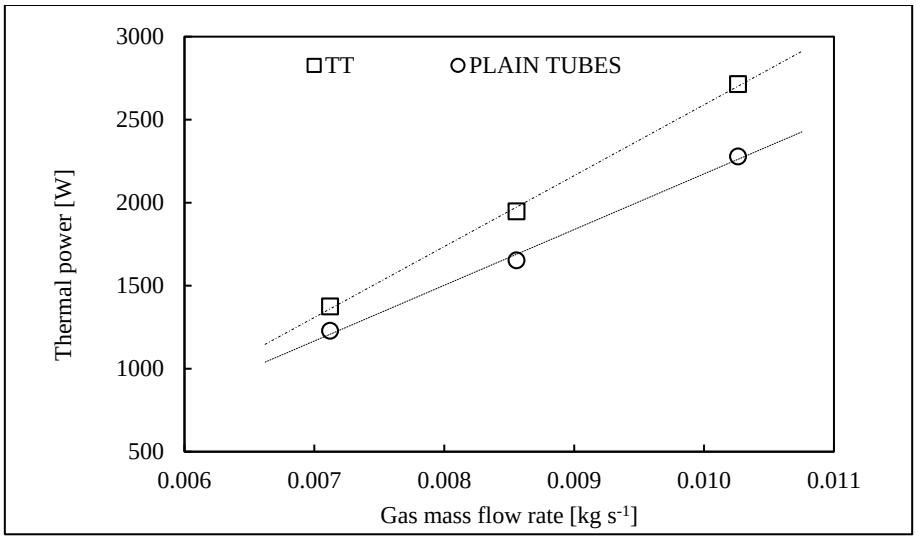

Figure 55. Thermal power dissipated by the producer-gas passing through the HX.

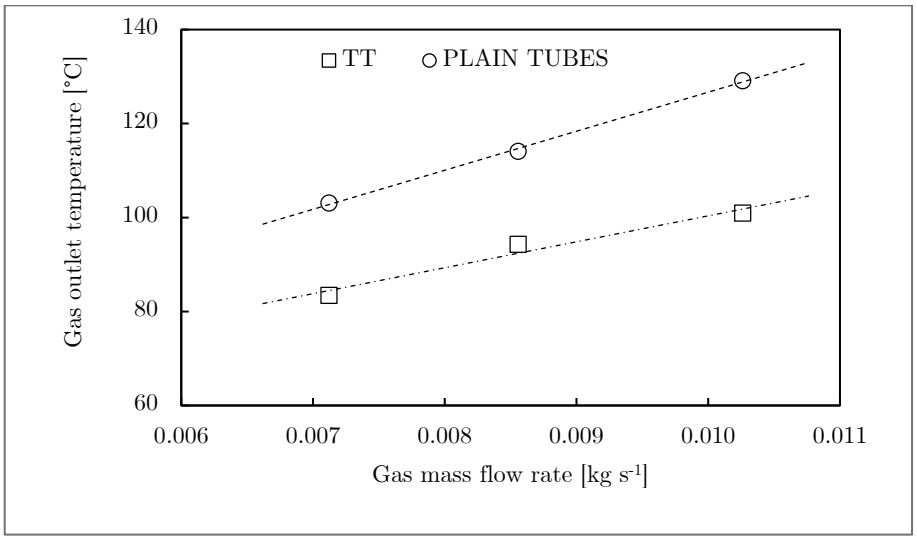

Figure 56. Syngas outlet temperature.

Table 12. Experimental results from the test campaign: gas mass flow and temperatures at inlet and outlet of the heat exchanger.

$\dot{m}_{gas}$ [kg s^{-1}]	TWISTED TAPES		PLAIN TUBES	
	$T_{gas,in}$ [°C]	$T_{gas,out}$ [°C]	$T_{gas,in}$ [°C]	$T_{gas,out}$ [°C]
$7.12 \cdot 10^{-3}$	234.4	83.4	237.6	103.1
$8.56 \cdot 10^{-3}$	271.3	94.3	264.0	114.1
$1.03 \cdot 10^{-2}$	305.6	100.9	300.5	129.1

The pressure drop of the heat exchanger was noticed to be negligible if compared to the total pressure drop of the gasification and filtering stage of the power plant (attested to 5÷10 kPa).

5.4 Chapter summary

In this work, twisted tape inserts were applied to a water-gas heat exchanger used to cool down the producer-gas generated from a small-scale wood gasification power plant. Results shown an increase of the overall *HTC* between 57 and 76 % and of the thermal power output from 12 to 19 %. Further tests are needed in order to assess the long-term performances of the system and the influence of pipes fouling on heat transfer. The *TT* applied to the *HX* were not

increasing the pressure drop of the device in a meaningful way. For this reason, the HX, in this configuration, does not affect engine performance in terms of volumetric efficiency and, therefore, in terms of maximum electrical power output.

5.5 Future works

5.5.1 Fouling effect in a tubes-in-shell heat exchanger with twisted tape inserts applied to a small-scale biomass gasification power plant

During the several hours of tests shown in this chapter it was noticed that the gas temperature difference between inlet and outlet increase, leading to an increased effectiveness of the heat exchanger during the first hours of run. The heat exchanger maintenance after the tests shown a reduced clearance between the twisted tapes and the tubes due to the deposition of soot and tar contained in the gas stream (Figure 58). According to the literature findings (Al-Fahed et al., 1996; Ayub et al., 1993), the fouling seems to generate a tight-fit configuration that tends to increase the heat transfer coefficient, more than counterbalance the reduction of HTC due to soot layer formation (Figure 57). In Figure 59 the temperature trend is shown and further studies should be conducted to address the duration of this phenomenon over the lifetime of the heat exchanger.

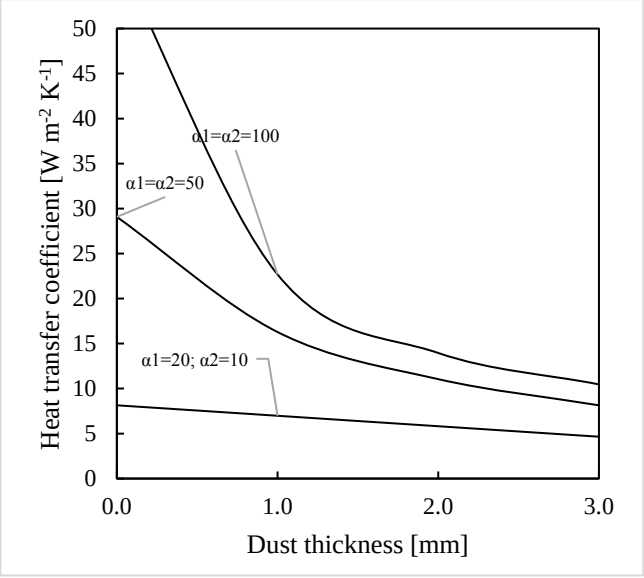

Figure 57. Influence of the dust film formation on the HTC of cooling surfaces. α_1 and α_2 are the convective HTC at the gas and air side respectively. (SERI, 1979)

Figure 58. Soot deposition on the top of the heat exchanger: rack of twisted tapes after the tests.

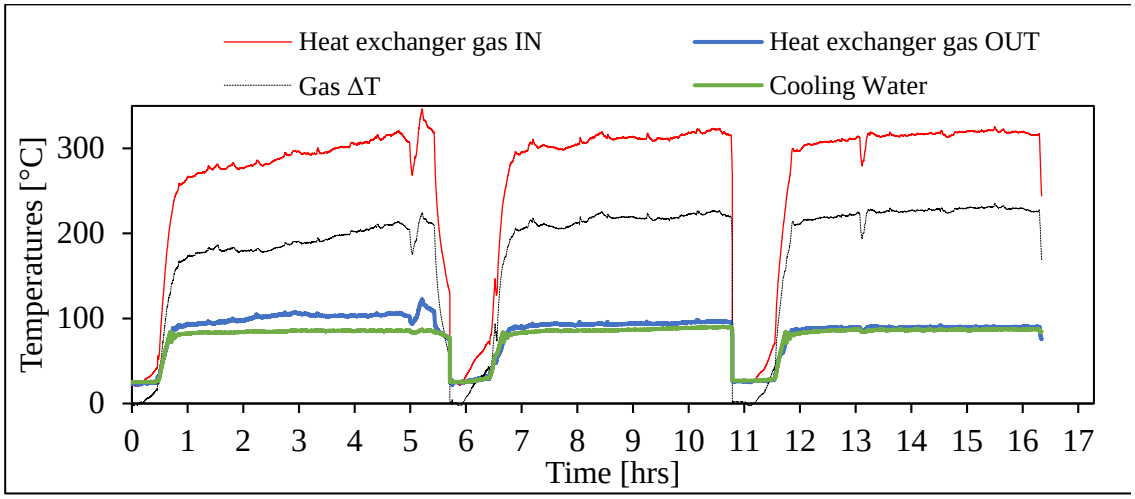

Figure 59. Temperature trends during the tests at constant engine power output. The increasing temperature difference is shown.

5.5.2 Enhanced heat transfer in tubes-in-shell heat exchanger for syngas cooling: a comparison between conventional and perforated twisted tape inserts

Perforated twisted tapes are known to perform better in terms of pressure loss maintaining the same effectiveness of plain tapes (Bipin et al., 2018; Eiamsa-ard et al., 2012). For this reason, two different sets of tapes will be tested in the same tubes in shell HX as shown in this chapter. The twisted tapes have the length of 1.6 m and the width of 33 mm in order to guarantee a sufficient clearance between the tape and the tube (36 mm ID), even in presence of soot deposition. The pitch of the tapes was set to 82.5 (calculated on 180°) and the second set of tapes has, in addition, equispaced square holes. A comparison between the two sets of tapes will be carried out by evaluating the heat transfer coefficient (HTC), the pressure loss and the total amount of thermal power transferred from the syngas to the coolant.

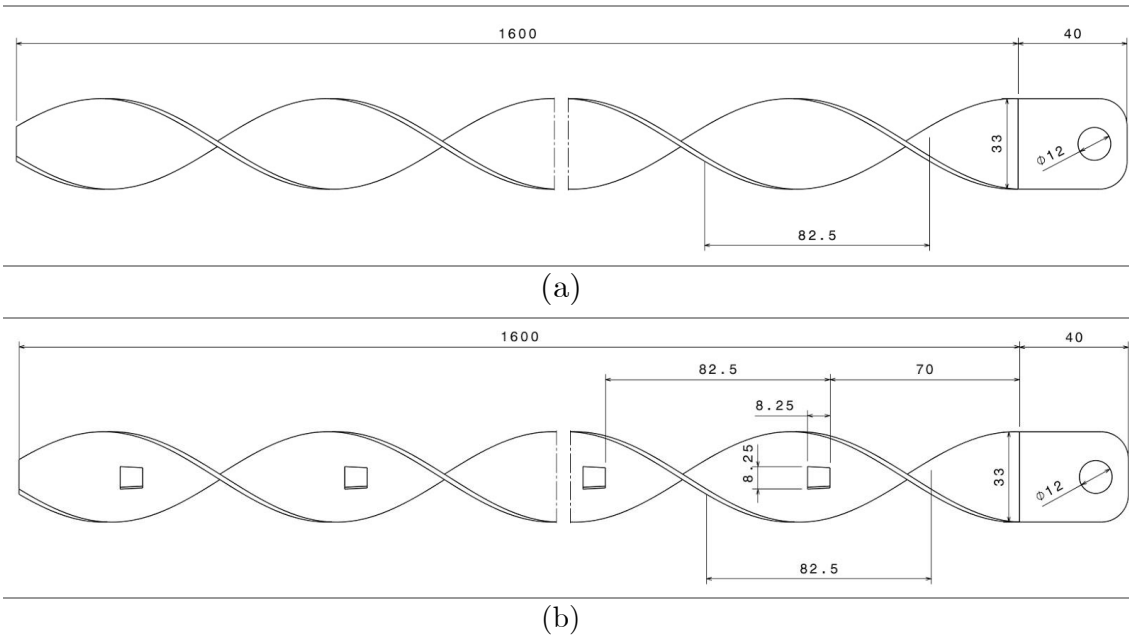

Figure 60. Designed twisted tape object of the tests: (a) plain tapes and (b) perforated tapes.

Chapter 6

Use of fabric filters for syngas dry filtration in small-scale gasification power systems

6.1 Introduction

The main objective of this chapter is the study of the effectiveness and efficiency of a baghouse filtering system for the producer gas generated by the PP30 downdraft gasifier system made by All Power Labs. As mentioned in Table 6 the syngas produced contains pollutants such as tar and particulate matter that must be kept under 30 mg Nm^{-3} and 50÷100 mg Nm^{-3} respectively to prevent the engine failure (Milne et al., 1998; Quinlan et al., 2017a; Quinlan et al., 2017b). Tar and particulate are not the sole contaminants in the gas stream, in fact a significant amount of steam (Allesina et al., 2017a) ranging from 1 % to 8 % can be found in the gas stream (Puglia et al., 2017).

For this purpose, a filtering system that works above the water dew point of the producer gas is needed to avoid tarry water condensation. Water requires specific disposal procedures that increase the variable costs of the plant. For this reason, the water-gas heat exchanger described in chapter 5 was used to control the temperature of the gas stream entering the filtration stage and, considering the commercial nature of the gasifier, several standard filtering bags were tested.

Tests were carried out using different bag materials such as polypropylene (PP), polyester (PE), PTFE coated fabric[8] and different filtering meshes ranging from 1 to 5 micron were compared too.

If the minimum working temperature of the filter is important to avoid the light tar and water condensation, the maximum working temperature is determined by the material of the bags, ranging from 120 to 150 °C. For this reason, during each test the filter temperature was measured at the filter outlet and, since the

[8] A micrometric PTFE layer is deposited over a polypropylene support increasing the filtration performances of the bag and activating the surface filtration process.

pressure drop generated by the filtration stage strongly affects the engine performances, the gauge pressures at the filter inlet and outlet, were measured too.

To assess the filtration performances, tar content gravimetric tests were performed using a simplified methodology taken by the tar sampling procedure (CEN 143). The tests shown that the behavior of the bags in terms of pressure drop is strongly correlated to the formation of condensates on them and that this can be reduced by maintaining the working temperature of the filter above the calculated (Allesina et al., 2017a) syngas dew point. Felt bags seemed to be more prone to get drenched compared to PTFE coated bags that gave higher but stable pressure drop during all the runs.

It has been proven that the Power Pallet has remarkable performances even fueling it with agricultural and river maintenance residues (Allesina et al., 2018c; Pedrazzi et al., 2017). In order to standardize the biomass entering in the system and then to keep the reactor operation under control, during these tests, the Power Pallet was feed with standard pine wood pellets mixed with vine pruning pellet.

6.2 Materials and methods

6.2.1 Syngas filtration system

On the Power Pallet 30, the filtration system is divided into two different stages. The first stage is composed by a single cyclone tasked with removing the majority of the soot that is collected in a sealed vessel on the base of the cyclone. In this first stage, the gas is filtered at temperatures that range from 300 °C to 550 °C not allowing the condensation of the tar contained into the gas stream (Reed, 1988). The adopted cyclonic separator is effective only for hundreds of microns large particles and, for this reason, a second stage was necessary in order to trap the remaining soot and tar aiming at concentrations for this pollutants that are respectively of 30 mg Nm^{-3} for the soot and between 50-100 mg Nm^{-3} for tar (Milne et al., 1998).

The second stage is made by a round SS vertical vessel in which 4 fabric bags are placed. The vessel is 420 mm diameter, 900 mm tall and it is clamped at the bottom to the “base-pan” and at the top to its lid that provides the connection for the gas outlet. The fabric bags are connected by means of clamps to 4 metal collars, 140 mm diameter, that are welded on a plate to the base-pan (b).

Since the gas exists from the cyclone from 250 °C to 450 °C and the second filtering stage materials has a limiting temperature due to the materials of the bags, a gas-water heat exchanger (*HX*) is placed between the cyclone and the filter vessel. The *HX* is a tubes in shell type with gas into the tubes and water in the shell. As cooling fluid, the coolant liquid of the engine was used. During normal engine operation, the temperature of the coolant ranges from 78 to 90 °C and this enables us to keep the minimum temperature of the gas stream under control, avoiding the condensation of the water that is carried in the gas in vapor phase.

In Figure 61a a schematic of the gasification facility is shown (p,T indicates the pressure and temperature logging port while TSP 1 and TSP 2 represent the gas sampling ports respectively for the pre and post filter measurements) and Figure 61c shows a picture of the installation of 4 fabric bags.

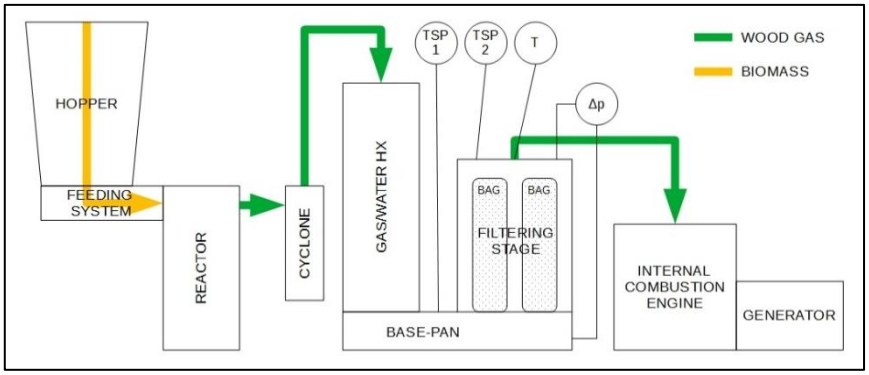

(a)

(b)

(c)

(d)

Figure 61. A schematic of the gasification facility with the instrumentation used during the tests (a). In (b) a picture of the collar where the bag are clamped at and in (c) a phase of the bags replacement.

6.2.2 Filter bags description and test methodology

Since the PP30 is designed for power-on-demand applications it is necessary to take into account the effect of the tar and water vapors condensation on the fabric bags during the cool down period (e.g. overnight). For this reason, a first series of tests was carried out on the finest mesh bags commercially available (1 µm PTFE coated bags and 1 µm PE felt bags - Figure 62 and Figure 63) in order to investigate the effect of condensation phenomena over the fabric. The PTFE layer is deposited over a PP support that reduces the maximum working temperature to 120 °C, while, for the PE felt bags, the maximum operating temperature is 150 °C. During each test the bags were subjected to periods of run and periods of cooling down. Temperature and pressure drop across the filtering stage were logged with the aim of tracking the dependency of the two measured properties over time.

A second series of tests was conducted to assess the effectiveness of pre-coating the felt bags using the part of the biochar byproduct that the gasification plants generates during operation and stores under the cyclonic separator.

In this case, two sets of new 5 µm polyester felt bags were consequently tested both with and without the pre-coating. For each run, the filter temperature and pressure drop were logged and a series of gas sampling were performed to investigate the concentration of PM and tar down and upstream the filtering stage during several hours of running.

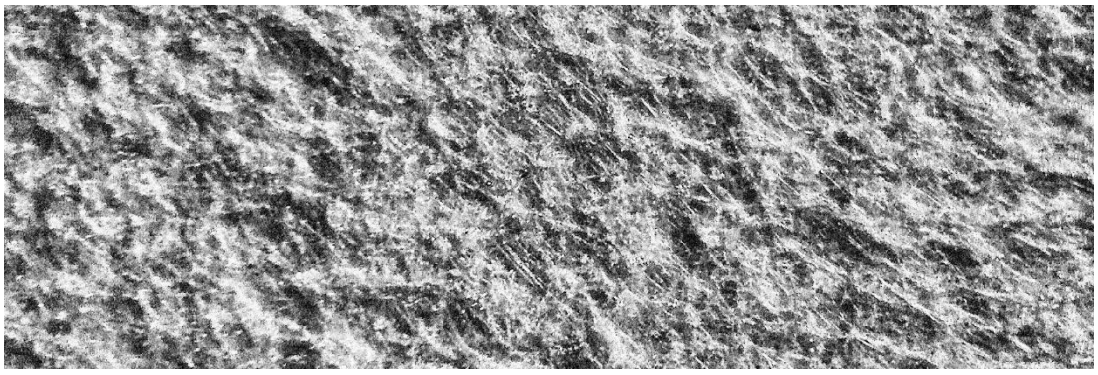

Figure 62. Texture of the filtrating mesh of a PE bag.

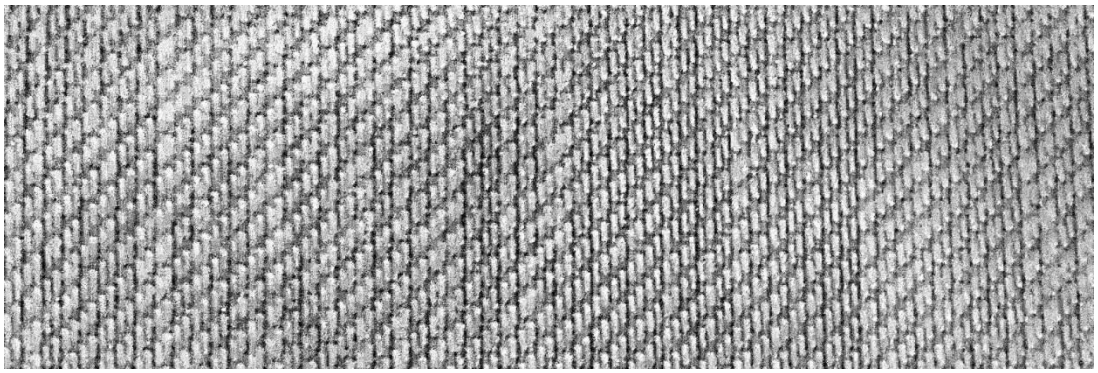

Figure 63. Texture of the PP filtrating support of a PTFE-coated bag.

6.3 Results and discussion

6.3.1 Producer gas vapors condensation: effect on felt filter bags

In Figure 64 a comparison between 1μm felt bags and membrane bags is shown. Both the tests were carried out after a run period of the bags and a subsequent overnight period, in order to simulate the typical discontinued use of the Power Pallet. The electrical power output of the engine was set at 14 kW_e to have a constant producer gas flow rate through the bags. The figure shows that PTFE bags generates more than four times the pressure drop of the felt bags at the same load condition. In the (b) plot is also shown a fast decrease in the pressure drop of the bags due to the failure of one of the four bags. Despite the failure, the pressure drop trend of the PTFE coated bags tends to increase during the hours of run while, as can be seen in (a), the felt bags were more prone to drenching phenomena that rises the pressure drop in the first moments of the test and tends to decrease with the increasing of the filter temperature.

For this reason, the drenching effect of the felt bags was investigated in a second series of tests and in Figure 65a a data-log of two consequent tests is shown. The test started with a new set of felt bags and, as reported in the plot, during the first run the pressure drop of the bags increases almost linearly. Then, the gasification power plant was turned off, sealed and let to cool down during overnight period and a new run was performed the day after. It can be seen, in the second part of the plot, that the pressure drop increases rapidly during the first minutes of operation, then, as soon as the filter temperature reaches almost 40°C the pressure drop starts to decrease again. In the last part of the plot the linear trend of pressure drop increasing is fully recovered. Due to the higher pressure drop in the first moments of the second run, the electrical power output of the second test was lowered from 18 kW_e to 15 kW_e and this explains the lower pressure drop at steady state in last part of the second run.

In Figure 65b a magnification of the pressure drop trend inversion is shown. Steady state temperature profiles were noticed during the heating up period and are highlighted with black arrows in the plot.

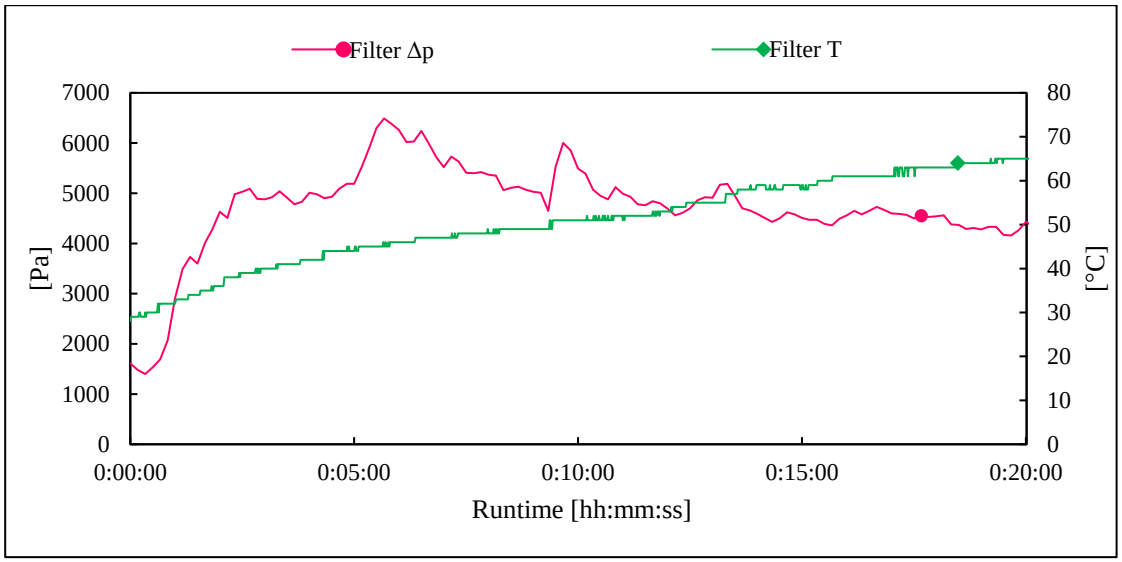

(a)

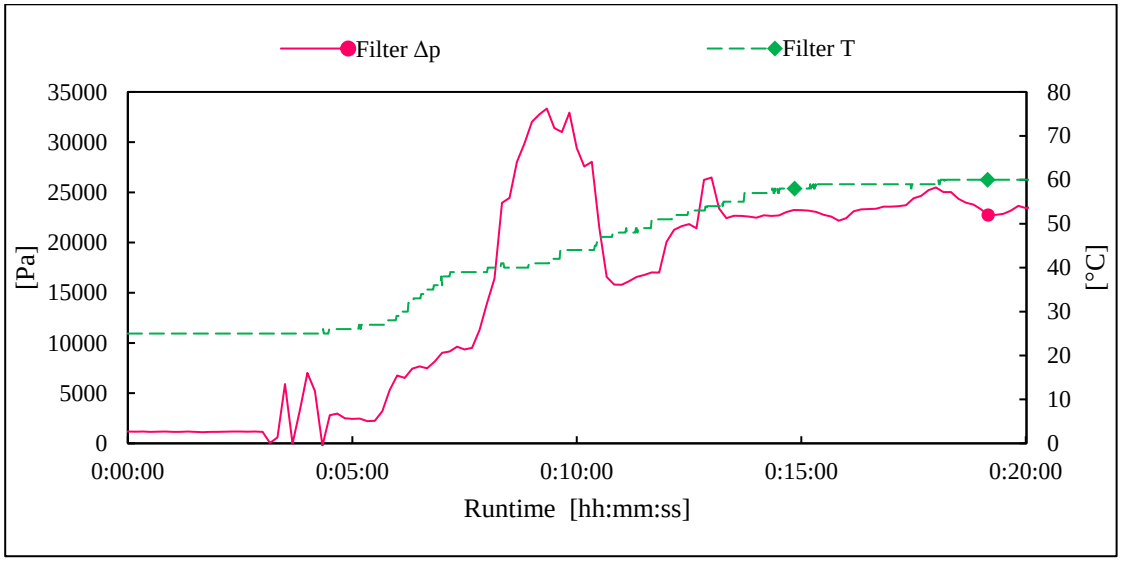

(b)

Figure 64. The plot (a) shows the pressure and temperature behavior of the polyester felt filter bags while in (b) the trend of PTFE polypropylene bags is shown.

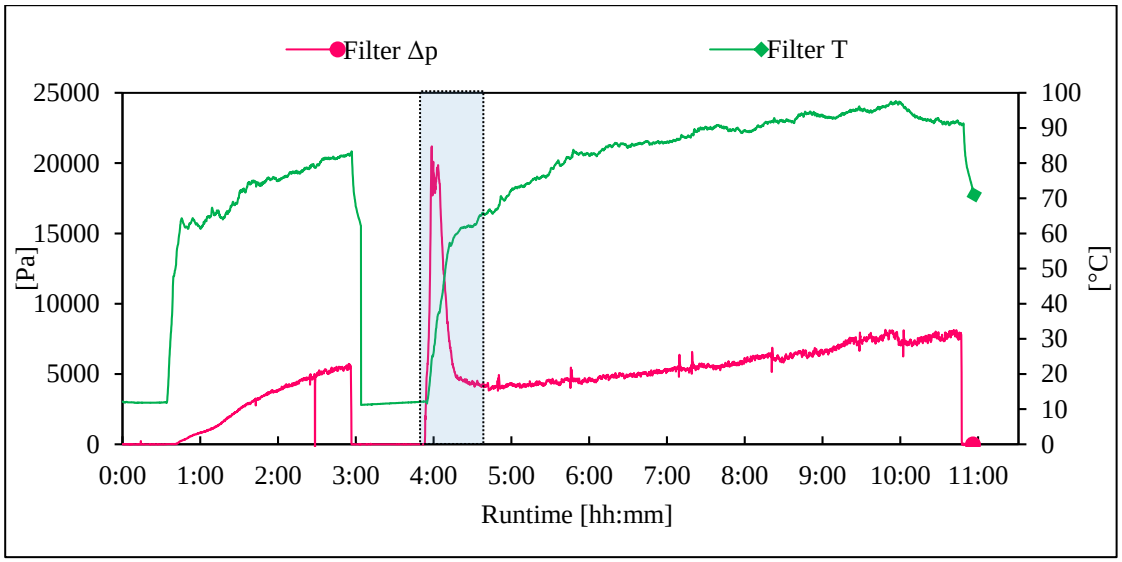

(a)

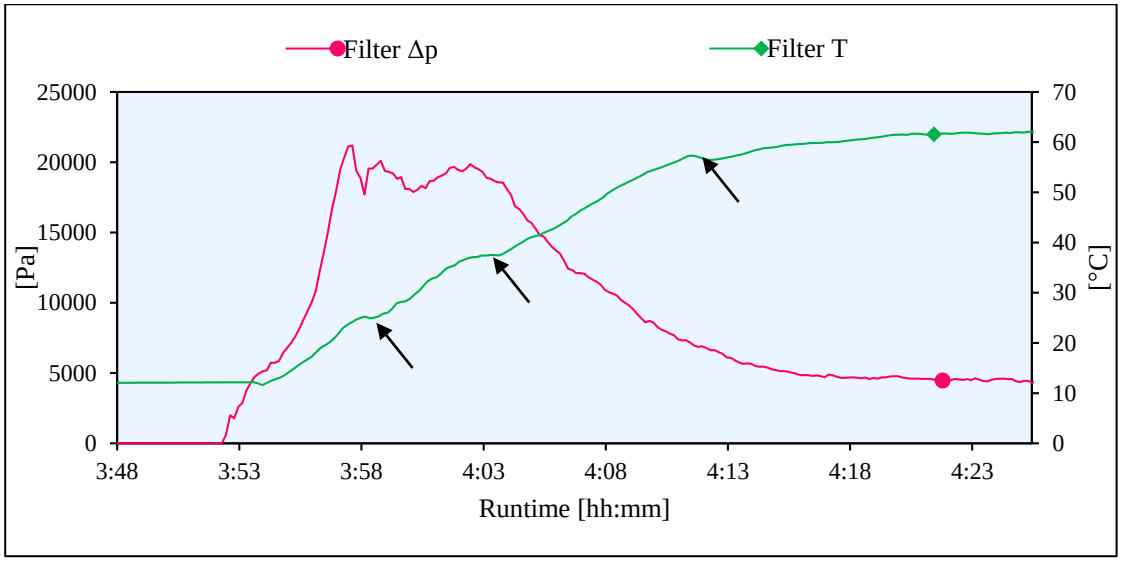

(b)

Figure 65. (a) two consequent runs on the PE 1µm felt bags. (b) magnification of the rectangle area that shows the dependency between filter temperature and filter pressure drop.

6.3.2 Filtration performances of felt bags: effect of pre-coating with char

In Table 13 the results of the gas sampling pollutants analysis is reported. Here the tested bags were the PE 5 μm felt bags and the cases are subdivided into non pre-coated felt bags and pre-coated ones. Each case has many sub-categories named from A to E that indicates a gas sample point during the test which is correlated to a specific age of the installed bags expressed in kWh_e of electrical energy generated from the engine connected to the gasification facility.

Table 13. Gas sampling results in terms of particulate matter and tar concentration before (PRE) and after (POST) the filtering bags. Comparison between not pre-coated and pre-coated bags.

			Particulate [mg Nm^{-3}]	Tar [mg m^{-3}]	Total electrical energy generated [kWh_e]
NOT PRE-COATED	A	PRE	339	1965	21.9
		POST	124	1543	
	B	PRE	219	1538	47.8
		POST	108	2284	
Bags replacement					
PRE-COATED	C	PRE	248	1502	18.0
		POST	188	1619	
	D	PRE	121	915	46.0
		POST	77	1256	
	E	PRE	176	1971	105.9
		POST	90	2173	

In Figure 66a the gas sampling results are shown and Figure 66b resumes the effectiveness of the filtering bags in capturing particulate matter and tars. It was noticed that for the not pre-coated bags the soot filtration effectiveness is stable around the 50-60% while for the pre-coated ones it is shown a rising trend for the soot filtration over time that ranges between the 24 %, with the bags brand new, and the 47 % after 105.9 kWh_e of electrical energy generated (approximately 7.5 h of engine running at 14 kW_e of electrical power output).

The same behavior was not noticed for tar that tends to incoherently increase passing through the filtering stage.

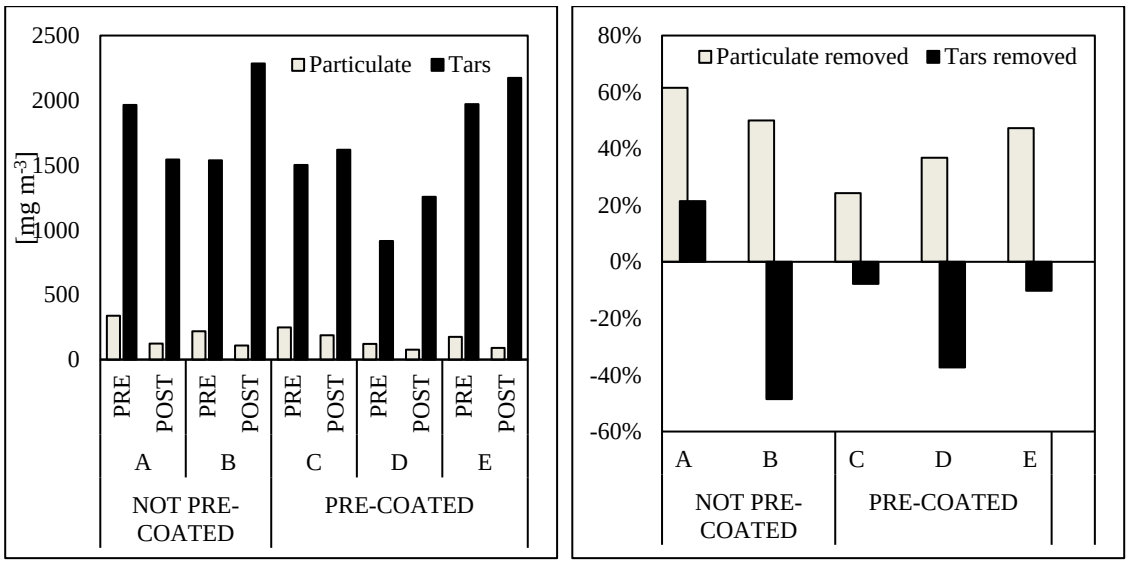

(a) (b)

Figure 66. The plot (a) shows the particulate and tar collected during the gas samplings shown in Table 13 while (b) reports the effectiveness of the bags in terms of particulate and tar removal.

In Figure 67 the comparison, in terms of pressure drop over time, between the pre-coated and not pre-coated 5 μm felt bags is shown. According to the previous test (Figure 65a), the not pre-coated bags maintain a linear trend of the pressure drop during the test, even if here (Figure 67) the values of Δp are lower because of the lower gas flow rate (lower engine electrical power output) and because of the higher spacing of the filtering mesh (5 μm instead of 1 μm). The pre-coated bags maintained a low value of Δp, even lower than the not pre-coated until the hour 2:30. Starting from that time, the pressure drop increased faster that what happened for the not pre-coated, and a nonlinear trend appeared.

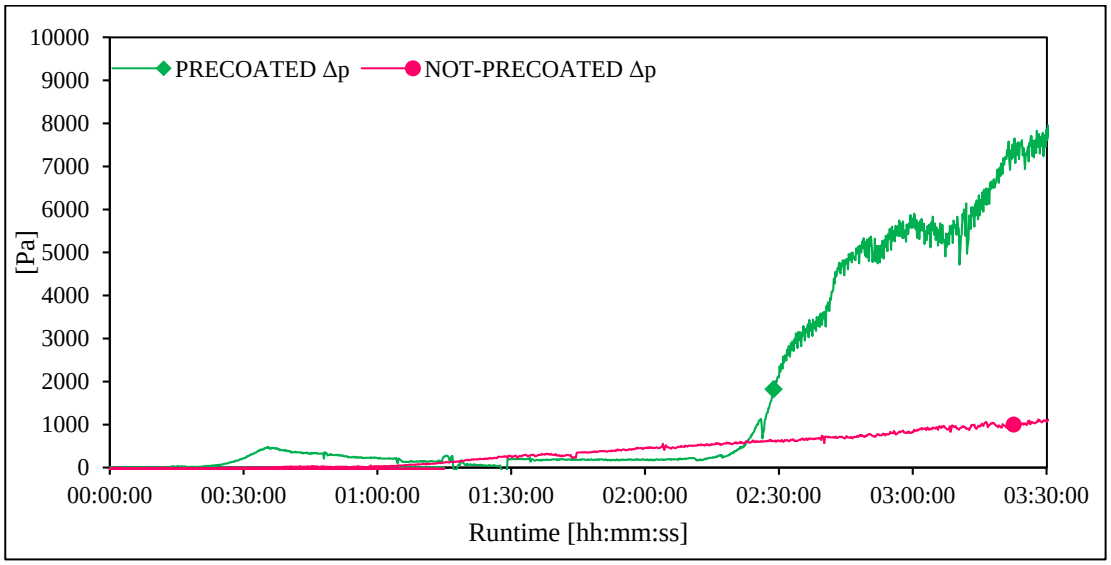

Figure 67. Comparison between the pressure drop over time both for the pre-coated and for the not pre-coated 5 μm felt bags.

6.4 Chapter summary

In this work, a series of comparisons were made in order to assess the effectiveness of fabric filter bags in the wood gas filtration of a commercial small-scale gasification power plant by All Power Labs. The comparison took into account different bag materials and it shown that PTFE bags tends to create a 4-time higher pressure drop at the same gas flow rate conditions and mesh spacing (1μm). This directly affects the volumetric efficiency of the engine, reducing then its maximum power output (Heywood, 1988). Moreover, PTFE-coated bags are not suited to resist to such high pressure drop (up to 30 kPa during the tests) and this caused rips in the bags with the consequent complete loss of the filtering effectiveness of the filtering stage.

On the other hand, felt bags are more prone to suffer of tar and water vapors condensation, during cool down periods of the power plants, generating high pressure drops at the subsequent startup. It was noticed that, if the producer gas flow rate is enough high to quickly heat up the filter stage, then the bags can be dried up and the pressure drop spike can be recovered. According to Figure 65b the drying process of the bags seemed to went through different compounds vaporization that generates steady filter temperature periods during filter heating up.

Lastly, a preliminary study on the effectiveness of the use of fine char for the bags pre-coating was carried out. Results shown that there is not the evidence that proof that the pre-coating increases the filtering performances of the bags.

In fact, the gas sampling campaign shown that the not pre-coated bags performed better in terms of PM filtering capacity, generating lower pressure drop if compared to the pre-coated ones.

The simplified tar sampling procedure adopted led to inconsistent results on the tar concentration in the gas, before and after the filtering stage: in most of the cases, higher concentrations of tar were measured downstream the filter. This could be caused by the fact that the soot is not separated at high temperature (300°C) from the gas stream but it is directly collected in the isopropyl alcohol along with tars. A standard tar sampling procedure should be adopted in order to properly estimate the pollutant content in the gas stream. Moreover, the time that the PP30 needs to reach steady state conditions is comparable to the duration of the tests reported in this chapter. Longer tests will likely increase the reliability of the simpler procedure adopted, reducing the transient effects of the filter bags warming up.

Concluding, the PM and tar concentration measured during the tests are higher than what the literature suggest as a maximum limit for wood gas used to fuel internal combustion engine. However, a cost-benefit analysis should be carried out in order to assess when is worth to increase the complexity and performances of the filtration stage instead of accepting higher O&M cost on the engine side. Future works should aim to investigate the effect of biomass quality on tar and PM production during the gasification process. The implementation of a numerical model based on (Pedrazzi et al., 2012; Allesina et al., 2013) should be explored in order to correlate the expected gasification efficiency to the lifespan of the filter bags.

Chapter 7

Concluding remarks

This research aims at the investigation and implementation of a series of technical solutions to define the boundaries of a simple and effective filtration system for small-scale biomass gasification power plants. In Chapter 1, a brief introduction to the European energy scenario is reported, showing the key role of biomasses in fulfilling the target of renewable share in the next decades.

Among the different biomass-to-energy processes presented, the gasification is still the most promising for the combined heat and power generation in small-scale applications. At this scale, the internal combustion engine is the most common end-user application, which guarantees high energy conversion coefficient, compactness and low investments but has strong limits on the contaminants concentration in the producer gas. It is shown in Chapter 3, how tar condensation and soot deposition can cause the failure of engine components. In particular, the case of the air-fuel mixture throttle valve was studied, investigating the phenomenon of tar and water condensation across the throttle plate at partial engine load. It was found that the coupling of numerical and psychrometric models is a reliable strategy to correlate the strong pressure and temperature drop across the governor with tar and water condensation. As output of the models combination, condensation risk is reduced when the gas-air mixture is above 27 °C and the engine is running at wide open throttle ($>$ 37°).

Since the throttle opening angle (i.e. the engine load) is often imposed by the application, the only parameter that can still be conditioned to avoid condensation is the air-syngas mixture temperature, that can be varied by cooling or heating both the syngas or the mixing air. While the mixing-air temperature is an independent parameter, the syngas temperature is often related to the adopted filtration strategy and, as described in Chapter 2, warm cleanup systems has been identified as the most promising filtration systems for small-scale applications. In Chapter 4 the influence of filtration temperature and mixing-air temperature was investigated. This study was based on the Power Pallet 20 gasification facility, where the main filter was modified by introducing two candle filters filled with gasification char used as filtrating medium. This material, byproduct of the gasification process, was proven to be effective in the

filtration of the particulate matter but, as every barrier filtration system, its performances and pressure drop are sensible to the cake formation on the filtrating surface. It was found that tarry water condensation in the filter vessel can be avoided by maintaining the filter temperature above 60 °C, while temperatures higher than 80 °C reduce the filtration performance not guaranteeing a sufficient collection efficiency of tars within the filter medium. On the other side, engine mixture temperature of 70 °C was found to avoid tar and water condensation across the throttle body at every load conditions, reducing the maintenance interval. A temperature of the mixing-air above 80 °C is then suggested.

Filtration temperature plays thus a crucial role in tar and water management and attention must be paid in the design of a cooling system able to cool down the producer gas by maintaining this parameter within an acceptable range. For this reason, in the Power Pallet 30 the engine coolant is used to cool down the syngas by means of a gas-water heat exchanger, providing a stable and fixed syngas temperature (80-100 °C) at the filter inlet in any weather condition. Engine coolant is often used in gasification power plants because it keeps the syngas above the water dew point, avoiding thus the generation of tarry water. In Chapter 5, the standard producer gas cooling system of the PP30 was replaced with a tubes and shell heat exchanger with syngas in the tubes and engine coolant in the shell. Having the producer gas in the tubes gives the opportunity to test different methods of heat transfer enhancing in the gas side and the study focused on the investigation of twisted tapes inserts effect in enhancing the gas heat transfer coefficient. Results shown that the twisted tapes increase the thermal power output of the heat exchanger of 12÷19 % depending on the gas flow rate (i.e. the engine power output). Moreover, these devices can be, at the same time, actuated as a cleaning mechanism of the tubes increasing the maintenance interval of the heat exchanger. Future works need to assess both the effect of tape-tube clearance on the heat exchange effectiveness and the enhancing performances of perforated twisted tapes in terms of drag and HTC compared to standard ones.

The heat exchanger described in Chapter 5 and the flexibility of the PP30, paved the way for the implementation and testing of a filtration system that reduces the O&M costs and time if compared to the char candles filter. Staying within the warm gas cleanup system, the standard filter was replaced with 4 cloth filters, testing different mesh size (from 1 to 5 µm) and different cloth material (PTFE-coated and PE). The tests reported in Chapter 6 proves that PE felt bag-house filters are suitable for small-scale gasification power plant applications if the filter temperature is kept above 60 °C, confirming the findings of the study in Chapter 4. Under this temperature, cloth filters tend to suffer of tar and water

condensation over the fabric that generates high pressure drops affecting the maximum power output of the internal combustion engine.

This thesis condenses the experimental and numerical work done in the woody biomass gasification field during the PhD course in Industrial and Environmental Engineering. As a conclusion, in small-scale biomass power plant, the filtration strategy seems to be more focused on cost reduction rather than performance targets, aiming at *reducing* instead of *solve* tar and particulate matter collection problem. The tests reported in this work shown the effectiveness of tubes-and-shell HX and bag-house filter coupling. The application of twisted tape inserts in syngas cooling opens new research paths for compact and cost-effective solutions in syngas conditioning.

List of Tables

List of Figures

Bibliography

Abatzoglou N., N. Barker, P. Hasler, and H, Knoef, The Development of A Draft Protocol for the Sampling and Analysis of Particulate and Organic Contaminants in the Gas from Small Scale Gasifiers. Version 1998. *Biomass and Bioenergy*, Vol. 18, pp. 5-17, 2000.

Abdoulmoumine N., Adhikari S., Kulkarni A., Chattanathan S., 2015. A review on biomass gasification syngas cleanup. *Appl. Energy*, Vol. 155 pp. 294-307, 2015.

Ahmad A. A., Zawawi N. A., Kasim F. H., Inayat A., Khasri A., Assessing the gasification performance of biomass: A review on biomass gasification process conditions, optimization and economic evaluation. *Renewable and Sustainable Energy Reviews*, Vol. 53 pp. 1333–1347, http://dx.doi.org/10.1016/j.rser.2015.09.030, 2016.

Ahmed O. Y., Ries M. J., Northrop W. F., Emissions factors from distributed, small-scale biomass gasification power generation: Comparison to open burning and large-scale biomass power generation. *Atmospheric Environment*, Vol. 200, pp. 221–227, 2019.

AI-Fahed S., Chakroun W., Effect of tube-tape clearance on heat transfer for fully developed turbulent flow in a horizontal isothermal tube. *Int. J. Heat and Fluid Flow*, Vol 17 pp 173-178, 1996.

Akagi, S.K., Yokelson, R.J., Wiedinmyer, C., Alvarado, M.J., Reid, J.S., Karl, T., Crounse, J.D., Wennberg, P.O., Emission factors for open and domestic biomass burning for use in atmospheric models. *Atmos. Chem. Phys.* 11, 4039–4072, 2011.

All Power Labs, GEK Gasifier Datasheet, www.allpowerlabs.com

Allesina G., Experimental and analytical investigation of downdraft stratified gasifiers, Ph.D. Thesis, Dept. of Engineering "E. Ferrari", Modena, Italy, 2013a.

Allesina G., Pedrazzi S. and Tartarini P., Modeling and investigation of the channeling phenomenon in downdraft stratified gasifiers. *Bioresource Technology*, Vol. 146 pp. 704-712, 2013b.

Allesina G., Pedrazzi S., Allegretti F., Morselli N., Puglia M., Santunione G. and Tartarini P. Gasification of cotton crop residues for combined power and

biochar production in Mozambique. *Applied Thermal Engineering*, vol. 139 pp. 387-394, 2018c.

Allesina G., Pedrazzi S., Ginaldi F., Cappelli G. A., Puglia M., Morselli N. and Tartarini P., Energy production and carbon sequestration in wet areas of Emilia Romagna region, the role of Arundo Donax. *Advances in Modelling and Analysis A*, Vol. 55 (3) pp. 108-113, 2018b.

Allesina G., Pedrazzi S., Montermini L., Giorgini L., Bortolani G. and Tartarini P., Porous filtering media comparison through wet and dry sampling of fixed bed gasification. *J. Phys. Conf. Series*, vol. 547, 2014.

Allesina G., Pedrazzi S., Puglia M., Morselli N., Allegretti F., Tartarini P., Gasification and Wine Industry: Report on the Use Vine Pruning as Fuel in Small-scale Gasifiers *European Biomass Conference and Exhibition Proceedings (26thEUBCE)* pp. 722-725, 2018a.

Allesina G., Pedrazzi S., Puglia M., Morselli N., Mason J., Tartarini P., Multi-phase fluid dynamic of syngas flow across a throttle body in a gasifier-engine system. *European Biomass Conference and Exhibition Proceedings (25thEUBCE),* pp. 738-742, 2017a.

Allesina G., Pedrazzi S., Puglia M., Tartarini P., A psychrometric approach to fixed bed biomass gasifier design. *23th European Biomass Conference and Exhibition, Wien, Austria*, 2015a.

Allesina G., Pedrazzi S., Rinaldini C.A., Di Paola G, Morselli N, Savioli T, Vidoni A, Mattarelli E, Tartarini P. Effect of Syngas-CNG co-combustion on automotive engines for micro CHP applications. *ASME-ATI-UIT Conference 2015*, Napoli, Italy, 17-20 May, 2015b.

Allesina G., Pedrazzi S., Sgarbi F., Pompeo E., Roberti C., Cristiano V., Tartarini P., Approaching sustainable development through energy management, the case of Fongo Tongo, Cameroon. *International Journal of Energy and Environmental Engineering*, Volume 6, Issue 2, pp 121–127, 2015c.

Allesina G., Pedrazzi S., Tebianian S. and Tartarini P., Biodiesel and electrical power production through vegetable oil extraction and byproducts gasification: Modeling of the system. *Bioresource Technology*, vol. 170 pp. 278-285, 2014b.

Allesina, G., Pedrazzi, S., Guidetti, L., Tartarini, P., Modeling of coupling gasification and anaerobic digestion processes for maize bioenergy conversion. *Biomass and Bioenergy*, Vol. 81 pp. 444–451, 2015d.

Anca-Couce A., Reaction mechanisms and multi-scale modelling of lignocellulosic biomass pyrolysis. *Prog Energy Combust Sci.*, Vol. 53 pp. 41–79, 2016.

Arthur M. James R,Wenqiao Yuan,Michael D. Boyette,Donghai Wang, Airflow and insulation effects on simultaneous syngas and biochar production in a top-lit updraft biomass gasifier, *Renewable Energy*, Vol. 117 pp 116-124, 2018.

Atimtay A. T., Cleaner energy production with integrated gasification combined cycle systems and use of metal oxide sorbents for H2S cleanup from coal gas. *Clean Technol Environ Pol,* Vol. 2(4) pp. 197-208, 2001.

Aurell, J., Gullett, B.K., Tabor, D., Emissions from southeastern U.S. grasslands and pine savannas: comparison of aerial and ground field measurements with laboratory burns. Atmos. Environ. 111, 170–178, 2015.

Ayub Z. H., AI-Fahed S. F., The effect of gap width between horizontal tube and twisted tape on the pressure drop in turbulent water flow. *Int. J. Heat and Fluid Flow*, Vol. 14, No. 1, 1993.

Banja M., Jégard M., Motola V., Sikkema R, Support for biogas in the EU electricity sector – A comparative analysis. *Biomass and Bioenergy*, 2019.

Beachler D.S., Joseph J., Pompelia M., Fabric filter operation review. North Carolina State University, EPA Cooperative Assistance Agreement CT-901889, 1995.

Beenackers A. A. C. M., Van Swaaij W. P. M., Gasification of biomass, a state of the art review (keynote paper). *Thermochemical Processing of Biomass. London*, UK: Butterworth's, pp. 91–136, 1984.

Beohar H., Gupta B., Sethi V.K., Pandey M., Parametric study of fixed bed biomassvgasifier: a review. *Int J Therm Technol* Vol. 2(1) pp. 134–40, 2012.

Bethea R. M., Air pollution control technology: an engineering analysis point of view. 1978.

Bhattachary S. C., Hla S. S., Pham H. L., A study on a multi-stage hybrid gasifier engine system. *Biomass and Bioenergy*, Vol. 21 pp. 445-60, 2001.

Bhattacharya, S.C., Albina, D.O., Salam, P.A., Emission factors of wood and charcoal-fired cookstoves. Biomass Bioenergy 23, 453–469, 2002.

Bhuiya M.M.K., M.S.U. Chowdhury, M. Shahabuddin, M. Saha, L.A. Memon, Thermal characteristics in a heat exchanger tube fitted with triple twisted tape inserts, Int. Commun. *Heat Mass Transf.,* Vol. 48 pp. 124–132, 2013.

Bipin K., Gaurav P. S., Manoj K., Anil K. P., A review of heat transfer and fluid flow mechanism in heat exchanger tube with inserts. *Chemical Engineering & Processing: Process Intensification* Vol. 123 pp 126–137, 2018.

Bisht A. S., Thakur N. S., Small scale biomass gasification plants for electricity generation in India: Resources, installation, technical aspects, sustainability criteria & policy. *Renewable Energy Focus*, Vol. 28, 2019.

Bocci E., Sisinni M., Moneti M., Vecchione L., Di Carlo A., Villarini M., State of art of small scale biomass gasification power systems: a review of the different typologies. *Energy Procedia*, Vol 45, pp. 247 – 256, 2014.

Borjesson M., Ahlgren E. O., Biomass gasification in cost-optimized district heating systems – A regional modelling analysis. *Energy policy,* Vol. 34 pp. 168-180, 2010.

Brammer J.G., Bridgwater A.V., The influence of feedstock drying on the performance and economics of a biomass gasifier–engine chp system. *Biomass and Bioenergy*, Vol. 22(4) pp. 271–281, 2002.

Breag. G.R, Harker. A.C., Hollingdale, A.C..and Pearce, Experimental 1i'ials on a Spark Ignition Engine Fueled by Producer Gas from Charcoal to Provide up lo 4 kW Shaft Power, Report of the Tropi cal Products Institute, 56162 Gray's Inn Road, London WCIXBLU, England, Publication t50, ISBN 0-85954-154-1.

Bridgwater A.V., The technical and economic feasibility of biomass gasification for power generation. *Fuel*, Vol 74, pp. 631–653, 1995.

Brown R. C., Introduction to thermochemical processing of biomass into fuels, chemicals, and power. *Thermochemical processing of biomass. Conversion into fuels, chemicals and power.* Brown R. C., editor. Chichester: Wiley, pp. 1–12, 2011.

Buragohain B., Mahanta P., Moholkar V. S., Biomass gasification for decentralized power generation: The Indian perspective. *Renewable and sustainable energy reviews*, Vol. 14 pp. 73-92, 2010.

Burhenne L., Rochlitz L., Lintner C., Aicher T., Technical demonstration of the novel Fraunhofer ISE biomass gasification process fort he production of a tarfree synthesis gas. *Fuel Process Technol*, Vol. 106 pp. 751e60, 2013.

Callé S., P. Contal D. Thomas, D. Bémer, D. Leclerc, Evolutions of efficiency and pressure drop of filter media during clogging and cleaning cycles, *Powder Technol.*, Vol. 128 pp. 213–217, 2002.

Campbell J. E., Block E., Land-use and alternative bioenergy pathways for waste biomass. *Environ. Sci. Technol.*, Vol. 44, pp. 8665–8669, 2010.

Campuzano F., Brown R. C., Martínez J. D., Auger reactors for pyrolysis of biomass and wastes. *Renewable and Sustainable Energy Reviews,* Vol. 102 pp. 372–409, 2019.

Cashco, Fluid flow basics of throttling valves, Technical Report, 2017.

CEN BT/TF 143 "Organic contaminants ("tar") in biomass producer gases".

Cengel Y. A., Introduction to thermodynamics and heat transfer. McGraw-Hill, 1997.

Chaves L. I., da Silva M. J., de Souza S. N. M., Secco D., Rosa H. A., Nogueira C. E. C., Frigo E. P., Small-scale power generation analysis: Downdraft gasifier coupled to engine generator set. *Renewable and Sustainable Energy Reviews*, Vol. 58 pp. 491–498 http://dx.doi.org/10.1016/j.rser.2015.12.033, 2016.

Chawdhury M. A., Mahkamov K., Development of a small downdraft biomass gasifier for developing countries, *J Sci Res*, Vol. 3 pp. 51–64, 2013.

Chokphoemphun S., M. Pimsarn, C. Thianpong, P. Promvonge, Thermal performance of tubular heat exchanger with multiple twisted-tape inserts. *Chin. J. Chem. Eng.*, Vol. 23 pp. 755–762, 2015.

Chopra S., Jain A. K., A review of fixed bed gasification systems for biomass. *Agric Eng Int*: CIGR E-J 2007;9, [ISSN:1682-1130], 2007.

Christian, T.J., Kleiss, B., Yokelson, R.J., Holzinger, R., Crutzen, P.J., Hao, W.M., Saharjo, B.H., Ward, D.E., Comprehensive laboratory measurements of biomass-burning emissions: 1. Emissions from Indonesian, African, and other fuels. J. Geophys. Res. 108 (D23), 148–227, 2003.

Cui H., Turn S. Q., Keffer V., Evans D., Tran T., Foley M., Contaminant Estimates and Removal in Product Gas from Biomass Steam Gasification, *Energy Fuels,* Vol. 24 pp. 1222–33, 2010.

Cummer K. R., Brown R. C., Ancillary equipment for biomass gasification. *Biomass Bioenerg,* Vol. 23(2) pp. 113-28, 2002.

Dagle R. A., Ayman Karim, Guosheng Li, Yu Su, David L. King, Syngas Conditioning. Pacific Northwest National Laboratory, 902 Battelle Boulevard, Richland, WA 99352, USA *Fuel Cells: Technologies for Fuel Processing* pp. 361-408, 2011.

Del Toro A., Computational Fluid Dynamics Analysis of Butterfly Valve Performance Factors. All Graduate Theses and Dissertations. Paper 1456. Utah State University, 2012.

Demirbas A., Arin G., An overview of biomass pyrolysis, *Energy Sources* Vol. 24 pp. 471–482, 2002.

Devi L., Ptasinski K. J., Janssen F. J. J. G., A review of the primary measures for tar elimination in biomass gasification processes. *Biomass Bioenergy*, Vol. 24 pp. 125–40, 2003.

EC-Bioeconomy-KC, *European Commission's Knowledge Center for Bioeconomy*, doi:10.2760/546943, 2019.

ECN, Energy research Centre of the Netherlands. Phyllis2, database for biomass and waste. 2017 https://phyllis.nl/Browse/Standard/ECN-Phyllis#3121 , Accessed date: 22 November 2019.

ECN, website for tar dew point calculations of Energy research Centre of the Netherlands (ECN). ⟨http://www.thersites.nl/⟩. Accessed date: 31 December 2019.

Eiamsa-ard S., C. Thianpong, P. Eiamsa-ard, Turbulent heat transfer enhancement by counter/co-swirling flow in a tube fitted with twin twisted tapes, *Exp. Therm Fluid Sci.* Vol. 34 pp. 53–62, 2010.

Erbach G., Promotion of renewable energy sources in the EU. *European Parliamentary Research Service Members' Research Service*, PE 583.810, doi:10.2861/062931EPRS, June 2016.

FAO Forestry Department Mechanical Wood Products Branch. Woodgas as engine fuel, volume ISBN 92-5-102436-7. F.A.O., 1986.

Ferrari G., Motori a combustione interna, Il capitello, 1996.

Fjellerup J., Ahrenfeldt J., Henriksen U., Gobel B., Formation, Decomposition and Cracking of Biomass Tars in Gasification. Technical University of Denmark – Department of Mechanical Engineering, Biomass Gasification Group, 2005.

Fritz H., Kern W., Reinigung von Abgasen (Flue gascleaning). Vogel, Wurzburg, 1990.

Gardner B., Guan X., Martin R. A., Spain J., Hot gas filtration meeting turbine requirements for particulate matter. *Reno-Tahoe, NV, United states: American Society of Mechanical Engineers*; pp.439-451, 2005.

Gautam G., Adhikari S., Gopalkumar S. T., Brodbeck C., Bhavnani S., Taylor S., Tar analysis in syngas derived from pelletized biomass in a commercial stratified biomass in a commercial stratified downdraft gasifier. *Bioresources*, Vol. 6(4) pp. 4652–61, 2011.

Glover J. D., M. Sarma, T. Overbye Glover, Power System Analysis and Design. 5th Edition. Cengage Learning. 2012.

Gonzalez P., Rong B. G., A review of the current state of biofuels production froml ignocellulosic biomass using thermochemical conversion routes, *Chinese Journal of Chemical Engineering* Vol. 27 pp. 1523–1535 https://doi.org/10.1016/j.cjche.2018.09.018, 2019.

Göransson K., Söderlind U., He J., Zhang W., Review of syngas production via biomass DFBGs. *Renew. Sust. Energy Rev.* Vol. 15(1) pp. 482-492, 2011.

Goyal H., Seal D., Saxena R., Bio-fuels from thermochemical conversion of renewable resources: a review. *Renewable and Sustainable Energy Reviews*, Vol. 12 pp. 504-517, 2008.

H. de Coninck, A. Revi, M. Babiker, P. Bertoldi, M. Buckeridge, A. Cartwright, W. Dong, J. Ford, S. Fuss, JC. Hourcade, D.Ley, R. Mechler, P. Newman, A. Revokatova, S. Schultz, L. Steg, T. Sugiyama, Strengthening and implementing the global response. In: Global warming of 1.5°C. *An IPCC Special Report on the impacts of global warming of 1.5°Cabove pre-industrial levels and related global greenhouse gas emission pathways, in the context of strengthening theglobal response to the threat of climate change, sustainable development, and efforts to eradicate poverty* [V. Masson-Delmotte, P. Zhai, H. O. Pörtner, D. Roberts, J. Skea, P.R. Shukla, A. Pirani, W. Moufouma-Okia, C. Péan, R. Pidcock,S. Connors, J. B. R. Matthews, Y. Chen, X. Zhou, M. I. Gomis, E. Lonnoy, T. Maycock, M. Tignor, T. Waterfield (eds.)]. In Press, 2018.

Han J., Kim H., The reduction and control technology of tar during biomass gasification/pyrolysis: an overview. *Renew Sustain Energy Rev,* Vol. 12(2) pp. 397e416, 2008.

Hasler P., Th. Nussbaumer, Gas cleaning for IC engine applications from fixed bedbiomass gasification. *Biomass and Bioenergy*, Vol. 16 pp. 385-395, 1999.

Heidenreich, S., Foscolo, P. U., New concepts in biomass gasification. *Prog. Energy Combust. Sci.* Vol. 46 pp. 72-95. http://dx.doi.org/10.1016/j.pecs.2014.06.002, 2015.

Henriksen U., Ahrenfeldt J., Jensen T. K., Gobel B., Bentzen J. D., Hindsgaul C., et al.,

Heywood J. B., Internal combustion engine fundamentals. Mc Graw Hill, 1998.

Hoel M., Sletten T. M., Climate and forests: The tradeoff between forests as a source for producing bioenergy and as a carbon sink. *Resource and Energy*

Economics Vol. 43 pp. 112–129 http://dx.doi.org/10.1016/j.reseneeco.2015.11.005, 2016.

Hoffmann A. C., Stein L. E., Gas cyclones and swirl tubes: principles, design, and operation. 2nd ed., vol. xxvi. Berlin ;New York: Springer; 422 pp, 2008.

Honga Y, Dua J, Lib Q, Xua T and Lia W 2019 Thermal-hydraulic performances in multiple twisted tapes inserted sinusoidal rib tube heat exchangers for exhaust gas heat recovery applications. *Energy Conversion and Management,* Vol. 185 pp. 271–290, 2019.

Hrbek J., Status report on thermal gasification of biomass and waste 2019. *IEA Bioenergy Task 33 special report*, 2019.

Huang J., Schmidt K. G., Bian Z., Removal and Conversion of Tar in Syngas from Woody Biomass Gasification for Power Utilization Using Catalytic Hydrocracking. Energies, vol. 4, pp. 1163-1177, 2011.

Hurley S., Xu C., Preto F., Shao Y., Li H., Wang J., et al., Catalytic gasification of woody biomass in an air-blown fluidized-bed reactor using Canadian limonite iron ore as the bed material, *Fuel*, Vol. 91 pp. 170–6, 2012.

IBI, 2013. International Biochar Initiative, Standardized Product Definition and Product Testing Guidelines for Biochar that is used in Soil. <http://www.biochar-international.org/sites/default/files/IBI_Biochar_Standards_V1.1.pdf>.

Imbert G., Patent Gas Producer US 1821263 A

IPCC, 2012. Renewable Energy Sources and Climate Change Mitigation. Special report prepared by Working Group III of the Intergovernmental Panel on Climate Change. *Intergovernmental Panel on Climate Change (IPCC)*, https://www.ipcc.ch/pdf/special-reports/srren/SRREN_FD_SPM_final.pdf, 2012.

Jain A. K., Biomass gasification under oxygen medium. J Agric Eng Vol. 36(3) pp. 27–31, 1999.

Jayamurthy M., Dasappa S., Paul P. J., Sridhar G., Sridhar H. V., Mukunda H. S., et al. Tar characterisation in new generation agro-residue gasifiers-cyclone and downdraft open top twin air entry systems. *Gasif Pyrolysis-State Art Futur Prospect*, pp. 235–48, 1997.

Jenkins B. M., Downdraft gasification Characteristics od Major California Residue-Derived Fuels, Ph.D. Thesis, Dept. of Engineering, University of California, Davis, 1980.

Kan T, Strezov V. Combustion of biomass. In: Strezov V, Evans TJ, editors. Biomass processing technologies. Boca Raton: CRC Press, pp. 53–80, 2014.

Kaupp A., Goss J. R., History of Small Gas Producer Engine Systems. In: Small Scale Gas Producer-Engine Systems. *Vieweg+Teubner Verlag*, Wiesbaden https://doi.org/10.1007/978-3-663-06868-6_2, 1984.

Khummongkol D., Arunlaksadamrong W., Performance of an updraft mangrove-wood gasifier. *Energy*, Vol. 15(9) pp. 781–784, 1990.

Kihedu, J.H., Yoshiie, R., Nunome, Y., Ueki, Y., Naruse, I., Counter-flow air gasification of woody biomass pellets in the auto-thermal packed bed reactor. *Fuel*, Vol. 117, pp. 1242–1247, 2014.

Kirkels A. F., Verbong G. P. J., Biomass gasification: Still promising? A 30-year global overview. *Renewable and Sustainable Energy Reviews*, Vol. 15(1) pp. 471–481, 2011.

Kirsanovs V., Blumberga D., Karlinka K., Veidenbergs I., Rochas C., Vigants E., Vigants G., Biomass gasification for district heating. *Energy procedia,* Vol. 113 pp. 2017-223, 2017.

Kjellstrom B.. Stassen H., and Beenackers, A.A.C.M., Producer Gas 1982: A Collec tion of Papers on Producer Gas With Emphasis on Ap pli cations in Developing Cowitries, Producer Gas Conference, Sri Lanka, SBN:91-86618-00-8,The Beijer Institute, Stockholm, Sweden, 1983.

Knoef H. A. M., Handbook of Biomass Gasification. *BTG*, 2005

Korens N., Simbeck D. R., Wilhelm D. J., Process screening analysis of alternative gas treating sulfur removal for gasification: Revised final report, 2002.

Kouhia M., Biomass gasification. *Department of Energy Technology Aalto University School of Engineering*, 2011.

Krasulina J., Luik H., Palu V., Tamvelius H., Thermochemical co-liquefaction of Estonian kukersite oil shale with peat and pine bark. *Oil Shale,* Vol. 29 pp. 222–36, 2012.

Kumar A, Jones DD, Hanna MA. Thermochemical biomass gasification: a review of the current status of the technology. *Energies,* Vol. 2 pp. 556–81, 2009.

Kunii D., Levenspiel O., Fluidization engineering. Oxford, UK: Butterworth-Heinemann, 1991.

Kurkela E., Ståhlberg P., Simell P., Leppälahti J., Updraft gasification of peat and biomass. *Biomass*, Vol. 19(1-2) pp. 37–46, 1989.

Lapuerta M., Hernández J. J., Tinaut F. V., Horrillo A., Thermochemical behaviour of producer gas from gasification of lignocellulosic biomass in SI engines. *SAE Paper* 2001-01-3586, 2001.

Launder B. E., Spalding D. B., The numerical computation of turbulent flows. *Computer methods in applied mechanics engineering,* Vol. 3 pp. 269-289.

Lien F. S., Chen W. L., and Leschziner M. A., Low-Reynolds number eddy-viscosity modelling based on non-linear stress-strain/vorticity relations. *Proc. 3rd Symp. on Engineering Turbulence Modelling and Measurements*, 27-29 May, Crete, Greece, 1996.

Liu, Y., Goodrick, S., Heilman, W., Wildland fire emissions, carbon, and climate: wildfire-climate interactions. For. Ecol. Manag. 317, 80–96, 2014.

Lozza G., Syngas cooling in IGCC systems, Editor(s): Ting Wang, Gary Stiegel, Integrated Gasification Combined Cycle (IGCC) Technologies, Woodhead Publishing, pp. 357-371, ISBN 9780081001677, https://doi.org/10.1016/B978-0-08-100167-7.00009-3, 2017.

Lyczkowski R. W., Bouillard J. X., State-of-the-art review of erosion modeling in fluid/solids systems. *Prog Energy Comb Sci*, Vol. 28(6) pp. 543e602, 2002.

Macìas-Machìn A., Socorro M., Verona J. M., Macı´as M., New granular material for hot gas filtration: use of the "Lapilli". *Chem Eng Process*, Vol. 45(9) pp. 719e27, 2006.

Mahinpey N., Gomez A., Review of gasification fundamentals and new findings: Reactors, feedstock, and kinetic studies, Chemical Engineering Science Vol. 148 pp. 14–31 http://dx.doi.org/10.1016/j.ces.2016.03.037, 2016.

Malaguti V., Lodi C., Sassatelli M., Pedrazzi S., Allesina G. and Tartarini P., Dynamic behavior investigation of a micro biomass CHP system for residential use. *International Journal of Heat and Technology*, Vol. 35 pp. 172-178, 2017.

Malico I., Pereira R. N., Gonçalves A. C., Sousa A. M. O., Current status and future perspectives for energy production from solid biomass in the European industry. *Renewable and Sustainable Energy Reviews*, Vol. 112 pp. 960–977, 2019.

Malik A., Mohapatra S. K., Biomass-based gasifiers for internal combustion (IC) engines—A review. *Indian Acad Sci*, Vol. 38(3) pp. 461–76, 2013.

Mallick D., Mahanta P., Moholkar V. S., Co-gasification of coal and biomass blends: chemistry and engineering. *Fuel,* Vol. 106e28. Elsevier, 2017.

Mao N., Y. Yao, M. Hata, M. Wada, C. Kanaoka, Comparison of filter cleaning performance between VDI and JIS testing rigs for cleanable fabric filter, *Powder Technol.* Vol. 180 pp. 109–114, 2008.

Marini F., Monitoraggio e valutazione delle prestazioni di un impianto di cogenerazione a cippato di legno con gassificatore e motore Stirling. *CISA*, http://www.centrocisa.it/ImpiantiRealizzati/stirlingCasteldaiano.php, 2012.

Martínez J. D., Mahkamov K., Andrade R. V., and Silva Lora E. E., Syngas production in downdraft biomass gasifiers and its application using internal combustion engines *Renewable Energy*, Issue 38 pp. 1-9, 2012.

McDonald J. R., Dean A. H., Electrostatic precipitator manual, vol. xi. Park Ridge, N.J: Noyes Data Corp; 1982. 484 pp. 122. Lloyd DA. Electrostatic precipitator handbook, vol. xiv. Bristol [England] ; Philadelphia: A. Hilger; 239 pp., 1998.

McKendry P. Energy production from biomass (part 2): conversion technologies. *Bioresources Technology,* Vol. 83 pp. 47-54, 2002b.

Mckendry P., Energy production from biomass (Part 1): overview of biomass. *Bioresources Technology,* Vol. 83 pp. 37–46, 2002a.

Mckendry P., Energy production from biomass (Part 3): gasification technologies. *Bioresour Technol,* Vol. 83 pp. 55-63, 2002c.

Melissari B., Ash related problems with high alkali biomass and its mitigation experimental evaluation. *Mem Invest En Ing*, Vol. 12 pp. 31–44, 2014.

Miles P. E. T. R., Miles J. T. R., Baxter L. L., Bryers R. W., Jenkins B. M., Oden L. L., Alkali deposits found in biomass power plants – a preliminary investigation of their extent and nature. *Cole, Boulevard, Golden, CO: Summary report for National Renewable Energy Laboratory*, 1995.

Milne T., Evans R., Abatzaglou N., Biomass gasifier ‘‘tars’’ their nature, formation, and conversion. *NREL/TP-570-25357. Golden, CO: National Renewable Energy Laboratory*, 1998.

Mitsakis P., Lehrstuhl für Energiesysteme Online analysis of the tar content of biomass gasification producer gas [Ph.D. dissertation]. Technische Universität München, 2011.

Mondal P., Dang G. S., Garg M. O., Syngas production through gasification and cleanup for downstream applications—recent developments. *Fuel Process Technol,* Vol. 2(8) pp. 1395–410, 2011.

Morselli N., Studio e progettazione di un microgeneratore a biomassa legnosa per applicazioni rurali, *M.D. Thesis in Vehicle Engineering, Dept. of Engineering "E. Ferrari" Modena Italy*, 2012.

Neeft J.P.A., Knoef H.A.M., Zielke U., Sjöström K., Hasler P., Simell P.A., Dorrington M.A., Abatzoglou N., Deutch S., Greil C., Buffinga G.J., Brage C., Soumalainen M., *Guideline for Sampling an Analysis of Tar and Particles in Biomass Producer Gas*, 1999.

Neves D., Thunman H., Matos A., Tarelho L., Gómez-Barea A., Characterization and prediction of biomass pyrolysis products, *Prog Energy Combust Sci* Vol. 37 pp. 611–30, 2011.

Ntalos G.A., Athanasios H., Characterization and utilisation of vine prunings as a wood substitute for particleboard production, *Industrial Crops and Products*, 2002.

Nuss P., Gardner K.H., Jambeck J.R., Comparative life cycle assessment (LCA) of construction and demolition (C&D) derived biomass and U.S. northeast forest residuals gasification for electricity production. *Environ. Sci. Technol.*, Vol. 47, pp. 3463–3471, 2013.

Ohtsuka Y., Tsubouchi N., Kikuchi T., Hashimoto H., Recent progress in Japan on hot gas cleanup of hydrogen chloride, hydrogen sulfide and ammonia in coal-derived fuel gas, *Powder Technol*, Vol. 190 pp. 340–7, 2009.

Ordys A. W., Grimble M. J., Kocaarslan I., Combined cycle and combined heat and power processes. *Control Syst, Robot Autom* Vol. 18 https:/www.eolss.net/Sample-Chapters/C18/E6-43-33-06.pdf, 2004.

Ouadi M., Brammer J.G., Kay M., Hornung A., Fixed bed downdraft gasification of paper industry wastes. *Applied Energy*, Vol. 103 pp. 692–699, 2013.

Ozgen, S., Caserini S, Galante, S., Giugliano, M., Angelino, E., Marongiu, A., Hugony, F., Migliavacca, G., Morreale, C., Emission factors from small scale appliances burning wood and pellets. Atmos. Environ. 94, 144–153, 2014.

Pan Z., Ting M., Wei-Dong L., Guang-Yu M. and Qiu-Wang W., Design and optimization of a novel high temperature heat exchanger for waste heat cascade recovery from exhaust flue gases, *Energy*, Vol. 160 pp. 3-18, 2018.

Pang S., Advances in thermochemical conversion of woody biomass to energy, fuels and chemicals. *Biotechnology Advances*, Vol. 37 pp. 589–597, https://doi.org/10.1016/j.biotechadv.2018.11.004, 2019.

Papurello D., Lanzini A., Leone P., Santarelli M., The effect of heavy tars (toluene and naphthalene) on theelectrochemical performance of an anode-supported SOFC running on bio-syngas. *Renewable Energy*, Vol. 99 pp. 747-753 http://dx.doi.org/10.1016/j.renene.2016.07.029, 2016.

Park H. J., S.H. Park, J.M. Sohn, J. Park, J.K. Jeon, S.S. Kim, Y.K. Park, Steam reforming of biomass gasification tar using benzene as a model compound over various Ni supported metal oxide catalysts, *Bioresour. Technol.*, Vol. 101 pp. S101–S103, https://doi.org/10.1016/j.biortech.2009.03.036, 2010.

Pathak B.S., S.R. Patel, A.G. Bhave, P.R. Bhoi, A.M. Sharma, and N.P. Shah. Performance evaluation of an agricultural residue-based modular throat-type down-draft gasifier for thermal application. *Biomass and Bioenergy*, Vol. 32(1) pp. 72–77, 2008.

Patuzzi F., Prando D., Vakalis S., Rizzo A. M., Chiaramonti D., Tirler W., Mimmo T., Gasparella A., Baratieri M., Small-scale biomass gasification CHP systems: Comparative performance assessment and monitoring experiences in South Tyrol (Italy), *Energy*, Vol. 112 pp. 285-293 http://dx.doi.org/10.1016/j.energy.2016.06.077, 2016.

Pedrazzi S., Allesina G. and Tartarini P., Aige conference: A kinetic model for a stratified downdraft gasifier. *International Journal of Heat and Technology*, Vol. 30 pp. 41-44, 2012.

Pedrazzi S., Allesina G., Morselli N., Puglia M., Barbieri L., Lancellotti I., Ceotto E., Giorgini L., Malcevschi A., Pederzini C. and Tartarini P., The energetic recover of biomass from river maintenance: the REBAF project. *European Biomass Conference and Exhibition Proceedings, 25thEUBCE*, pp. 52-57, 2017.

Pedrazzi S., Santunione G., Minarelli A., Allesina G., Energy and biochar co-production from municipal green waste gasification: A model applied to a landfill in the north of Italy. *Energy Conversion and Management*, vol. 187 pp. 274-282, 2019a.

Pemen A. J. M., Nair S. A., Yan K., van Heesch E. J. M., Ptasinski K. J., Drinkenburg A. A. H., Pulsed corona discharges for tar removal from biomass derived fuel gas. *Plasma Polym*, Vol. 8(3) pp. 209-24, 2003.

Perkins G., Bhaskar T., Konarova M., Process development status of fast pyrolysis technologies for the manufacture of renewable transport fuels from biomass. *Renew Sustain Energy Rev*, Vol. 90 pp. 292–315, 2018.

Permadi D.A., Oanh N.T.K., Assessment of biomass open burning emissions in Indonesia and potential climate forcing impact. *Atmos. Environ.*, Vol. 78, pp. 250–258, 2013.

Petrov O., Bi X., Lau A., Impact assessment of biomass-based district heating systems in densely populated communities. Part II: would the replacement of fossil fuels improve ambient air quality and human health?. *Atmos. Environ.* Vol. 161, pp. 191–199, 2017.

Prando D., Shivananda Ail S., Chiaramonti D., Baratieri M., Dasappa S., Characterization of the producer gas from an open top gasifier: assessment of different tar analysis approaches. *Fuel*, Vol. 181 pp. 566-72. https://doi.org/10.1016/ j.fuel.2016.04.104. Elsevier, 2016.

Prasad Lalta. Experimental study on gasification of jatropha shells in a downdraft open top gasifier. *Waste Biomass Valorization*, Vol. 6 pp. 117-22. https://doi.org/10.1007/s12649-014-9321-8. Springer, 2015.

Proll T., Rauch R., Aichernig C., Fluidized bed steam gasification of solid biomass performance characteristics of an 8 MWth combined heat and power plant. *Int J Chem React Eng*, Vol. 5, http://dx.doi.org/10.2202/1542-6580.1398, 2007.

Pruksakit W., Dejterakulwong C., Patumsawad S., Performance prediction of a downdraft gasifier using equilibrium model: effect of different biomass. Proceedings of the 5th international conference on sustainable energy and environment (SEE: Science, Technology and Innovation for ASEAN Green Growth, Bangkok, Thailand, pp. 19-21, 2014.

Quaak P., Knoef H., Stassen H. E., Energy from biomass: a review of combustion and gasification technologies. *Washington D. C.: World Bank Publications*, Vol. 23,1999.

Quinlan B., Kaufmann B., Allensina G., Pedrazzi S. and Whipple S., Application of OLTT in gasification power systems. *International Journal of Heat and Technology*, Vol. 35 pp. 773-778, 2017b.

Quinlan B., Kaufmann B., Allesina G., Pedrazzi S., Hasty J., Puglia M., Morselli N. and Tartarini P., The use of on-line colorimetry for tar content evaluation in gasification systems. *International Journal of Heat and Technology*, Vol. 35 (Special Issue 1) pp. S145-S151, 2017a.

Rabou L. P. L. M., Zwart R. W. R., Vreugdenhil B. J., Bos L., Tar in biomass producer gas, the energy research Centre of the Netherlands (ECN) experience: an enduring challenge. *Energy Fuel,* Vol. 23(12) pp. 6189-98, 2009.

Rajvanshi A.K., Biomass gasification. Boca Raton, Florida, United States: CRC Press, pp. 83–102, 1986.

Rakesh N., Dasappa S., A critical assessment of tar generated during biomass gasification -Formation, evaluation, issues and mitigation strategies. *Renewable and Sustainable Energy Reviews*, Vol. 91 pp. 1045–1064, 2018.

Ramalingam S. et al., Recent advances in the performance of Co-Current gasification technology: A review. *International Journal of Hydrogen Energy*, https://doi.org/10.1016/j.ijhydene.2019.10.185, 2019.

Rauch R., Biomass gasification to produce synthesis gas for fuels and chemicals. *Technical report, IEA Bioenergy Agreement*, 2003.

Raveendran K., Ganesh A., Khilar K. C., Influence of mineral matter on biomass pyrolysis characteristics. *Fuel*, Vol. 74(12) pp. 1812-22, 1995.

Ravenni G., Elhamib O.H., Ahrenfeldta J., Henriksena U.B., Neubaue Y., Adsorption and decomposition of tar model compounds over the surface ofgasification char and active carbon within the temperature range250–800 °C. Applied energy, vol. 241, pp. 139-151, 2019.

Reed T. B., Das A., Handbook of Biomass Downdraft Gasifier Engine Systems. The biomass energy foundation press, 1988.

Richardson Y., Blin J., Julbe A., A short overview on purification and conditioning of syngas produced by biomass gasification: Catalytic strategies, process intensification and new concepts. *Progress in Energy and Combustion Science,* Vol. 38 pp. 765e781 10.1016/j.pecs.2011.12.001, 2012.

Rios M. L. V., González A. M., Silva Lora E. E., Almazán del Olmo O. A., Reduction of tar generated during biomass gasification: A review. *Biomass and Bioenergy,* Vol. 108 pp. 345–370, https://doi.org/10.1016/j.biombioe.2017.12.002, 2018.

Risnes H., High Temperature Filtration in Biomass Combustion and Gasification Processes. A thesis submitted to The Norwegian University of Science and Technology for the degree of Doktor Ingeniør August 2002 - The Norwegian University of Science and Technology Faculty Engineering Science and Technology Department of Thermal Energy and Hydropower, 2002.

Rogelj J., den Elzen M., Höhne N., Fransen T., Fekete H., Winkler H., Schaeffer R., Sha F., Riahi K., Meinshausen M., Paris Agreement climate proposals need a boost to keep warming well below 2 °C. *Nature* Vol. 534, 631–639, http://dx.doi.org/10.1038/nature18307 , 2016.

Rüegsegger M., Kast M., Lessons Learned about Thermal Biomass Gasification. *Report elaborated 2016-2018 under IEA Bioenergy, Task 33 Thermal gasification of Biomass and waste*, 2019.

Ruiz J., Juarez M., Morales M., Munoz P., Mendivil M., Biomass gasification for electricity generation: review of current technology barriers. *Renew. Sust. Energy Rev.*, Vol. 18, pp. 174–183, 2013.

Ruiz J.A., Juàrez M.C., Morales M.P., Muñoz P., Mendìvil M.A., Biomass logistics: Financial & environmental costs, *Biomass & Bioenergy*, 2013.

Russo F., Basseb N.T., Scaling of turbulence intensity for low-speed flow in smooth pipes. Flow measurement and instrumentation, Vol. 52 pp. 101-114, 2016.

Saha S. K., Gaitonde U. N., Date A. W., Heat transfer and pressure drop characteristics of Turbulent flow in a circular tube fitted with regularly spaced twisted-tape elements *Experimental Thermal Fluid Science*, Vol. 3 (6) pp 632–640, 1990.

Salcedo R.L., Pinho M.J., Pilot- and industrial-scale experimental investigation of numerically optimized cyclones. *Ind Eng Chem Res,* Vol. 42(1) pp. 145e54, 2002.

Salzmann R., Kaufmann H. P., Hasler P., Guideline for sampling and analysis of tars, condensates and particulate from biomass gasifiers, 1996.

Samiran N.A., Jaafar M.N.M., Ng J.N., Lam S.S., Chong C.T., Progress in biomass gasification technique with focus on Malaysian palm biomass for syngas production. *Renew. Sust. Energy Rev.* Vol. 62 pp. 1047-1062, 2016.

Sandeep K., Dasappa S., Oxy–steam gasification of biomass for hydrogen rich syngas production using downdraft reactor configuration. *Int J Energy Res*, Vol. 38 pp. 174–88, 2014.

Sansaniwal S. K., Pal K., Rosen M. A., Tyagi S. K., Recent advances in the development of biomass gasification technology: A comprehensive review. *Renewable and Sustainable Energy Reviews,* Vol. 72 pp. 363–384, 2017.

Savutoa E., Andrea Di Carloa, Andrew Steeleb, Steffen Heidenreichc, Katia Galluccia, Sergio Rapagnad Syngas conditioning by ceramic filter candles filled with catalyst pellets and placed inside the freeboard of a fluidized bed steam gasifier. *Fuel Processing Technology*, Vol. 191 pp. 44–53, 2019.

Schifftner K. C., Hesketh H. E., Wet scrubbers. 2nd ed., vol. xv. Lancaster, Pa: Technomic, 206 pp., 1996.

SERI Generator Gas: The Swedish Experience from 1939-1945, Di Ingenjörsvetenskapsakademien (Sweden). Solar Energy Research Institute, United States. Dept. of Energy, Golden, Colorado, 1979.

Sharma S. D., Dolan M., Park D., Morpeth L., Ilyushechkin A., McLennan K., et al., A critical review of syngas cleaning technologies-fundamental limitations and practical problems. *Powder Technol*, Vol. 180(1-2) pp. 115-21, 2008.

Sheth P. N., Babu B. V., Production of hydrogen energy through biomass (waste wood) gasification. *International journal of hydrogen energy*, Vol. 35(19) pp. 10803–10810, 2010.

Shih T.H., Liou W.W., Shabbir A., Yang Z., and Zhu J., A new k-e eddy viscosity model for high Reynolds number turbulent flows-model development and validation. *Institute for Computational Mechanics in Propulsion and Center for Modeling of Turbulence and Transition Lewis Research Center*. Cleveland, Ohio, 1994.

Siedlecki M., Jong W. D., Verkooijen A. H. M., Fluidized bed gasification as a mature and reliable technology for the production of. Energies, Vol. 4 pp. 389–434, 2011.

Sinaiski E. G., Eugeniy J. Lapiga, Separation of Multiphase, Multicomponent Systems, Wiley, 2007.

Sinha, P., Hobbs, P.V., Yokelson, R.J., Blake, D.R., Gao, S., Kirchstetter, T.W. .Emissions from miombo woodland and dambo grassland savanna fires. J. Geophys.Res. 109, 2004.

Situmorang Y. A., Zhao Z., Yoshida A., Abudula A., Guan G., Small-scale biomass gasification systems for power generation (< 200 kW class): A review, *Renewable and Sustainable Energy Reviews* Vol. 117, https://doi.org/10.1016/j.rser.2019.109486, 2019.

Smid J., Hsiau S. S., Peng C. Y., Lee H. T., Hot gas cleanup: new designs for moving bed filters. *Filtrat Separ*, Vol. 42(10) pp. 36-9, 2005.

Soares J., Oliveira A. C., Experimental assessment of pine woodchips gasification at steady and part load performance. *28th European Biomass Conference and Exhibition Proceedings*, pp 513-519, 2019.

Sokhansanj, S., and Fenton, J., *Cost benefit of biomass supply and pre-prossessing.* Biocap Research Integration Program Synthesis Paper, 2006.

Song C.B., H.S. Park, K.W. Lee, Experimental study of filter clogging with monodisperse PSL particles. *Powder Technol.*, Vol. 163 pp. 152–159, 2006.

Souza G. M., Ballester M. V. R., Cruz C. H., Chum H., Dale B., Dale V. H., Fernandes E. C. M., Foust T., Karp A., Lynd L., Filho R. M., Milanez A., Nigro F., Osseweijer P., Verdade L. M., Victoria R. L., Van der Wielen L., The role of bioenergy in a climate-changing world. *Environmental Development*, Vol. 23 pp. 57–64 http://dx.doi.org/10.1016/j.envdev.2017.02.008, 2017.

Srivastava T. Renewable energy (gasification). *Adv Electron Electr Eng, Vol. 3*(9) pp. 1243–50, 2013.

Stanghelle D., Slungaard T., Sønju O. K., Granular bed filtration of high temperature biomass gasification gas. *J Hazard Mater*, Vol. 144(3) pp. 668-72, 2007.

Stevens D. J., Hot gas conditioning: recent progress with larger-scale biomass gasification systems. Update and Summary of recent progress. Golden, Colorado (US): NREL/SR-510e29952, National Renewable Energy Laboratory, 2001.

Sthal K., Nergaard M., IGCC power plant for biomass utilization, Värnamo, Sweden. *Biomass and Bioenergy*, Vol. 15, No. 3, pp. 205-211, 1998.

Strandberg M., Olofsson I., Pommer L., Wiklund-Lindström S., Åberg K., Nordin A., Effects of temperature and residence time on continuous torrefaction of spruce wood, *Fuel Process. Technol.* Vol. 134 pp. 387–398, 2015.

Susastriawan A. A. P., Saptoadi H., Small-scale downdraft gasifiers for biomass gasification: a review. *Renew Sustain Energy Rev,* Vol. 76 pp. 989–1003, 2017.

Taeroe A., Mustapha W. F., Stupak I., Raulund-Rasmussen K., Do forests best mitigate CO2 emissions to the atmosphere by setting them aside for maximization of carbon storage or by management for fossil fuel substitution? *Journal of Environmental Management*, Vol. 197 pp. 117e129, http://dx.doi.org/10.1016/j.jenvman.2017.03.051, 2017.

Tanabe E.H., P.M. Barros, K.B. Rodrigues, M.L. Aguiar, Experimental investigation of deposition and removal of particles during gas filtration with various fabric filters. *Separation and Purification Technology*, Vol. 80 pp. 187–195, 2011.

Tanger, P., Field, J.L., Jahn, C.E., DeFoort, M.W., Leach, J.E., 2013. Biomass for thermochemical conversion: targets and challenges. Front. Plant Sci. 4, 218.

The design, construction and operation of a 75 kWtwo-stage gasifier. *Energy,* Vol. 31 pp. 1542e53, 2006.

Tomei Roberto, La meccanica italiana, vol. n. 148, 1981.

Tregrossi A., Ciajolo A., Barbella R., The combustion of benzene in rich premixed flames at atmospheric pressure. *Combust Flame*, Vol. 117(3) pp. 553e61, 1999.

Vashistha C., A.K. Patil, M. Kumar, Experimental investigation of heat transfer and pressure drop in a circular tube with multiple inserts, *Appl. Therm. Eng.* Vol. 96 pp.117–129, 2016.

Verma R., An analysis of biomass technology and its impact on multi-fuel fired biomass boiler. *Int J Sci Eng Technol*, Vol. 3 pp.198–202, 2014.

Versteeg H.K., Malalasekera W., An introduction to computational fluid dynamics: the finite volume method, 2nd ed., Pearson Education Limited, London, 2007.

Wang C., Wang Y., Herath H. M. S. K., Polycyclic aromatic hydrocarbons (PAHs) in biochar – Their formation, occurrence and analysis: A review. *Organic Geochemistry*, Vol. 114, pp. 1–11, 2017.

Wang Y. et al., Characteristics of heat transfer for tube banks in crossflow and its relation with that in shell-and-tube heat exchangers. *Int. J. Heat Mass Transf.*, Vol. 93 pp. 584–594, 2016.

Warnecke R., Gasification of biomass: comparison of fixed bed and fluidized bed gasifier. Biomass. Bioenergy Vol. 18 pp. 489–497, 2000.

Wei C. N., Siming Y., Ran L., Yew-Hoong Gin Karina, Dai Yanjun, Wang Chi-Hwa. Co-gasification of woody biomass and chicken manure: syngas production, biochar reutilization, and cost-benefit analysis. *Energy.* https://doi.org/10.1016/j.energy.2017.07.165, 2017.

Wei L., Pordesimo L. O., Filip To S. D., Herndon C. W., Batchelor W. D., Evaluation of micro-scale syngas production costs through modeling. *American Society of Agricultural and Biological Engineers*, Vol. 52, pp. 1649-1659, 2009.

Well-to-Wheels Analysis of Fast Pyrolysis Pathways with GREET; *Argonne National Laboratory: Lemont, IL*, 2011.

Wihersaari, M., Evaluation of greenhouse gas emission risks from storage of wood residue. Biomass Bioenergy 28, 444–453, 2005.

Woodward, Product manual 26249 (revision F, 10/2014), original instructions. L-Series ITB LC-50.

Woolcock P. J., Brown R. C., A review of cleaning technologies for biomass-derived syngas, *Biomass Bioenergy*, Vol. 52 pp. 54–84. http://dx.doi.org/10.1016/j.biombioe.2013.02.036, 2013.

Wu K. T., Chein R. Y., Modeling of Biomass Gasification with Preheated Air at High Temperatures, *Energy Procedia*, Vol. 75 pp 214-219, 2015.

Yokelson, R.J., Burling, I.R., Urbanski, S.P., Atlas, E.L., Adachi, K., Buseck, P.R., Wiedinmyer, C., Akagi, S.K., Toohey, D.W., Wold, C.E., Trace gas and particle emissions from open biomass burning in Mexico. Atmos. Chem. Phys. 11, 6787–6808, 2011.

Yoon S.J., Choi Y., Son Y., Lee S., Lee J., Gasification of biodiesel by-product with air or oxygen to make syngas. Bioresour. Technol., Vol. 101 pp. 1227–1232, 2009.

Yunus A. Çengel, Introduction of Thermodynaics and heat transfert, McGraw-Hill, 1997.

Zainal Z.A., Rifau A., Quadir G.A., Seetharamu K.N., Experimental investigation of a downdraft biomass gasifier, Vol. 23 pp. 283–289, 2002.

Zanzi R., Sjostrom K., Bjornbom E., Rapid high-temperature pyrolysis of biomass in a free-fall reactor. *Fuel*, Vol. 75(5) pp. 545e50, 1996.

Zheng N., Fang Yan, Kang Zhang, Tian Zhou, Zhiqiang Sun, A review on single-phase convective heat transfer enhancement based on multi-longitudinal vortices in heat exchanger tubes. Applied Thermal Engineering, Vol. 164 https://doi.org/10.1016/j.applthermaleng.2019.114475, 2020.

Zhongqing M., Yimeng Z., Qisheng Z., Yongbiao Q., Jianbin Z., Hengfei Q., Design and experimental investigation of a 190 kWe biomass fixed bed gasification and polygeneration pilot plant using a double air stage downdraft approach. *Energy* Vol. 46 pp. 140-147, https://doi.org/10.1016/j.energy.2012.09.008. Issue 1, 2012.

Zhou J., Masutani S. M., Ishimura D. M., Turn S. Q., Kinoshita C. M., Catalytic gasification of woody biomass in an air-blown fluidized-bed reactor using Canadian limonite iron ore as the bed material, *Ind Eng Chem Res*, Vol. 39 pp. 626–34, 2000.

Ziqi Yanga, Yuanqing Wua, Zisheng Zhanga,b, Hong Lia, Xingang Lia, Roman I. Egorovc, Pavel A. Strizhakc, Xin Gaoa,2019, Recent advances in co-thermochemical conversions of biomass with fossil fuels focusing on the synergistic effects , Renewable and Sustainable Energy Reviews 103 (2019) 384–398 https://doi.org/10.1016/j.rser.2018.12.047

Ringraziamenti

Desidero ringraziare il Professor Tartarini per avermi dato la possibilità di iniziare il percorso di Dottorato e gli Ingegneri Allesina e Pedrazzi per avermi trasmesso conoscenza e passione, ed avermi dato tempo e modo di approfondire gli argomenti discussi in questo elaborato. Ringrazio tutti gli autori che hanno contribuito agli studi qui presentati e, in particolar modo, all'ingegnere compagno di viaggio Marco per i preziosi confronti e la quotidiana collaborazione. Un grazie infine a chi c'è sempre stato, ai più giovani e ai meno giovani, a chi c'era e non c'è più, a chi non c'era e sembra esserci sempre stato.

Appendix

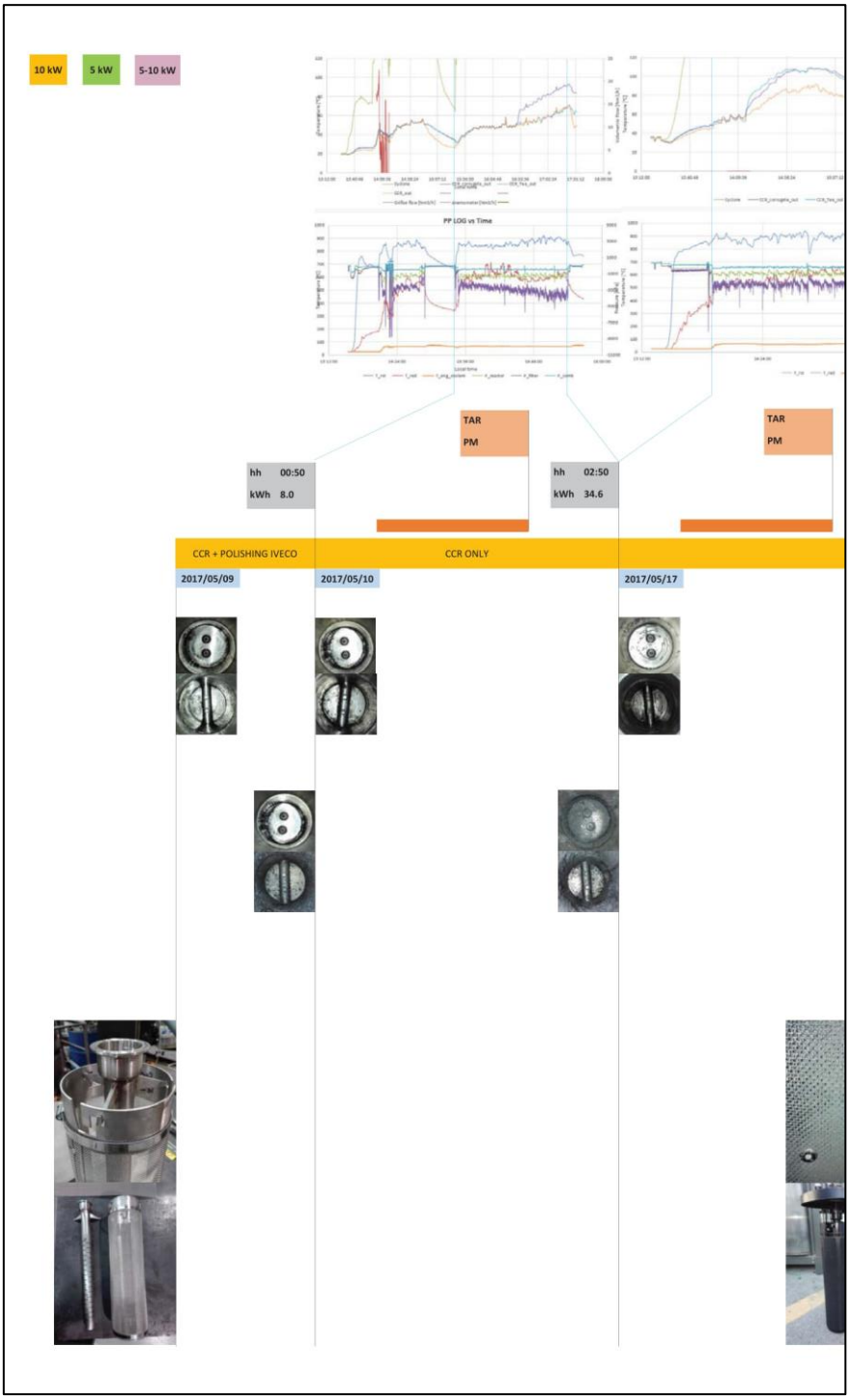

Figure 68. Timeline scheme of the tests reported in Chapter 4 – section 1.

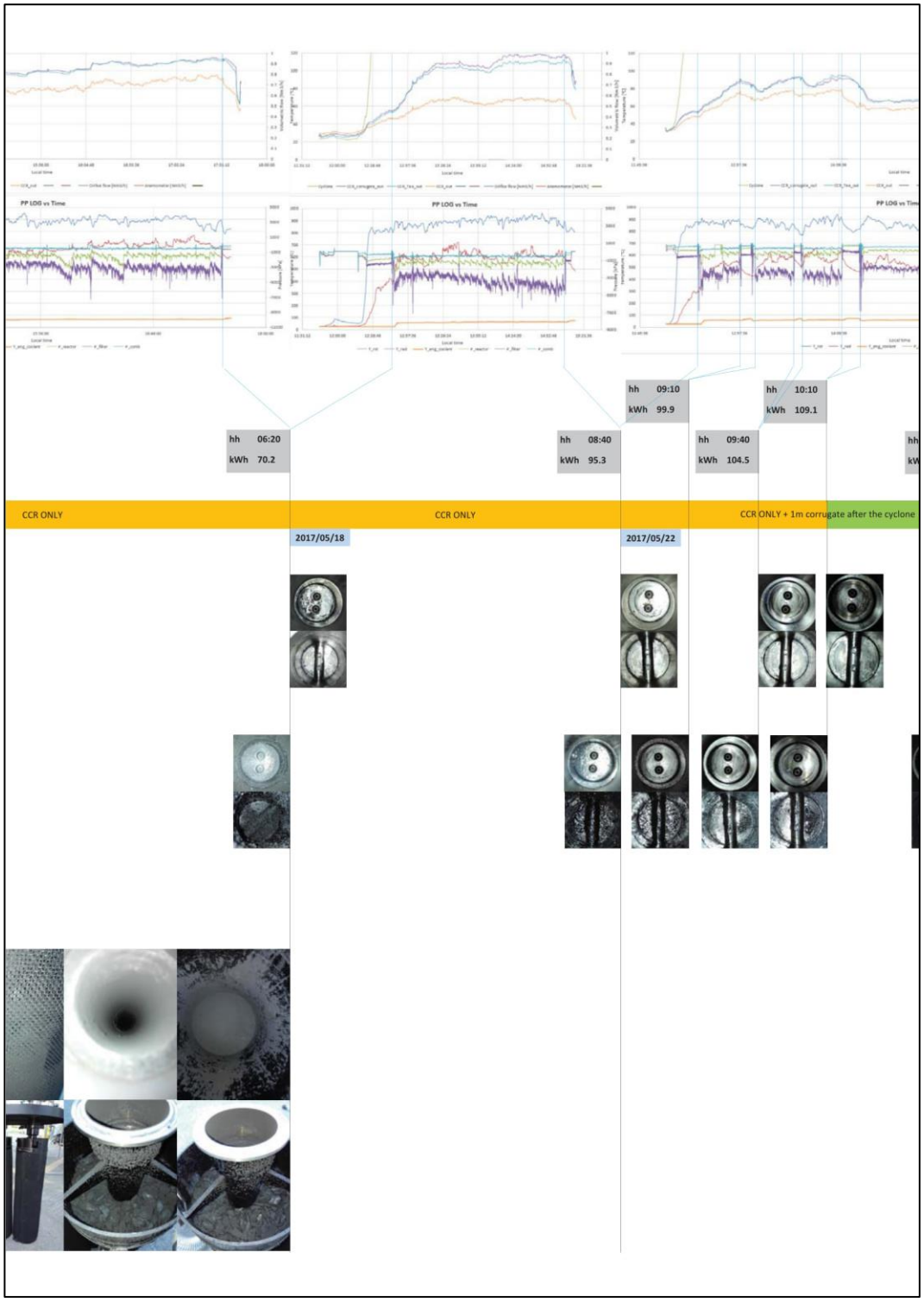

Figure 69. Timeline scheme of the tests reported in Chapter 4 – section 2.

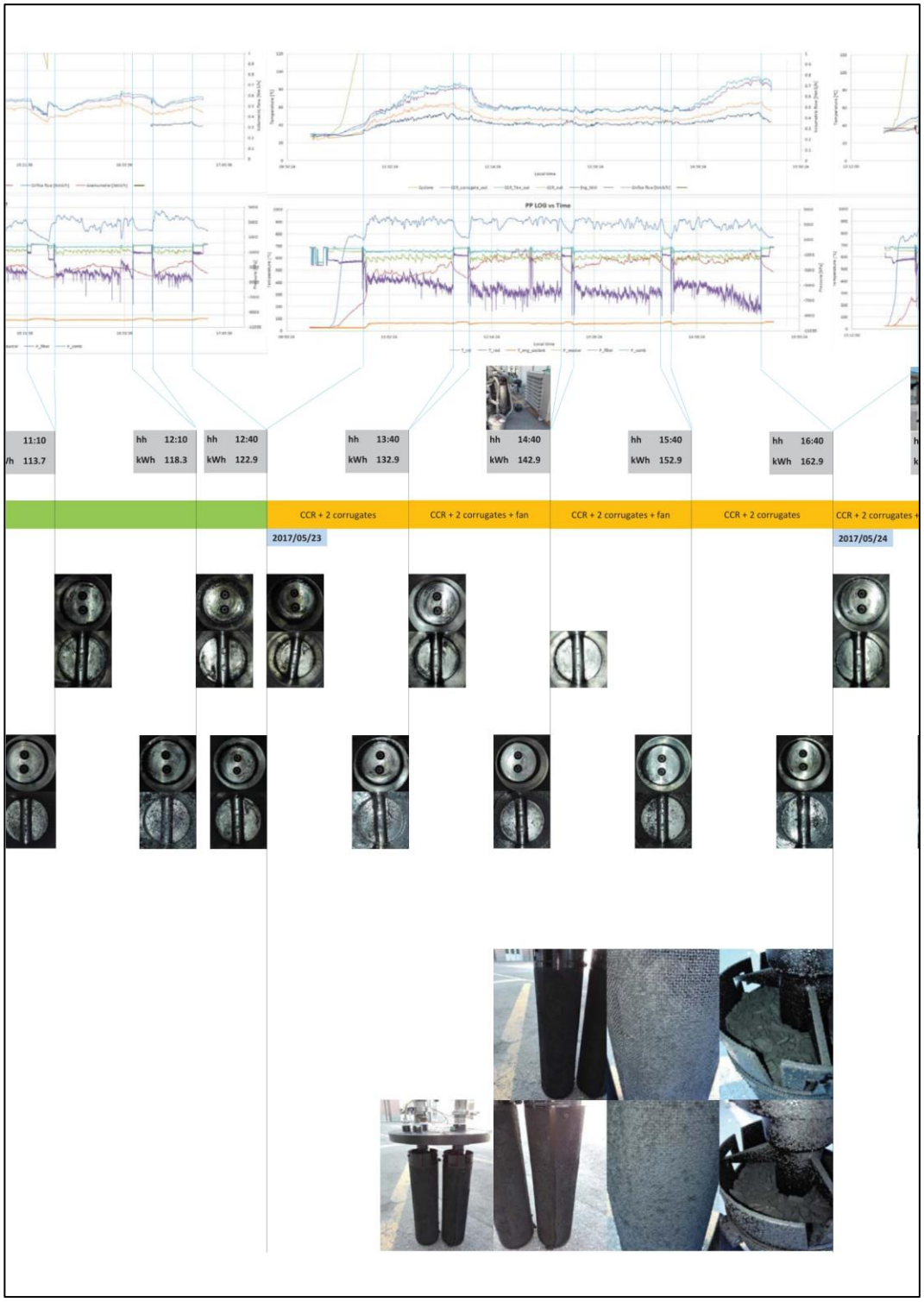

Figure 70. Timeline scheme of the tests reported in Chapter 4 – section 2.

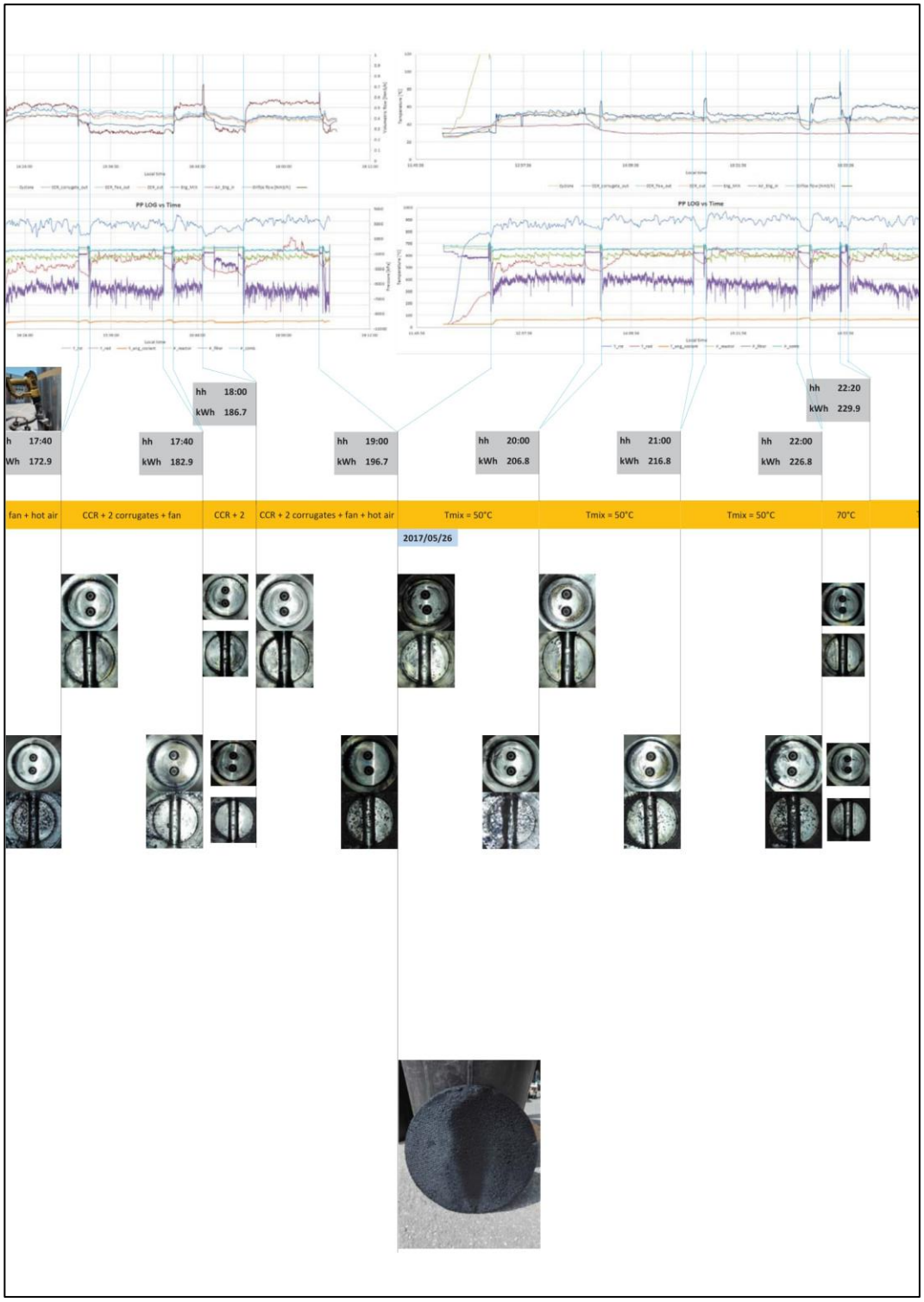

Figure 71. Timeline scheme of the tests reported in Chapter 4 – section 3.

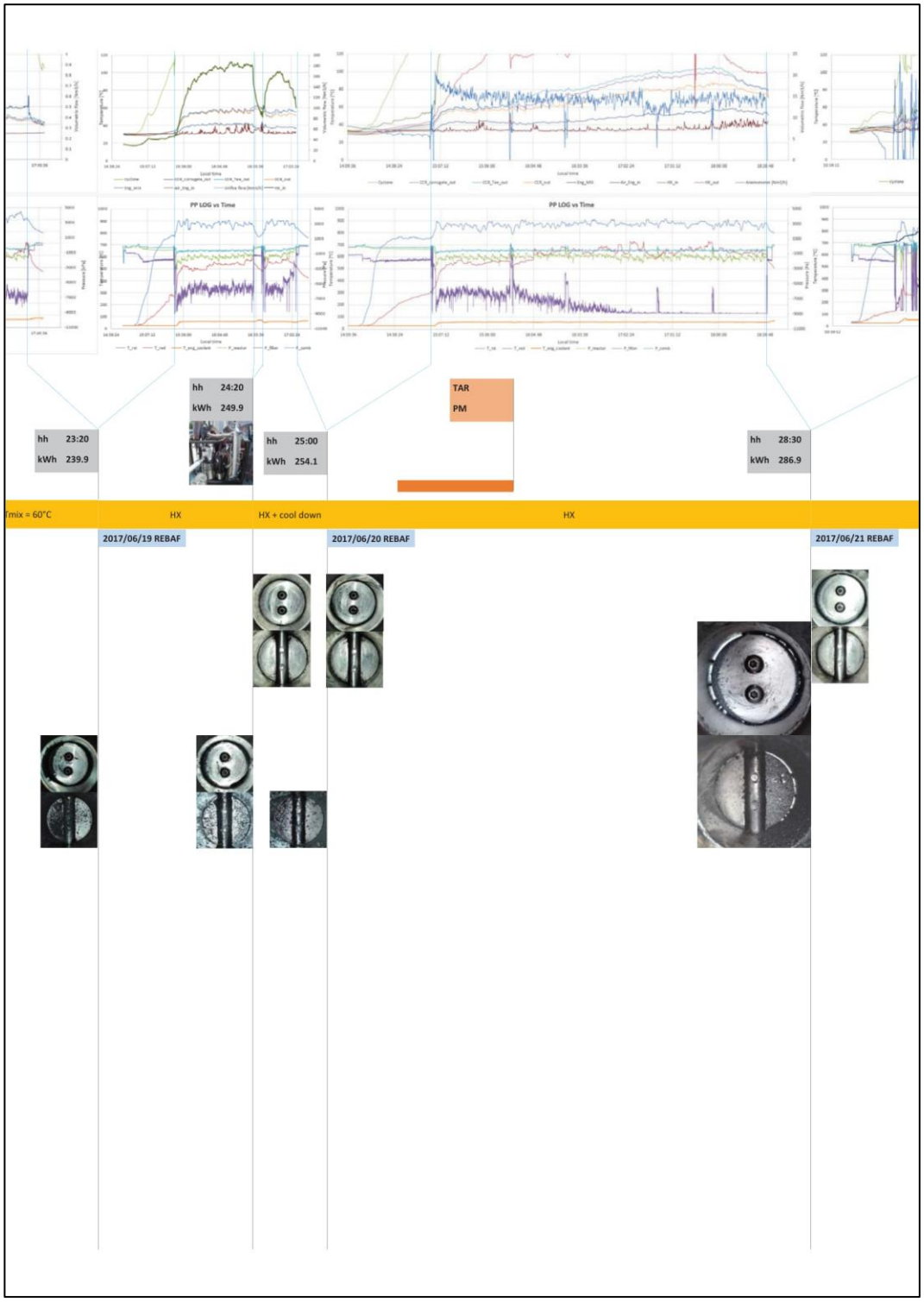

Figure 72. Timeline scheme of the tests reported in Chapter 4 – section 4.

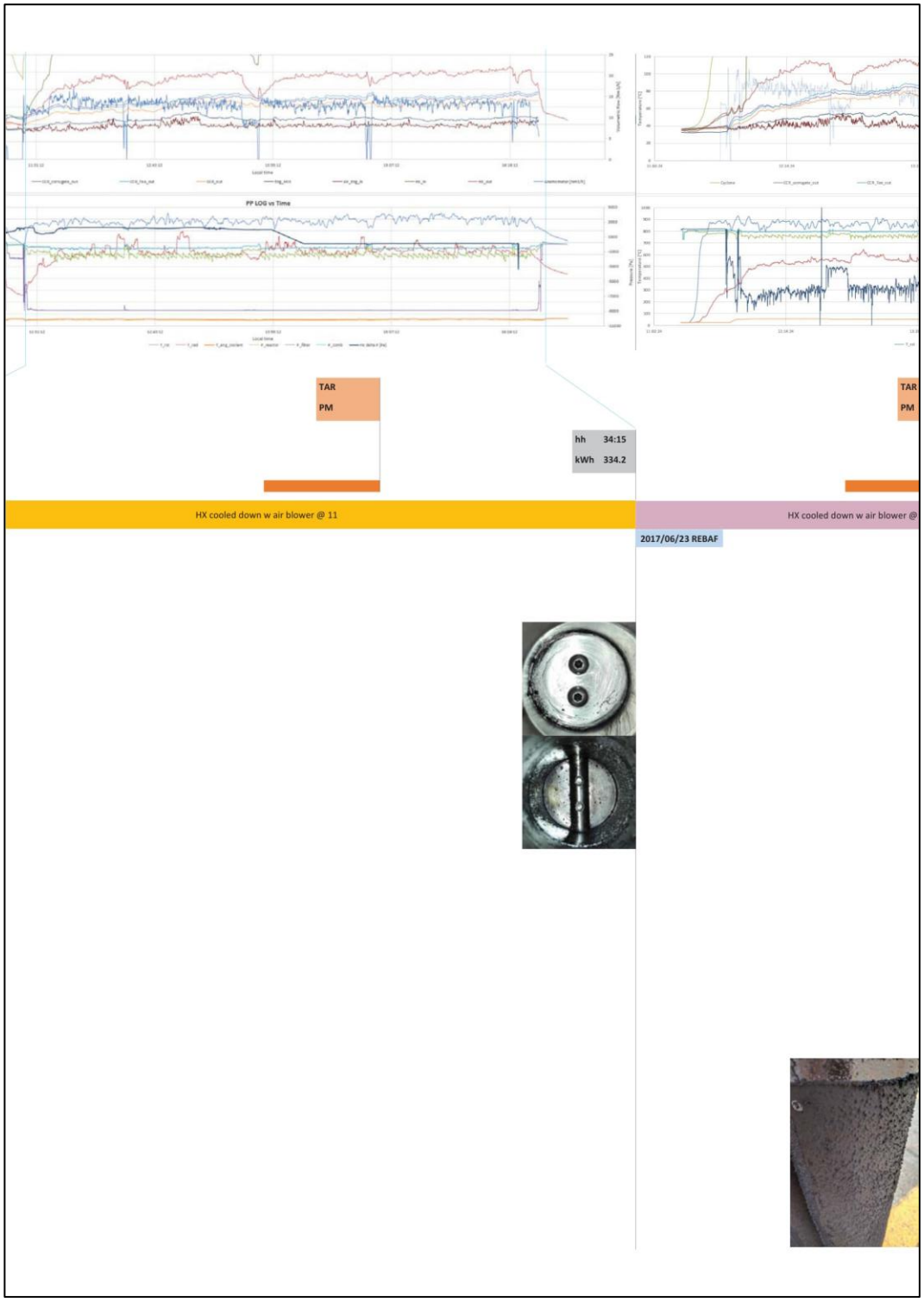

Figure 73. Timeline scheme of the tests reported in Chapter 4 – section 5.

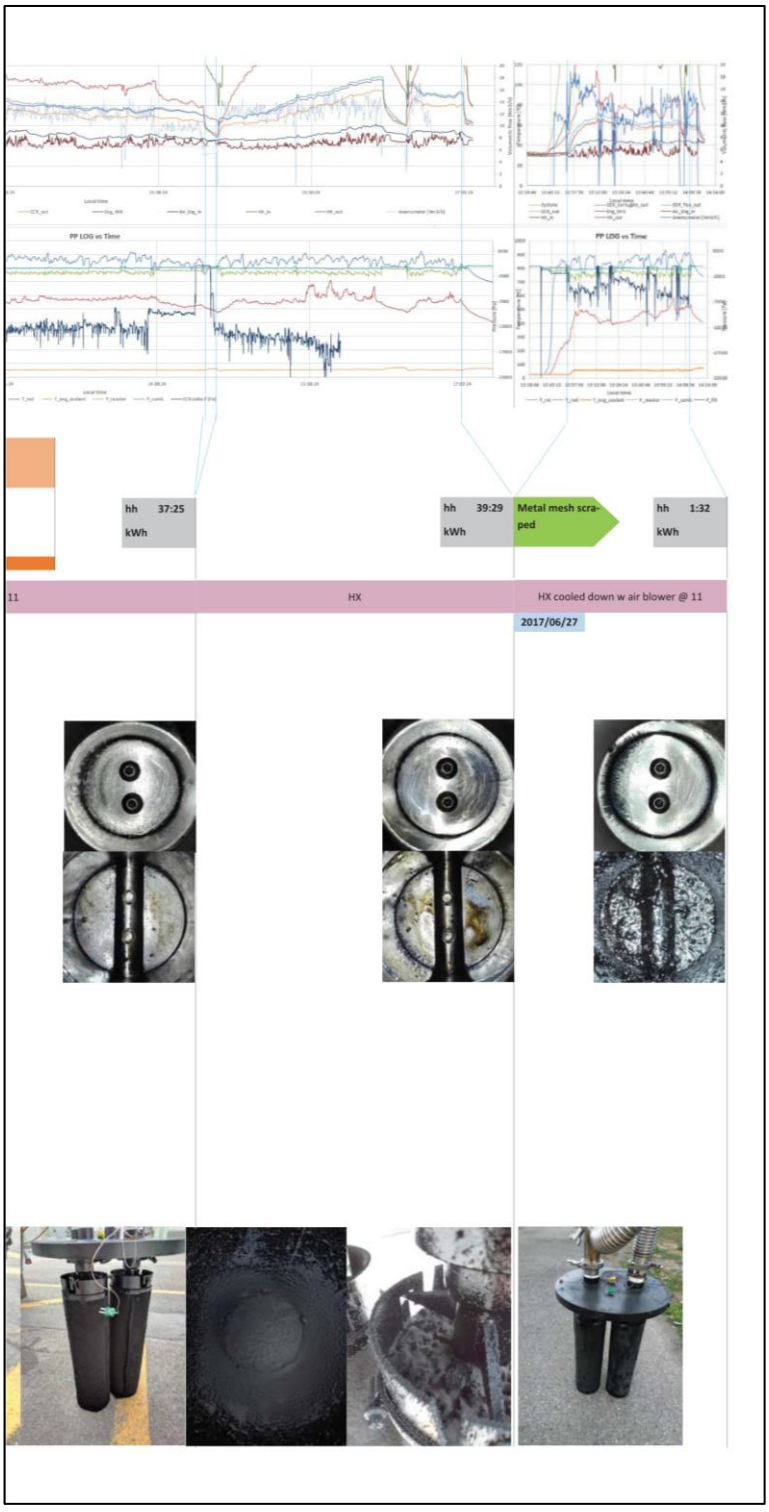

Figure 74. Timeline scheme of the tests reported in Chapter 4 – section 6.